DOKUZ EYLÜL UNIVERSITY

GRADUATE SCHOOL OF NATURAL AND APPLIED SCIENCES

HYDROGRAPHY OF THE BAYS ALONG THE EASTERN COAST OF THE AEGEAN SEA

by

Canan ERONAT

July, 2011

İZMİR

HYDROGRAPHY OF THE BAYS ALONG THE EASTERN COAST OF THE AEGEAN SEA

A Thesis Submitted to the
Graduate School of Natural and Applied Sciences of Dokuz Eylül University
In Partial Fulfillment of the Requirements for the Degree of Doctor of Philosophy in Marine Sciences and Technology, Coastal Engineering Program

by
Canan ERONAT

July, 2011
İZMİR

Ph.D. THESIS EXAMINATION RESULT FORM

We have read the thesis entitled **"HYDROGRAPHY OF THE BAYS ALONG THE EASTERN COAST OF THE AEGEAN SEA"** completed by **Canan ERONAT** under supervision of **Assoc. Prof. Dr. Erdem SAYIN** and we certify that in our opinion it is fully adequate, in scope and in quality, as a thesis for the degree of Doctor of Philosophy.

Assoc. Prof. Dr. Erdem SAYIN

Supervisor

Prof. Dr. Şükrü BEŞİKTEPE

Thesis Committee Member

Prof. Dr. Şükrü GÜNEY

Thesis Committee Member

Prof. Dr. Baha BÜYÜKIŞIK

Examining Committee Member

Assist. Prof. Dr. Hüsne ALTIOK

Examining Committee Member

Prof.Dr. Mustafa SABUNCU
Director
Graduate School of Natural and Applied Sciences

ACKNOWLEDGMENTS

First of all, I would like to express my gratitude to my Ph.D. supervisor, Assoc. Prof. Dr. Erdem SAYIN, whose expertise, understanding, and patience, added considerably to my graduate experience. I would like to thank the other members of my committee, Prof. Dr. Şükrü BEŞİKTEPE, Prof. Dr. Şükrü GÜNEY and Prof. Dr. Deniz ÜNSALAN for the assistance they provided at all levels of this study.

I thank the "Institute of Marine Science and Technology" and the "Graduate School of Natural and Applied Sciences" of Dokuz Eylül University for providing me the opportunity to work my thesis.

This work was supported by a TUBITAK Fellowship (BIDEB 2211). I would also like to convey thanks to the TUBITAK for providing the financial means.

Many thanks to all my friends who have been around these years, who have been helping me at different occasions and in one way or another have influenced this thesis.

I wish to express my love and gratitude to my beloved families; for their understanding & endless love, through the duration of this long-term study. Especially thanks to my brother Cem ÖZTÜRK who encouraged me to take first step in my academic life.

And special thanks to my husband, İlke ERONAT, who helped me get through all years of graduate school.

I want to ascribe this thesis to my son Çınar and my niece Bilge.

Canan ERONAT

HYDROGRAPHY OF THE BAYS ALONG THE EASTERN COAST OF THE AEGEAN SEA

ABSTRACT

Seasonal and interannual variability of the local hydrography and the water masses in the bays (Saros, Edremit, Çandarlı, İzmir, Kuşadası, Güllük and Gökova Bays) along the eastern coast of Aegean Sea are investigated using the data sets collected until 2010. The data covers the last major deep-water formation episode, and the EMT relaxation period. The concurrently intensive monitoring in Saros Bay, İzmir Bay and Gökova Bay have been conducted in spring 2001 and winter 2002.

Aegean Sea hydrology and water mass characteristics influence the water masses of the bays. The data suggests that the Saros Bay (North Aegean Sea), Edremit, Çandarlı and İzmir Bays (Central Aegean Sea) and Kuşadası, Güllük and Gökova Bays (South Aegean Sea) are the bays that have different physical processes inside and different water masses. They have their own dynamics independent from the Aegean Sea. At the same time they are occasionally influenced by the Aegean Sea's physical processes from time to time.

Besides the analysis of physical properties the time evolution of water masses inside the bays are investigated. The bays data shows the relaxation period of Eastern Mediterranean Transient (EMT) which continued well until the winter 2000. It is known that this variability depends on the changing climate over the Mediterranean area.

Our analysis reveals that the dense water formation in the Central Aegean Sea is considerably connected to the anomalous decrease in winter atmospheric temperature during EMT relaxation period. The isopycnal levels started to increase again and reached its maximum in the summer 2007 after relaxation period. The outcropping of isopycnals could have been a sign of a new formation of very dense water in the Aegean Sea.

Keywords: Aegean Sea; Saros Bay; Edremit Bay; Çandarlı Bay; İzmir Bay; Kuşadası Bay, Güllük Bay; Gökova Bay; Seawater properties; Water mass; Water movements; Eastern Mediterranean Transient (EMT).

EGE DENİZİNİN DOĞU KIYISINDAKİ KÖRFEZLERİN HİDROGRAFİSİ

ÖZ

Ege Denizi'nin doğu kıyısındaki körfezlerde (Saros, Edremit, Çandarlı, İzmir, Kuşadası, Güllük ve Gökova Körfezleri), su kütleleri ve yerel hidrografideki mevsimsel ve yıllık değişimler, 1940–2010 yılları arasında toplanan veri seti kullanılarak incelenmiştir. Veriler, son büyük yoğun su oluşumu zamanını ve duraklama dönemini kapsar. Saros, İzmir ve Gökova Körfezlerinde yoğun eş zamanlı araştırmalar bahar 2001 ve kış 2002'de gerçekleştirilmiştir.

Ege Denizi hidroloji ve su kütlesi özellikleri körfez suları üzerinde önemli bir etkiye sahiptir. Veriler, Saros Körfezi (Kuzey Ege Denizi), Edremit, Çandarlı ve İzmir Körfezleri (Orta Ege Denizi) ve Kuşadası, Güllük ve Gökova Körfezleri'nin (Güney Ege Denizi), içerisinde farklı fiziksel süreçler ve farklı su kütleleri olan üç körfez olduğunu göstermektedir. Körfezlerin Ege Denizi'nden bağımsız kendi dinamikleri vardır. Aynı zamanda, zaman zaman Ege Denizi'nin fiziksel süreçlerinden de etkilenmektedirler.

Körfezlerin fiziksel özelliklerinin analizinin yanı sıra, körfez içinde bulunan su kütlelerinin zamansal değişimi incelenmiştir. Körfezlerdeki veriler, Doğu Akdeniz Transienti'nin (EMT) kış 2000 yılına kadar devam eden durgunluk dönemini gösterir. Bu değişkenliğin, Akdeniz bölgesi üzerindeki iklim değişikliğine bağlı olduğu bilinmektedir.

Bizim yaptığımız analizler, Orta Ege Denizi'ndeki yoğun su oluşumunun, EMT dönemi boyunca kış mevsimlerinde atmosferik sıcaklığın anormal azalmasına bağlı olduğunu ortaya koymaktadır. EMT'nin durgunluk döneminden sonra eş yoğunluk seviyeleri tekrar artmaya başlamış ve yaz 2007'de maksimum seviyeye ulaşmıştır. Yüzeye çıkan eş yoğunluk eğrileri, Ege Denizi'ndeki yeni bir yoğun su oluşumunun bir işareti olabilir.

Anahtar sözcükler: Ege Denizi; Saros Körfezi; Edremit Körfezi; Çandarlı Körfezi; İzmir Körfezi; Kuşadası Körfezi; Güllük Körfezi; Gökova Körfezi; Deniz suyu özellikleri; Su kütlesi; Su hareketleri; Doğu Akdeniz Transienti (EMT).

CONTENTS

Page

CHAPTER ONE
INTRODUCTION

The present study provides an overview of the physical properties in the bays along the Eastern coast of the Aegean Sea. Within the framework of the various activities of the Research Vessel K. Piri Reis, 1991-2010, this work presents an integrated synthesis of the spatial and temporal heterogeneity of the bays, in terms of: i) main processes in the bays ii) formation and evolution of the water masses and iii) wind-induced water circulation patterns. Besides the analysis of physical properties the time evolution of water masses inside the bays are investigated.

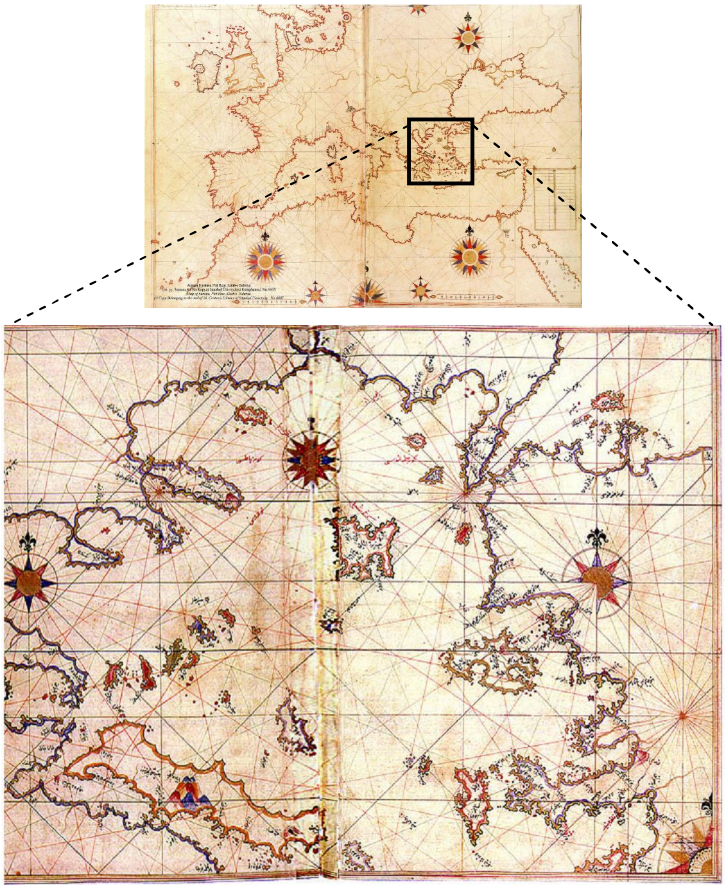

Figure 1.1 Historic map of Aegean Sea by Piri Reis.

Kitab-ı Bahriye (Book of Navigation-1525) of Piri Reis contained detailed information on the major ports, bays, gulfs, capes, peninsulas, islands, straits and

ideal shelters of the Aegean Sea (Figure 1.1). The current coastline dates back to about 4000 BC. The Aegean Sea is an elongated embayment of the Mediterranean Sea located between the southern Balkan and Anatolian peninsulas, i.e., between the mainlands of Greece and Turkey (Figure 1.2). In the north, it is connected to the Marmara Sea and Black Sea by the Çanakkale and İstanbul Straits (Dardanelles and Bosporus). The Aegean Islands are within the sea and some bound it on its southern periphery, including Crete and Rhodes. The Aegean Sea is 660 km long with a maximum width of 270 km in the north, 150 km in the central and 400 km in the south. It lies approximately between latitudes of 35 and 41 °N and the longitudes of 23 and 27/28 °E. Its surface area is 214000 km^2, surrounded by Europe and Asia. Its mean depth is 1500 m; it reaches a maximum depth of 3543 m off the east of Crete.

The bays and gulfs of the Aegean beginning at the south and moving clockwise include on Crete, the Mirabelli, Almyros, Souda and Chania bays or gulfs, on the mainland the Myrtoan Sea to the west, the Saronic Gulf northwestward, the Petalies Gulf which connects with the South Euboic Sea, the Pagasetic Gulf which connects with the North Euboic Sea, the Thermian Gulf northwestward, the Chalkidiki Peninsula including the Cassandra and the Singitic Gulfs, northward the Strymonian Gulf and the Gulf of Kavala and the rest are in Turkey; Saros Bay, Edremit Bay, Çandarlı Bay, İzmir Bay, Kuşadası Bay, Güllük Bay, Gökova Bay (Figure 1.2). The areas under investigation are located in the eastern part of the Aegean Sea (Figure 1.3).

Aegean Sea is one of the most interesting basins in the Mediterranean. However, there have been a few detailed oceanographic studies. The main reasons of this scarce is the difficulty of obtaining in-situ data over the whole Aegean Sea due to the regional problems such as complex bottom topography, continental shelf problem between Turkey and Greece, high cost rates for ship navigation (Uckac, 2004).

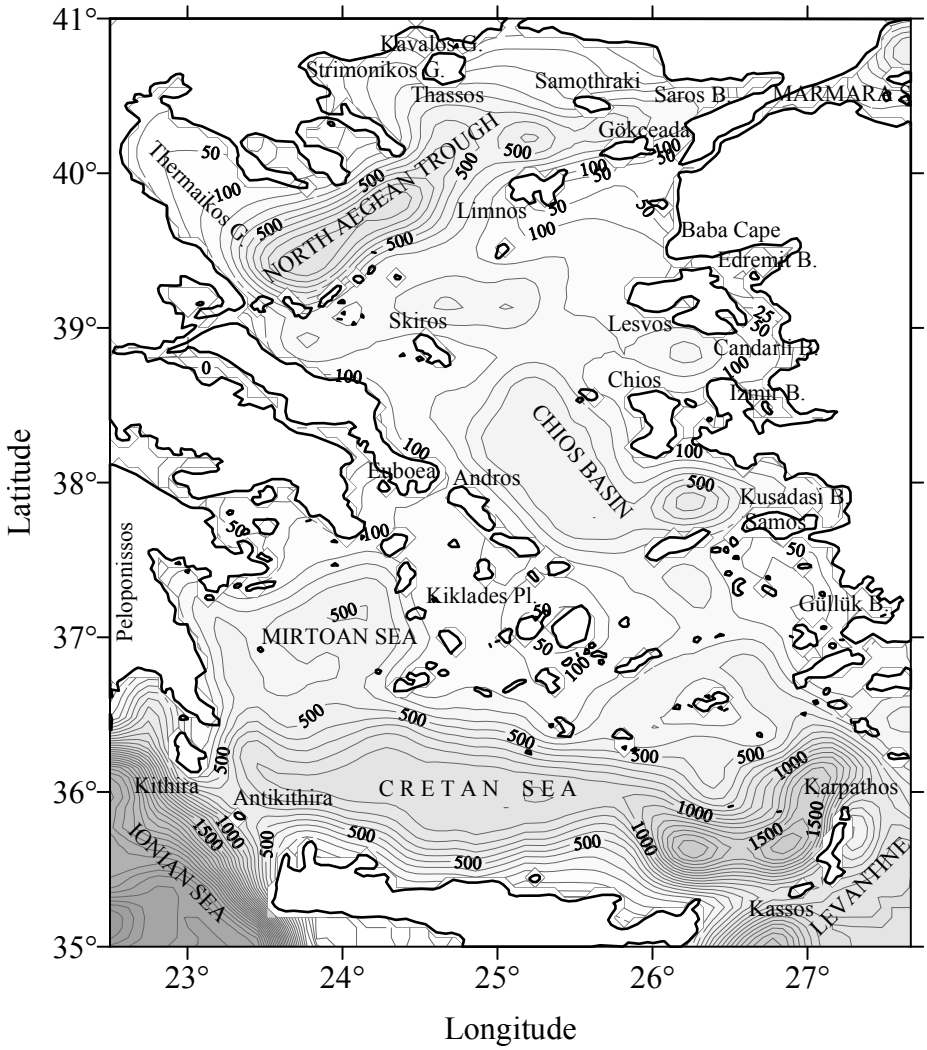

Figure 1.2 The map, the view from Google Earth and bathymetry of Aegean Sea and the location of the major basins and islands.

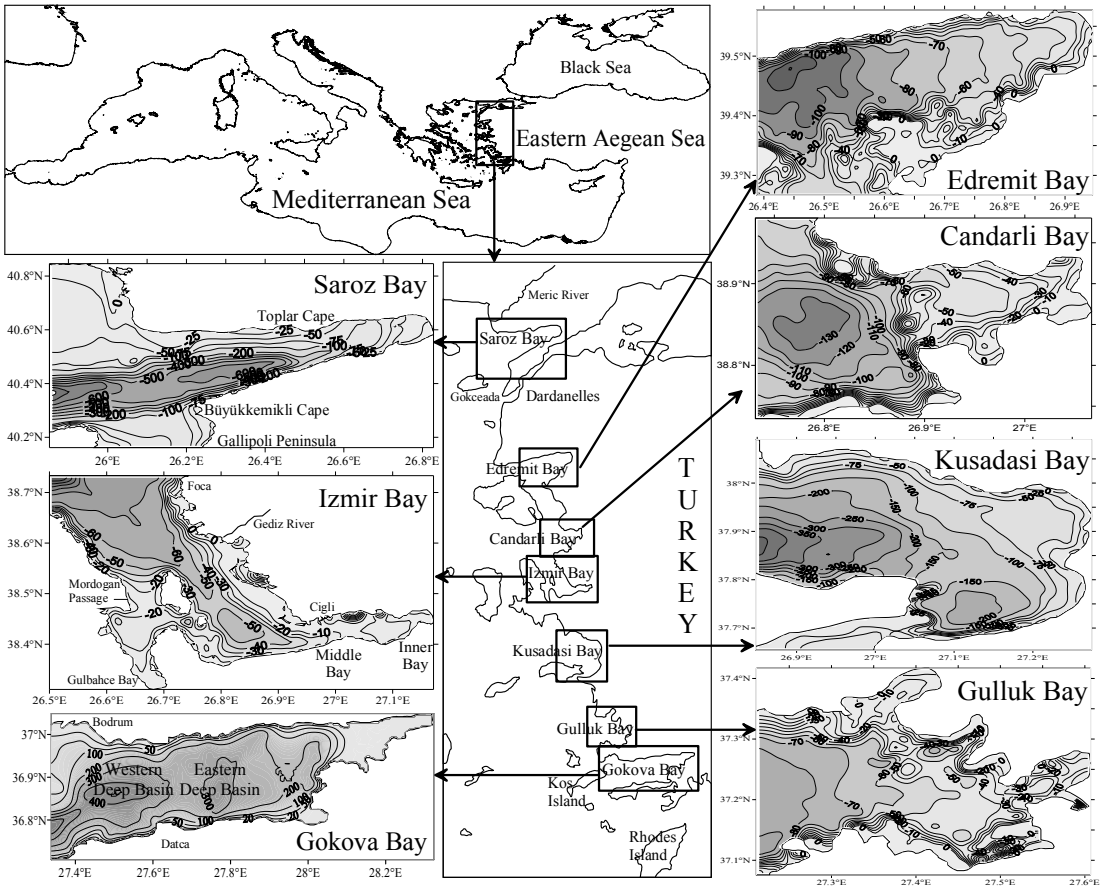

Figure 1.3 Bathymetry (from GEBCO-General bathymetric chart of the oceans, 2008 grided data) and location of the bays in the Eastern Aegean Sea.

The general circulation structure of the Aegean Sea has been described in detail in many papers, such as Zodiatis (1992), Theocharis & Georgopoulos (1993), Poulos et al. (1997), Oğuz & Tuğrul (1998), Theocharis et al. (1999), Zervakis et al. (2000), Sayın (2003), Velaoras & Lascaratos (2005). Intensive research has been underway for several years, coordinated by the international POEM (Physical Oceanography of the Eastern Mediterranean) program.

In the last decade, climatic and oceanographic studies have shown that there have been significant changes in the Aegean Sea. These changes lead to the variations in

physical properties not only in the Aegean Sea also in the Eastern Mediterranean deep water formation (Uckac, 2004).

Hydrology in the Aegean Sea area is mostly influenced by a number of external factors, such as the largely variable inflow of cold and less saline Black Sea Water (BSW), its mixing with the more saline Levantine Intermediate Water (LIW) and the presence of an extended continental shelf and an irregular bottom topography (Yuce, 1995; Poulos et al., 1997). BSW forms a strong surface current flowing through the Çanakkale Strait with an average speed of approximately 0.60 ms^{-1} (Bethoux, 1980; Malanotte-Rizzoli and Hecht, 1988).

The Aegean Sea water characteristics are different in every season. The Levantine Waters (LWs) enter to the Aegean Sea from Levantine basin and influence the off-shore of eastern coastal area up to Gökçeada Island in spring time especially after Eastern Mediterranean Transient (EMT) (Sayın et al. 2011). Therefore it is interesting to investigate the LWs if they exist in the Saros bay environment in spring 2001. Salty and warm water mass covers the eastern coastal area of the Aegean Sea with entering LWs.

Generally, the Levantine water masses can be observed up to North Aegean Sea mainly in spring time. In the Central Aegean Sea the frequently seen cold dense water mixes with the upwelling water and remains very dense water behind in summer time. The Levantine Surface Water (LSW) is blocked and does not penetrate further to the north because of the existing upwelling water seen near Saros (Büyükkemikli Cape) and off-shore side of Baba Cape (product of northerly wind) especially in summer and relatively less intense in fall time. The water masses are rather homogeneous vertically with the influence of strong wind mixing and convective mixing in winter time (Sayın et al. 2011).

The other important phenomenon for Saros bay is the upwelling taking place near the Büyük Kemikli Peninsula. The lasting northerly wind is prevailing all the year in the Saros area with high wind speed. Especially NE wind maintains a strong

upwelling in the south entrance of the Saros bay and cold and dense water covers the area. The third important water mass is the Black Sea Water occasionally enters the Saros bay mainly through its south entrance (Sayın et al. 2011).

The most important water mass is Central Aegean Intermediate Water (CAgIW). Gertman et. al (2006) found that the Central Aegean Basin is the site of the formation of Aegean Intermediate Water. Formation of cyclonic circulation in the Central Aegean Sea brings dense and cold intermediate water near surface (Sayin et al. 2011). The surface water temperature is further decreased due to open sea convection. In a modeling work by Nittis et al. (2003), open sea convection was identified as a mechanism for the deep water formation, where cyclonic circulation favors this mechanism in the Skyros and Chios basins. Winter mixing exacerbates cyclonic circulation (Zervakis et al. 2004). The existence of CAgIW in the bays means that the forming such intermediate water can affect the whole Aegean Sea even in the bays very close to the coast.

Another North Aegean water mass is “Cold Intermediate Layer” (CIL). Dense water is formed with the cooling of water from surface in winter period. This dense water sinks till it finds its density equal to the density of environment in a water column. CIL is a known feature in the Black Sea and Marmara Sea. A similar structure is found in the Aegean Sea in spring time in the study of Tokat (2006).

All the water masses mentioned above exist time to time in the Aegean Sea. Even South Aegean water masses can be seen in the Middle and North Aegean Sea.

Aegean Sea hydrology and water mass characteristics have influence on the waters of the bays along the eastern coastal area. Saros, Edremit, Çandarlı, İzmir, Kuşadası, Güllük and Gökova are the bays have different physical processes inside and different water masses. They have own dynamics independent from the Aegean Sea at the same time they are influenced by Aegean Sea dynamics time to time. The oceanography of the Edremit, Çandarlı, Kuşadası, Güllük and Gökova Bays has not been studied until now. But several studies on water masses and water quality can be

found for the İzmir Bay (Sayin, 2003; Sayin et al. 2006 and 2007) and Saros Bay (Tokat, 2006, Tokat and Sayin, 2007, Pazı, 2008, Uluturhan, 2010).

In-situ measurements and modeling studies enable us to identify how far the Aegean water masses (Black Sea Water (BSW), Levantine Surface Water (LSW), Levantine Intermediate Water (LIW), Central Aegean Intermediate Water (CAgIW), North Aegean Deep Water (NAgDW), Modified Atlantic Water (MAW), Transition Mediterranean Water (TMW)) influence the bays.

Three water masses are observed in the İzmir Bay as ASW (Aegean Sea Water) IBW (İzmir Bay Water) and IBIW (İzmir Inner Bay Water) (Sayin et al. 2006). In winter, ASW and IBW show a homogenous vertical distribution due to the winter convection and wind mixing. Fresh water discharge forces the establishment of a vertical and horizontal stratification all year around in IBIW.

Besides seasonal heating, the strong evaporation plays an important role in the two-layered system in the summer. The temperature in winter decreases gradually towards the Inner Bay. The IBIW mass is always colder, less saline, and denser than the other water masses and the ASW is always warmer, more saline and lighter than the water masses of other regions in winter. Temperatures decrease in summer from Inner Bay to Aegean Sea, because of differential warming. As a result of variation in temperature, density also changes in similar manner. It decreases from Middle Bay to Outer III in winter, but increases in summer. April and October are the transient months between winter and summer.

The upper and lower layers of İzmir Bay show summer and winter characteristics respectively, in April except for the surface of ASW. Because of its large volume, ASW water preserves its winter character. In the late April, the stratifications start to be stronger, but gradually, horizontally homogeneity takes place in time. A gyre evolves always in the middle of the Bay. It is cyclonic or anticyclonic manner depending on the wind condition over the area. IBW forms in this Middle Gyre area. The forming eddy in the Middle Gyre area has a cyclonic character in case of

southerly and easterly winds and has an anticyclonic character in case northerly and westerly winds.

The Levantine water masses LSW and LIW enter the south Aegean Sea. In-situ measurements and related modelling studies enable us to identify these water masses how far they influence the Gökova bay. Besides LSW and LIW, Modified Atlantic Water (MAW) and Transition Mediterranean Water (TMW) of low salinity, temperature and oxygen, but rich in nutrients into the South Aegean Sea at intermediate depths from the open sea areas of the Eastern Mediterranean occupy the South Aegean Sea. It is originating in the Levantine and Ionian basins (Balopoulos et al., 1999; Theocharis et al., 1999a). This water mass enters the south Aegean through the Cretan Arc Straits to balance the water budget (Zervakis et al., 2004).

Sayin & Besiktepe (2010) studied on TMW existing in the eastern Cretan Sea. In this study, the detection of TMW starts from fall 1992 up to spring 1995 in the Cretan Sea approximately in the depth of 250 to 600 m. The same information can be obtained in the study of Georgopoulos et al. (2000). They explain also the dipole characteristics and the changing the isopycnal levels parallel to water movements.

Kontoyiannis et al. (2005) noticed the overall decrease in the TMW volume from June 1997 to May 1998 into the Cretan Sea and Röther et al. (2007) mentioned about fresh TMW that were replacing the higher-salinity waters transferred downward; by 1998 the salinities had recovered toward the 1991-92 values.

In this study we will examine the general physical properties of the Aegean Sea, focusing on the bays (Saros Bay, Edremit Bay, Çandarlı Bay, İzmir Bay, Kuşadası Bay, Güllük Bay and Gökova Bay) dynamics. It will show the different characteristics of the water masses of the Bays and try to identify variabilities of these characteristics. Chapter 2 deals with the material and methods. In Chapter 3, we review the existing knowledge on water masses formed in the bays (Saros Bay, Edremit Bay, Çandarlı Bay, İzmir Bay, Kuşadası Bay, Güllük Bay and Gökova Bay) giving reference to the results of recent studies. This chapter presents a description of

the data set related to the observations done seasonally and the methods used, and we present the results of a numerical study and seasonal features. The results of the work are summarized and discussed in the Chapter 5.th of this study. And the last section is conclusion.

CHAPTER TWO
MATERIAL AND METHOD

2.1 Measurements

The measurements, especially CTD (Conductivity, Temperature and Depth) measurements have been initiated in the Eastern Aegean Sea covering Saros, Edremit, Çandarlı, İzmir, Kuşadası, Güllük and Gökova Bays based on the national projects since 1991 (Table 2.1). The concurrently intensive monitoring in Saros Bay, İzmir Bay and Gökova Bay has been conducted in 2001 spring and 2002 winter.

CTD (Conductivity, Temperature and Depth) Data was utilized in order to evaluate the robust features of the sea water properties and circulation. The simulations are used to define the seasonal circulation of the bays along the eastern coast of Aegean Sea. The potential temperature (θ) and potential density (σ_θ) values hereafter will be referred to as temperature and density.

The weather properties of the bays are analyzed using the data retrieved from these seven different areas in a long term period up to 2010. Hourly data on six meteorological factors were obtained from the meteorological centers in the bays of Saros, Edremit, Çandarlı, İzmir, Kuşadası, Güllük and Gökova are:

- Wind speed (m/s) and wind direction (degree)
- Air temperature (°C)
- Precipitation (mm)
- Evaporation (mm)
- Relative humidity (%)
- Air pressure (mbar)

Table 2.1 Data summary as year, season and month of cruises that provided in-situ data used in this work.

Cruise	Saros Bay	Edremit Bay	Çandarlı Bay	İzmir Bay	Kuşadası Bay	Güllük Bay	Gökova Bay
Summer 1991	July	July	July	August	July, August	August	August
Spring 1992	May	April	April	April	May	May	May
Fall 1992	September	September	September	September	October	October	October
Winter 1993	February		January				
Spring 1993	May			May	May	May	May
Fall 1993	October			September	October	October	October
Winter 1994				January			
Spring 1994				April			
Summer 1994		August		August	August	August	
Fall 1994						December	December
Spring 1995	April				April	April	May
Summer 1995	August				August	August	August
Fall 1995	November	November			November	November	November
Winter 1996				January			
Spring 1996	March	March			April	April	April
Summer 1996	June	June	June	June	June	June	June
Fall 1996	October	October	October	October	October	October	November
Winter 1997				January	January		
Summer 1997				July, August			
Fall 1997				November			
Winter 1998		January	January	January	February	February	February
Spring 1998				April			
Summer 1998						July	
Fall 1998				September, October			
Winter 2000				March			
Spring 2000				April, May			
Summer 2000				July			
Fall 2000				November			
Winter 2001				January			
Spring 2001	May			April			May
Summer 2001				August			
Fall 2001				December			
Winter 2002	January			February			January
Spring 2002				July			
Summer 2002				August			
Fall 2002				November			
Winter 2003				March			
Spring 2003				May			
Summer 2003			August	August			
Fall 2003					November		
Spring 2004				March			
Summer 2004				August			
Fall 2004				November			
Winter 2005			February	February			
Spring 2005				April			
Summer 2005			July	June			
Fall 2005			September	September			
Winter 2007				January			
Spring 2007				March			
Summer 2007	June		June	July	June	June	June
Fall 2007				October			
Winter 2008				January			
Spring 2008				April			
Summer 2008	June	June	June	July	June	June	June
Fall 2008				December			
Winter 2009				February			
Spring 2009				April			
Summer 2009		June	June	July	June	June	
Fall 2009				November			
Winter 2010				February			
Spring 2010				April			

2.2 Method

2.2.1 Analysis

The CTD data including depth, temperature, salinity and density were grouped and prepared with help of FORTRAN programs and were stored in DBF form using FoxPro Visual Studio for easy and fast access. Selected data with queries were posted on the map using the SURFER and ODV program to be sure if the data any location errors contain. In the vertical profiles (GRAPHER and ODV are used), physical parameters are plotted according to the depth. In order to identify water masses, the best way is to visualize the temperature salinity diagrams called T-S diagrams. In these diagrams, a set of observations of temperature and salinity for successive depths at that location are plotted on a graph with temperature on the vertical axis and salinity on the horizontal axis. At the end, the seasonal data was presented visually.

The daily mean values for air temperature, precipitation, evaporation, relative humidity and air pressure were calculated by averaging 24 hourly values for each day. Time series analysis comprises methods for analyzing data in order to extract meaningful statistics and other characteristics of the data. In atmospheric sciences an anomaly time series is the time series of deviations of a quantity from some mean. A moving average is commonly used with time series data to smooth out short-term fluctuations and highlight longer-term trends or cycles. The threshold between short-term and long-term depends on the application, and the parameters of the moving average will be set accordingly.

We present the data by using the time series monthly and yearly averaged values. Monthly anomalies are drawn to yield the deviation from the mean values. Running average is applied on the yearly anomalies in order to see long-term trends. All time series for all variables are displayed in figures.

2.2.2 The model

Modeling plays an important role in modern ocean scientific research. In order to have an idea on the water exchange between the bays and the Aegean Sea, and the residence time of water in the bays, the numerical simulations are carried out with a version of Bryan-Cox model (the three-dimensional, free surface, multi-layer, z-coordinate Killworth Model). It is an explicit free surface version of the Princeton model developed by Killworth et al. (1989). The chosen model parameters are given in Table 2.2.

Table 2.2 The chosen model parameters for the wind-driven circulation experiments.

Parameters	Saros Bay	İzmir Bay	Gökova Bay
Horizontal resolution	1000 m	500 m	500 m
Number of vertical layers	11	6	11
Layer thickness (m)	5, 5, 10, 5, 15, 10, 50, 100, 100, 200 and 100 m	5, 10, 15, 15, 15 and 10 m	5, 5, 10, 5, 15, 10, 50, 100, 100, 100 and 100 m

The model was forced using the wind data obtained from the Gökçeada (for Saros Bay), Çiğli (for İzmir Bay) and Marmaris Meteorological Center (for Gökova Bay), and selected hydrological cruise data. As for most coastal areas, wind stress is a major circulation forcing mechanism. The prevailing wind direction and intensity for the bays were calculated from the long term winter period wind analysis. As a result of wind analysis it is found that the prevailing wind directions of the bays coincide circumstantially with the dominant wind directions in the cruise time. Therefore the model runs were conducted using the prevailing wind intensity and direction in order to obtain general water movements in the bays. A detailed bathymetric data set (from GEBCO-General bathymetric chart of the oceans, 2008 grided data) has allowed for the detailed model topography. To set a realistic stratification, measured Winter 2002 CTD data is prescribed in the model as an initial condition.

2.2.2.1 The Model Equations

In this section a brief description of the model equations and some important properties of the model will be given. The model equations expressing momentum, mass heat and salt conservation, and the equation of state were written in spherical coordinates.

The basic equations of the model are the following. The momentum equations read

$$u_t + \Gamma(u) - f v = -ma^{-1}\left(\frac{p}{\rho_0}\right)_\lambda + F^u \qquad (1)$$

$$v_t + \Gamma(v) + f u = -a^{-1}\left(\frac{p}{\rho_0}\right)_\phi + F^v \qquad (2)$$

where ϕ is latitude, λ is longitude, and a is the radius of the earth. The velocity field is given by (u:east, v:north, w:up). ρ_0 is a reference density, F^u, F^v represent effects of horizontal turbulence as detailed by Cox (1984).

The continuity equation is given by

$$\Gamma(1) = 0. \qquad (3)$$

Here the operator Γ is an advective operator, defined by

$$\Gamma(\mu) = ma^{-1}\left[(u\mu)_\lambda + \left(v\mu m^{-1}\right)\right] + (w\mu)_z \qquad (4)$$

and μ represents any scalar quantity.

$$m = \sec\phi \qquad (5)$$

$$f = 2\Omega\sin\phi \qquad (6)$$

$$u = \frac{a\dot{\lambda}}{m} \qquad (7)$$

$$v = a\dot{\phi} \qquad (8)$$

The local pressure p is given by the hydrostatic relation

$$p = p_s + \int_z^0 \rho g\, dz \qquad (9)$$

where p_s is the pressure at the surface (z=0). It is defined as

$$p_s = \rho_0 g \eta(\lambda, \phi, t) \qquad (10)$$

where η is the free surface elevation.

The conservation of a tracer T is given by

$$T_t + \Gamma(T) = F^T \qquad (11)$$

where F^T represents diffusive and other effects acting on T. The equation of state is

$$\rho = \rho(\theta, S, z) \qquad (12)$$

where θ is potential temperature and S is salinity. A polynomial fit was usedfor the equation of state.

The lateral boundary conditions are

$$u = v = T_n = 0 \qquad (13)$$

where n is a coordinate normal to the wall. Kinematic boundary conditions are required at the surface and at the bottom, respectively

$$w = \eta_t + uma^{-1}\eta_\lambda + va^{-1}\eta_\phi \qquad z = 0 \quad \text{at surface} \qquad (14)$$

$$w = -uma^{-1}H_\lambda + va^{-1}H_\phi \qquad z = -H \quad \text{at bottom} \qquad (15)$$

The barotropic mode is defined by

$$u = \frac{U}{H} + u' \qquad v = \frac{V}{H} + v' \qquad (16)$$

where (U,V) is the vertically integrated (barotropic) mass flux

$$U = \int_{-H}^{z} u\, dz \qquad V = \int_{-H}^{z} v\, dz \qquad (17)$$

and (u', v') is the baroclinic flow which has no depth average.

$$\int_{-H}^{z} u'\, dz = 0 \qquad \int_{-H}^{z} v'\, dz = 0 \qquad (18)$$

Integration of the continuity equation with respect to z from –H to η together with the kinematic boundary conditions and the approximation η << H gives

$$\eta_t + a^{-1}\left[mU_\lambda + m\left(Vm^{-1}\right)_\phi\right] = 0. \qquad (19)$$

This equation yields a prognostic equation for η. If the momentum equations are integrated with respect to z from –H to η and applying the boundary condition on w, one obtains

$$U_t - f\,V = -ma^{-1}gH\eta_\lambda + X \qquad (20)$$

$$V_t + f\,U = -a^{-1}gH\eta_\phi + Y \qquad (21)$$

These equations are familiar from forced linear gravity wave theory, where (X, Y) are the forcing or residual forcing terms (described by Killworth et al., 1989).

CHAPTER THREE
ANALYSIS AND RESULTS

Hourly weather data (wind speed (m/s) and wind direction (degree), air temperature (°C), precipitation (mm), evaporation (mm), relative humidity (%) and air pressure (mbar)) is obtained from the meteorological centers in the Saros, Edremit, Çandarlı, İzmir, Kuşadası, Güllük and Gökova Bays, and it is analyzed in a long term period up to 2010. The selected parameters are related to the water properties and movements in the bays. The upper part of the water column is affected by them. Wind influences the water column up to the depth of Ekman. The surface salinity is affected by precipitation and evaporation. Air temperature plays an important role for the decrease of density of water by heating and the increase of density by evaporation and cooling at the surface. Air pressure influences directly the surface of water establishing sea level difference in space. Sea level difference is the main contributor by the generation of barotropic currents in the ocean. Evaporation from the sea and humidity in the air above the surface are two important and related aspects of the phenomenon of air-sea interaction.

The general circulation patterns that are frequently seen in the bays (Saros, İzmir and Gökova Bays) are studied three dimensional and shown schematically by presenting the net currents. The coastal current is mainly driven by the wind. The all current pattern are calculated with a concept assuming the general circulation occurs in the bays under the influence of prevailing wind in order to examine the mesoscale variability in the bays and determine the path ways of the water masses entering the bays from the Aegean Sea.

Tables 3.1-3.6 give an overview of the water masses and physical water characteristics existing in the bays for spring 2001 and winter 2002. They will be explained in detail by analysis of the cruise data.

The temperature, salinity and density profiles of the bays in spring 2001 and winter 2002 have been drawn. İzmir Bay is shallower in comparison to Saros and Gökova Bays. Temperature of İzmir Bay is less than the temperature of Gökova Bay and is higher than the temperature of Saros Bay. Salt content of İzmir Bay water is more than that of Saros Bay water. The salinity values of the upper layer of Gökova Bay are comparable with the salinity values of İzmir Bay. Therefore İzmir Bay water is the densest of three bays with its cold and salty water mass. Dense water cascade is likely to flow from the İzmir Bay to the Aegean Sea. Water masses that exist in three bays are shown on θ -S diagram and tables.

The peak EMT period has taken place during the period ranging from the late ’80s to the early ’90s (Gertman et al,.2006, Veloaras and Lascaratos, 2010). It is strongly related to the rising isopycnal level found especially at the intermediate layers of the Aegean Sea. In this study, the temporal evolution of the water mass characteristics was identified in the semi-enclosed bays along the eastern coast of the Aegean Sea, during the EMT and EMT post – peak period. This was accomplished by profiles of temperature, salinity and density from several cruises in the bays extending from 1991 to 2008 (to 2010 for İzmir Bay).

3.1 Saros Bay

3.1.1 Study area

Saros Bay, which is situated at the Northern Aegean Sea (Figure 3.1), is connected to the Lemnos basin with a depth of approximately 600 m to the west. The shelf extends at a water depth of 90–120 m. The island of Gökçeada lies in the Aegean Sea just outside of Saros Bay. The length of the bay is about 61 km long and the width that connects the Bay to the Aegean Sea is about 36 km long. It receives discharge from the Meric River. Meric River is, with a length of 480 km, the longest river that runs solely in the interior of the Balkans. The drainage area and annual average discharge rate of Meriç river are 45374 km^2 and 298.8 m^3/s respectively (Yasar, 1994).

The bay is generally under the influences of northerly winds called as Etesian winds. Cold and dense water can be observed as a result of upwelling processes taking place in this area as a result of this wind. Black sea waters (BW) can be observed circumstantially at the southern part of the Saros Bay (Tokat, 2006).

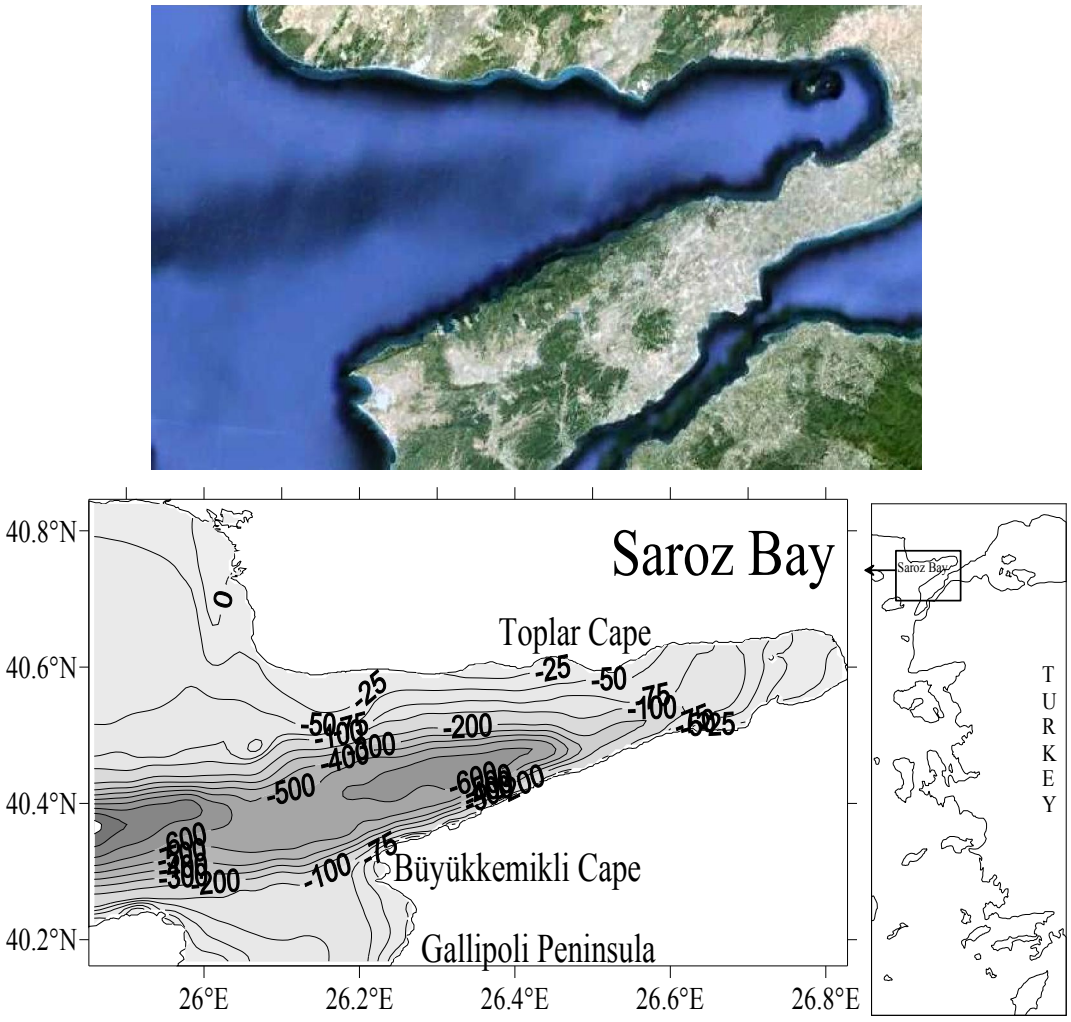

Figure 3.1 The view from Google Earth, bottom topography (from GEBCO, 2008 grided data) and location of the Saros Bay.

3.1.2 Meteorological Conditions

The meteorological data from Gökçeada Meteorological Centers for Saros Bay area were recorded as hourly and include wind speed, wind direction, air temperature, precipitation, relative humidity and air pressure. Figures 3.2-3.8 show the weather condition in the Saros Bay, Turkey.

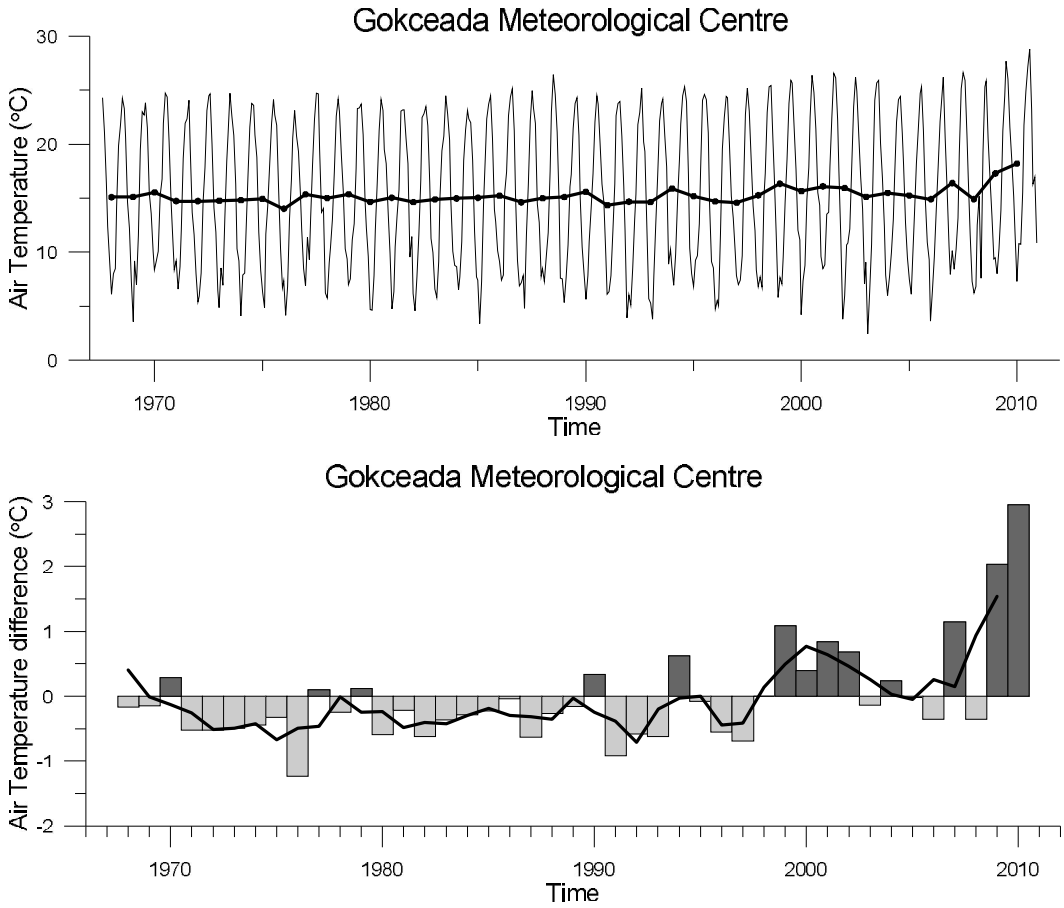

Figure 3.2 Time series of monthly average (thin line) and annual mean (thick line) air temperature (°C) (top), and yearly anomaly time series (bars) with moving averages (thick line) (bottom) for the Saros Bay.

The mean temperature average over 42 year is 15.27 °C. The temperature difference reaches approximately 20 °C between the summers and winters (Figure 3.2). The maximum value ever measured in hourly data is 49.8 °C in June 2008 and minimum value is -8.9 °C in January 2006.

The time series of yearly averaged data (Figure 3.2 bottom panel) shows slight negative air temperature anomalies before 1998, especially in 1976. Air temperature anomaly gradually increases after 1998 as a result of global warming. The negative anomalies in 1991, 1992 and 1993 are also remarkable. The air-sea interactions were strong during those years covering the major peak period and before. Exceptional

dense water formation occurs in 1996. This period is the last considerable negative air temperature anomaly taken place.

Monthly averaged precipitation data for the years 1959-2010 is shown in Figure 3.3. The maximum value ever measured in hourly data is 140.60 mm in November 1994. The average over 50 year is 7.88 mm. The rainfall is minimum in the months of late summer according to monthly averaged values.

Precipitation anomaly time series was used to detect the long-term trends calculating the deviations from mean of the all data (Figure 3.3 bottom). Precipitation plays an important role for the air-sea interactions. If precipitation increases a thin layer will be build at the surface of the ocean. It means less air-sea interactions between air and sea. Figure 3.3 shows the negative anomalies around the year 1990 suitable for strong air-sea interaction. Precipitation is not alone sufficient for the air-sea interactions. In spite of high negative anomalies in precipitation in the Saros area we can not expect formation of dense water because the increasing temperature that is more effective on the sea surface.

Hourly humidity data was retrieved from Gökçeada Meteorological Center for the years 1965-2010. Monthly averaged humidity time series is shown in Figure 3.4. The average relative humidity over 45 year is % 67.81. The humidity is minimum (% 41.16) in summer and the maximum (% 89.68) is in winter according to monthly averaged values.

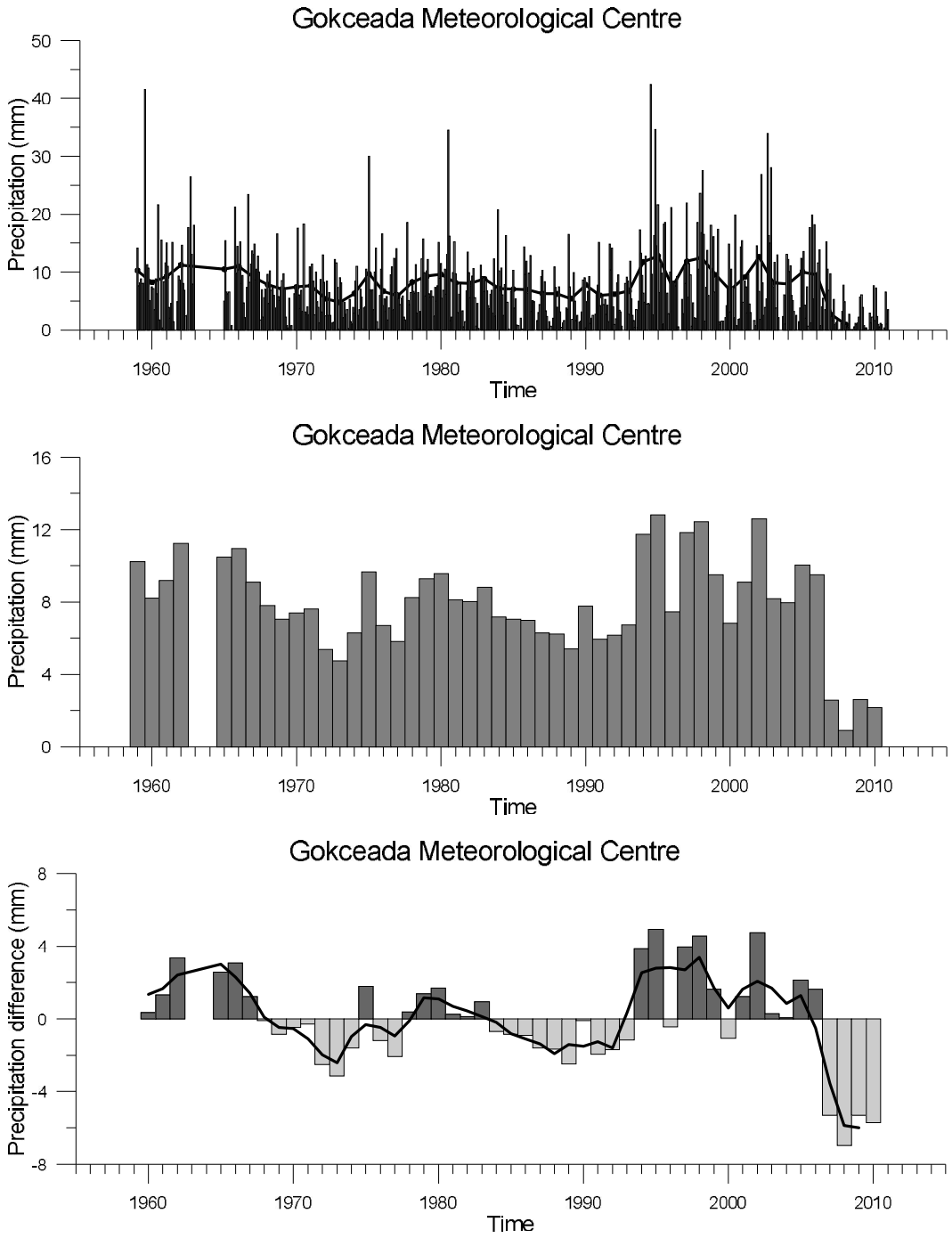

Figure 3.3 Time series of monthly averaged (top), annual mean precipitation (center) and yearly anomaly time series (bars) with moving averages (thick line) (bottom) for the Saros Bay.

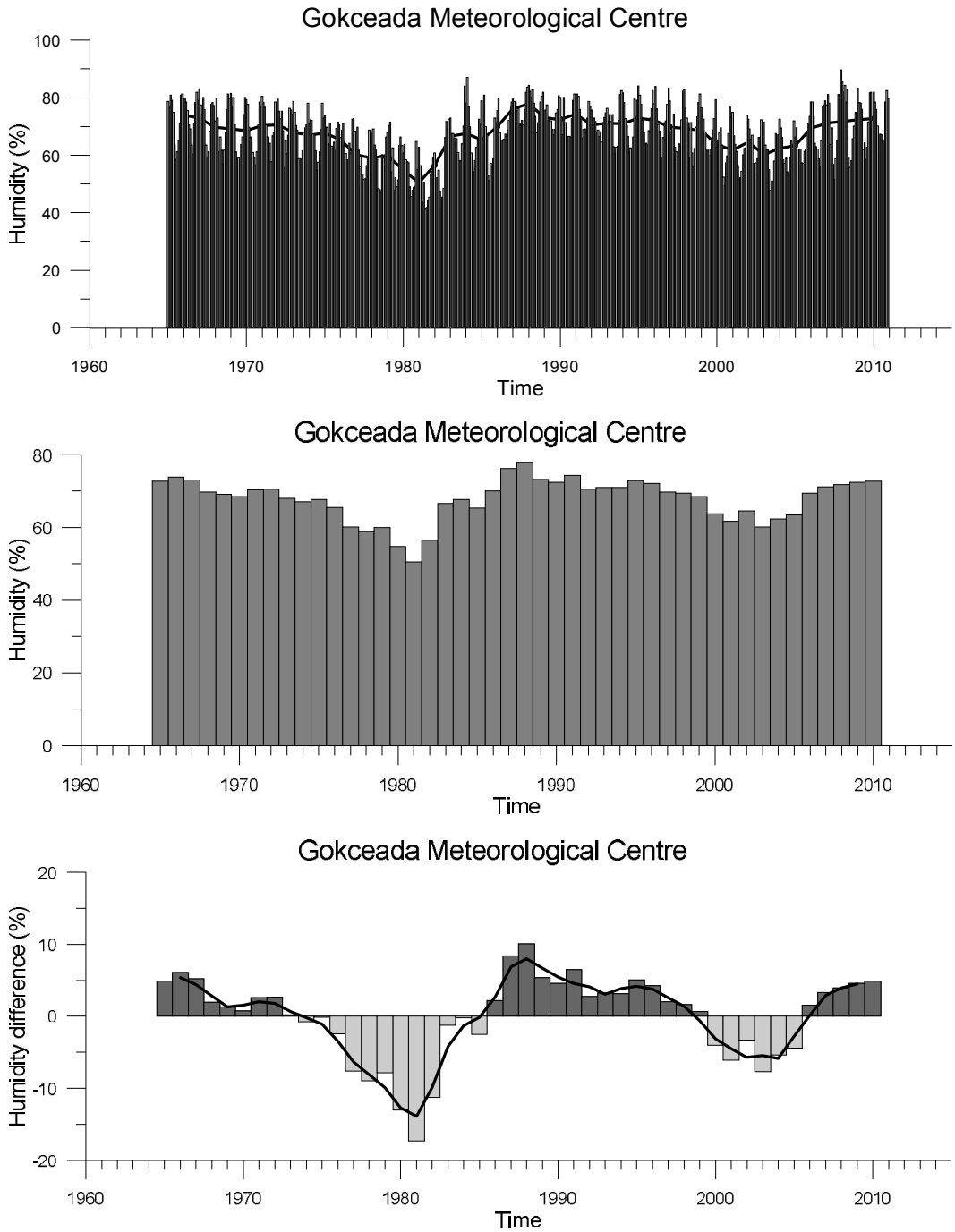

Figure 3.4 Time series of monthly averaged (top), annual mean humidity (center) and yearly anomaly time series (bars) with moving averages (thick line) (bottom) for the Saros Bay.

The anomaly time series of yearly averaged data (Figure 3.4, bottom panel) shows negative humidity anomalies between 1974-1985 and 1999-2006. The positive anomaly values are observed before 1974, between 1985 and 1999, and after 2006 probably affected by warm air.

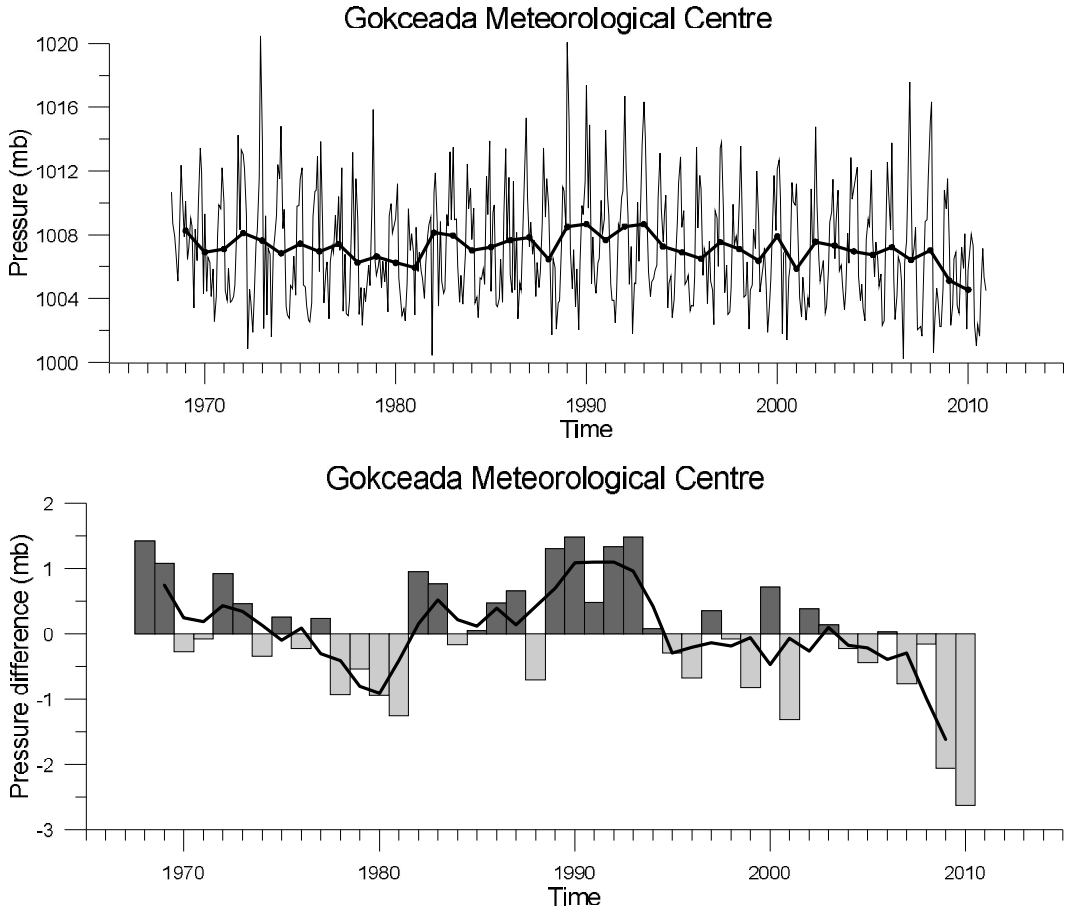

Figure 3.5 Time series of monthly average (thin line) and annual mean (thick line) pressure (mb) (top), and yearly anomaly time series (bars) with moving averages (thick line) (bottom) for the Saros Bay.

The highest pressure value ever recorded in Saros area is 1034.5 mbar in January 1973 and lowest value is 861.0 mbar in January 2004 (Figure 3.5). The average pressure over 42 year (between 1968 and 2010) is 1007.13 mbar.

Anomaly time series was used to see the deviations from the mean of the all pressure data in time. The time series of yearly averaged pressure data (Figure 3.5, bottom panel) shows very interesting evolution of high positive pressure anomalies during the years from 1989 until 1994. Any significant positive pressure anomalies have been not observed after this period. The big amount of Aegean Deep Water

(ADW) flowed over the sills of the Cretan Arc into the Levantine Basin during this time. It is the deep water formation period in the Aegean Sea.

3.1.3 Wind Analysis

In the region, wind from NNE direction dominates throughout the years with an average speed of 5.08 m/s is shown in Figure 3.6. The prevailing wind over the Saros area is NNE direction shown in the wind-rose map in Figure 3.6. Wind vectors of the monthly time series of wind speed and direction anomalies for 1968-2010, depending on the availability of the data, were constructed from hourly wind measurements in the Gökçeada Meteorological Centre. The wind vectors of the monthly prevailing wind with average wind speed values for Saros Bay data from Gökçeada Meteorological Centre is shown in Figure 3.7. The wind vectors show that the wind direction changes around the year 1989-1991. ENE direction is dominant in the year 1989-1991. The ENE wind is very important for the Saros Bay. Blowing ENE wind causes an upwelling near the coast of Büyükkemikli Cape.

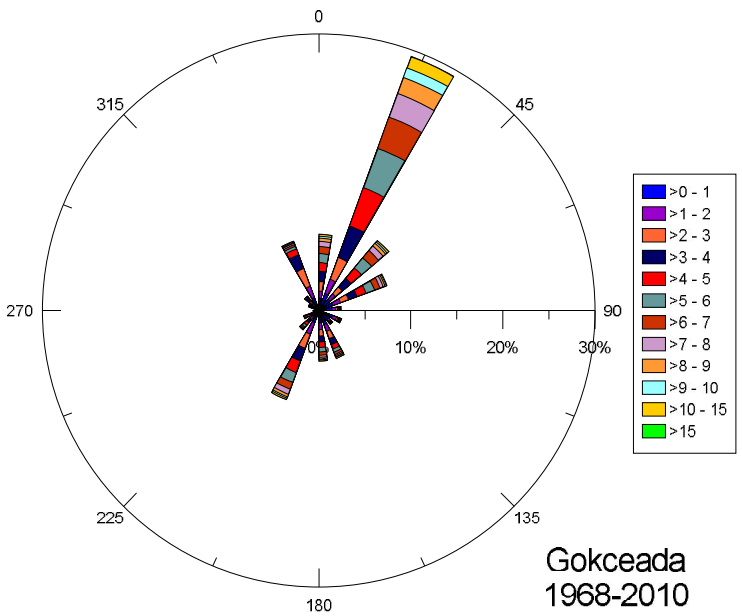

Figure 3.6 Wind chart of the prevailing wind for Saros Bay data from Gökçeada Meteorological Centre.

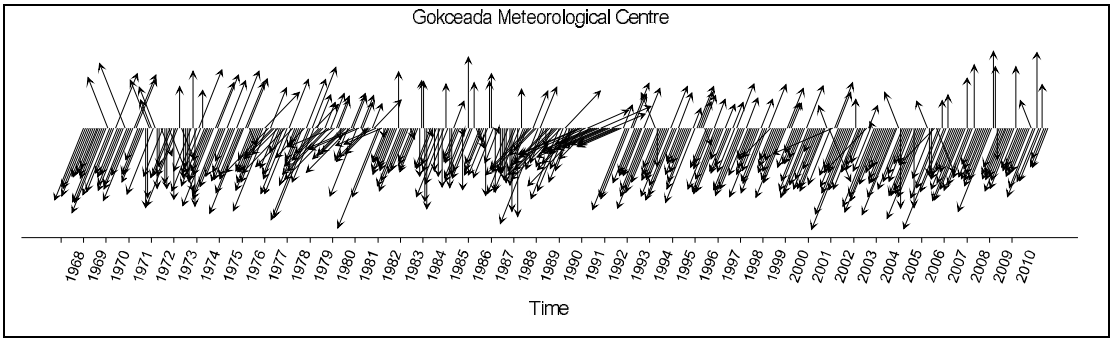

Figure 3.7 Wind vectors of the monthly prevailing wind with average wind speed values for Saros Bay data from Gökçeada Meteorological Centre. (V_{max}=21.5 m/s).

The currents need sufficient time to be established towards a certain direction. If the wind blows more than 12 hours, the establishing current will be the same direction as wind direction and the speed of current will be proportional to wind intensity for wind-driven circulation. The long duration (more than 12 hours) wind directions and speeds are selected for Saros region and shown in Figure 3.8. The prevailing wind direction is also dominant characteristics by the long duration wind (It is not always the case).

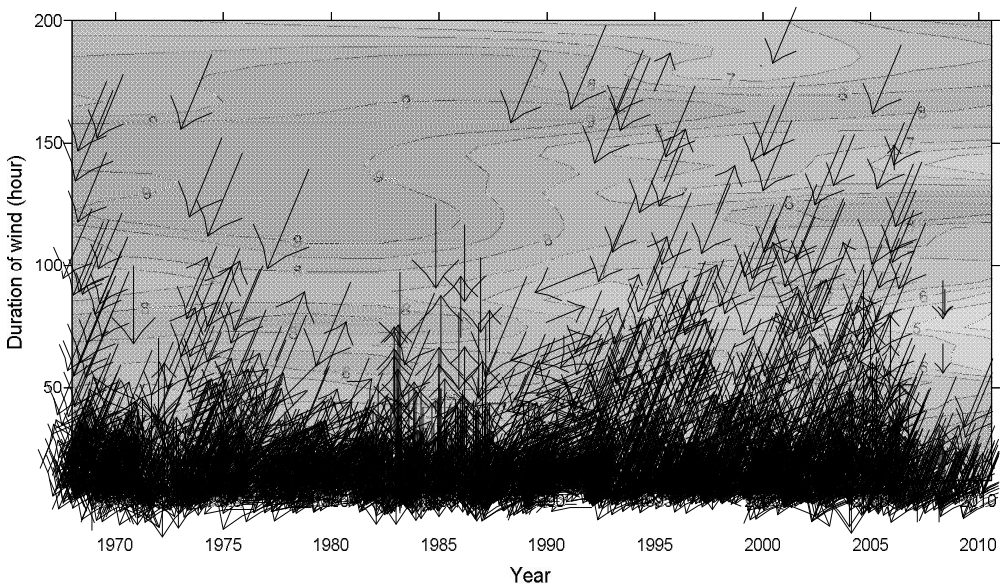

Figure 3.8 The wind vectors for the wind blowing more than 12 hours drawn on the average wind field.

3.1.4 Saros Bay General Circulation Pattern

As a result of wind analysis it is found that the prevailing wind direction of the Saros Bay (NNE) coincides circumstantially with the dominant wind direction in the winter cruise time. Therefore the model runs were conducted using the prevailing wind intensity and direction in order to obtain general water movements in the Bay. The circulation is based on the basin wide net current flowing along the water column.

The general circulation pattern that are frequently seen in the Saros bay under the influence of prevailing wind are shown schematically. Saros Bay general circulation pattern shows that the dipole structure is obvious near the southwest entrance of the bay (Figure 3.9). The cyclonic eddy of this dipole is located near Buyukkemikli Cape and is result of the upwelling process frequently taking place in this region. The water enters the bay from the North Aegean Sea in the middle of the bay to compensate the water outflowing near the coasts resulting from wind-driven circulation. It meanders into the bay. This current brings from time to time LIW to the southern coastal area across the Toplar Cape (Tokat and Sayin, 2007).

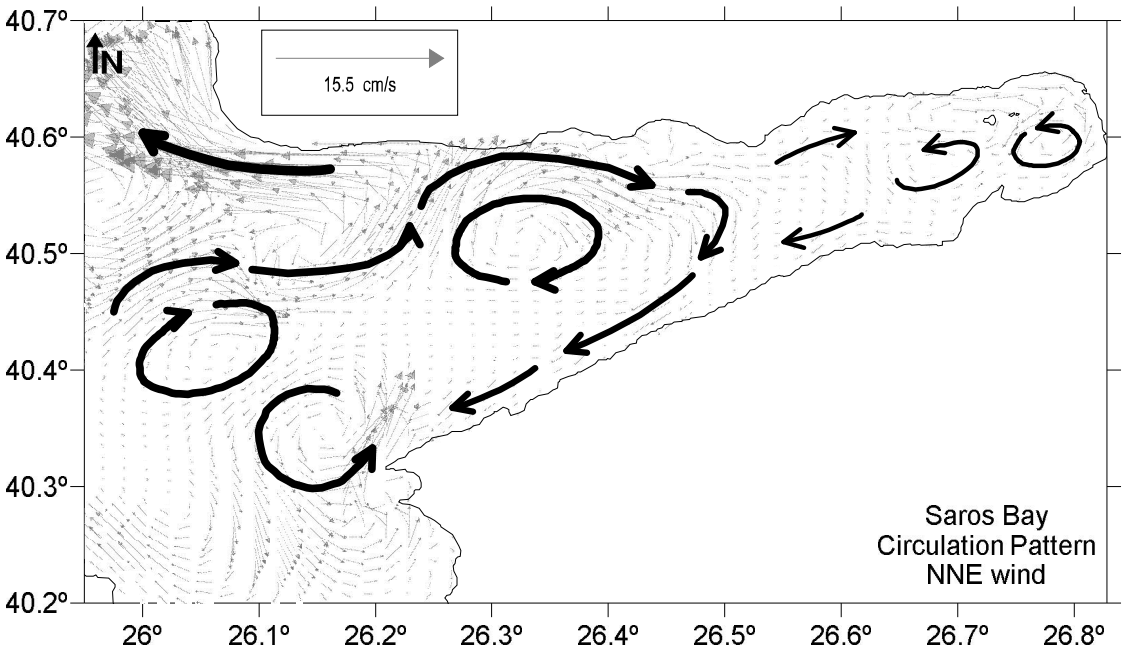

Figure 3.9 General circulation patterns of Saros Bay.

The residence or renewal time for the bays can be calculated dividing the water volume of the bays by the total water exchange through the vertical section in the entrance. The water exchange values were obtained from model run. The renewal time is important from the point of view of determining how the water exchange between the bays and the Aegean Sea extend. The residence time is 3 months for Saros Bay. The existing anticyclones found near the entrance of the Saros Bay could be responsible for the high residence time.

3.1.5 Time Series of the Saros Bay

The Saros Region is chosen to represent the northern shallow area of Aegean Sea under the influence of strong northerly winds which cause an upwelling along the Turkish coast. From time to time, occurring upwelling in the Saros Bay makes contribution for the density increase in the water column. It takes place in summer 1991 and spring 2001 (Figure 3.10).

Remarkable thing is the blowing wind from NE direction (prevailing wind direction for the Saros area) that causes the occurrence of upwelling in the Saros Bay. There have been no new severe deep–water producing episodes in the Aegean Sea since 1994. But some minor quantities of deep-water seem to have been produced in 1991 and 2001 already registered by Roether et al. (2007) and Veloaras and Lascaratos (2010). The depths of water column by CTD measurements are not same. Therefore it is not easy to conclude how the isopycnal levels developed before 1993 winter (Figure 3.10).

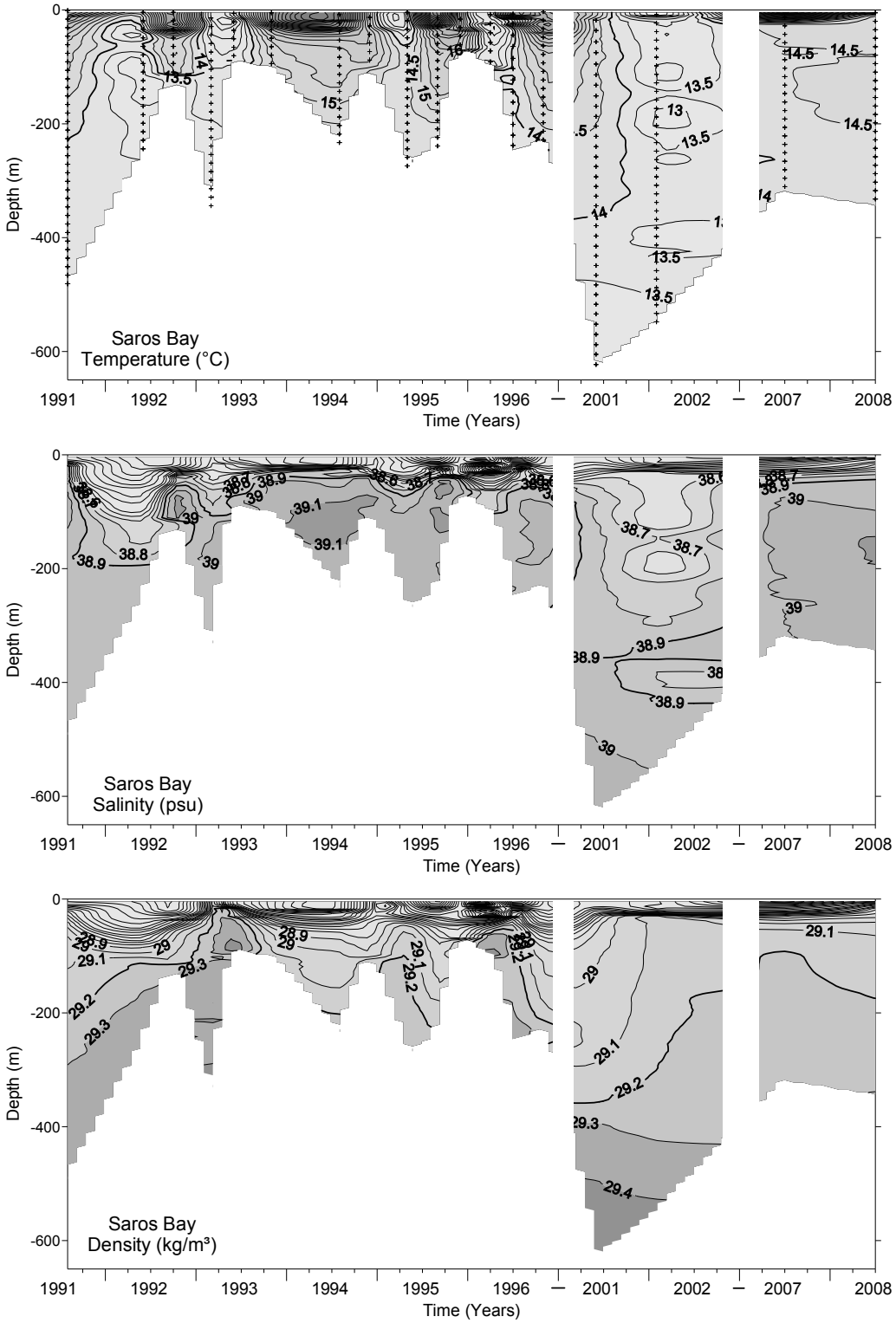

Figure 3.10 Temporal evaluations of temperature, salinity and density fields of Saros region starting from summer 1991 up to summer 2008. The areas in white represent where data was not collected.

The σ_θ density levels 29.0, 29.1 and 29.2 kg/m^3 in 1994 are comparable with the levels in main deep water formation episode. Density increases in the upper layers because of the decreasing in temperature, and isopycnals 29.1–29.3 start to shoal by up to 250 m from winter 1993 until the end of spring 1995. It is consistent with the study of Sayin & Besiktepe (2010). However in their study the time series were until 1996. Although the very cold weather condition was registered in spring 1996, the density levels continued to decrease gradually. The main reason for this decrease was the existing low saline water in the water column. It occupies the depth of 100 m to 400 m in the bay after spring 2001. The relaxation period continued until spring 2001, and some upper layer density levels started to rise namely the σ_θ = 29.1 kg/m^3 density level was about 250 m in spring 2001 and rises approximately up to 50 m in winter 2002. This level was same as the level detected in 1993. The lower layer isopycnal levels did not change much, other than a slight increase in spring 2001. The saline water was observed again in the Bay first in summer 2007 with a rising 29.2 kg/m^3 isopycnal level near the surface up to 100 m. This level is comparable with the levels forming during the major deep-water formation episode in the Aegean Sea (1993).

3.1.6 Hydrographic Characteristics of the Saros Bay

3.1.6.1 Spring 2001

The water properties of the bay were analyzed using the data retrieved from 26 stations during spring 2001 cruise (12-16.05.2001) (Figure 3.11- 3.14).

The NNE wind is the dominant wind in cruise time in spring 2001 and also in winter period in general. The lasted wind from NNE over the Saros area causes an upwelling in the southeastern part of the Saros Bay. Therefore the surface layer is occupied by a water mass slightly colder than its environment. This upwelling water is seen from the horizontal distribution and vertical sections with its high salinity and density in the surface layer (Figure 3.13 and 3.14).

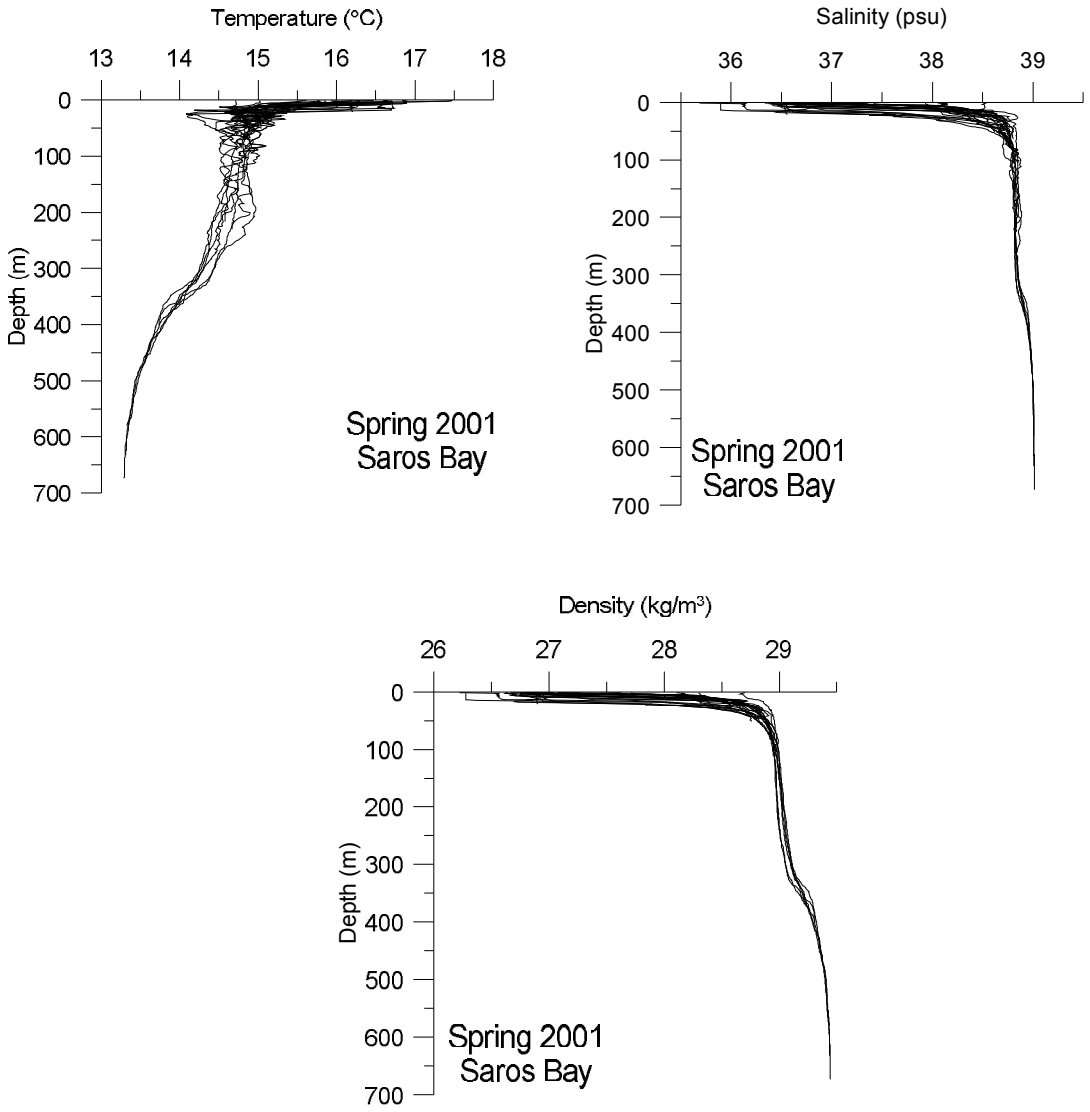

Figure 3.11 Temperature, salinity and density profiles of Saros bay in spring 2001.

Besides Saros Upwelling Water, there are other water masses also that exist in the Saros Bay; LIW, Saros Intermediate Water (SIW) and NAgDW. These mentioned all water masses were observed in spring 2001 in the Bay and are shown on the θ -S diagram (Figure 3.12) and Table 3.1. BSW can be determined in the offshore side of the Çanakkale Strait with low salinity (31.5 psu) and low density (23 kg/m^3) and spreads to the west and then slightly routes to the north. But can not enter the Saros Bay in spring 2001.

The strong upwelling water pushes the LIW to the south and west hinders it entering into the Bay more from the southwest corner. LIW is determined from the

θ-S diagram and the vertical section with its rich salt content and warmer water characteristics in the eastern part of the upwelling region in the depth of 200 m across the Toplar Cape.

The vertical profiles show that the permanent thermocline occurs between 300-400 m. The values do not change much down to this depth and approach the values of NAgDW.

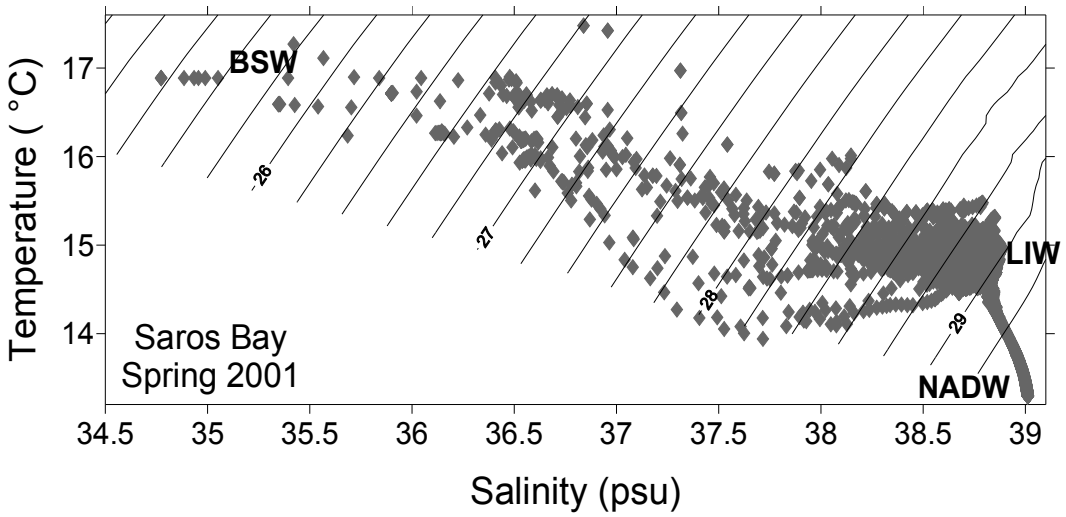

Figure 3.12 θ-S diagram of spring 2001 (Saros Bay).

Table 3.1 The water masses existing in the Saros bay and their range in spring 2001.

		Spring 2001		
	Water mass	Temperature (°C)	Salinity (psu)	Density (kg/m³)
SAROS BAY	SUW	< 15.0	> 38.68	> 28.3
	SIW	14.35-14.8	38.8-38.85	28.97-29.08
	NAg DW	13.29	39.01	29.44
	BSW	----	----	----
	LIW	14.95	38.89	28.98

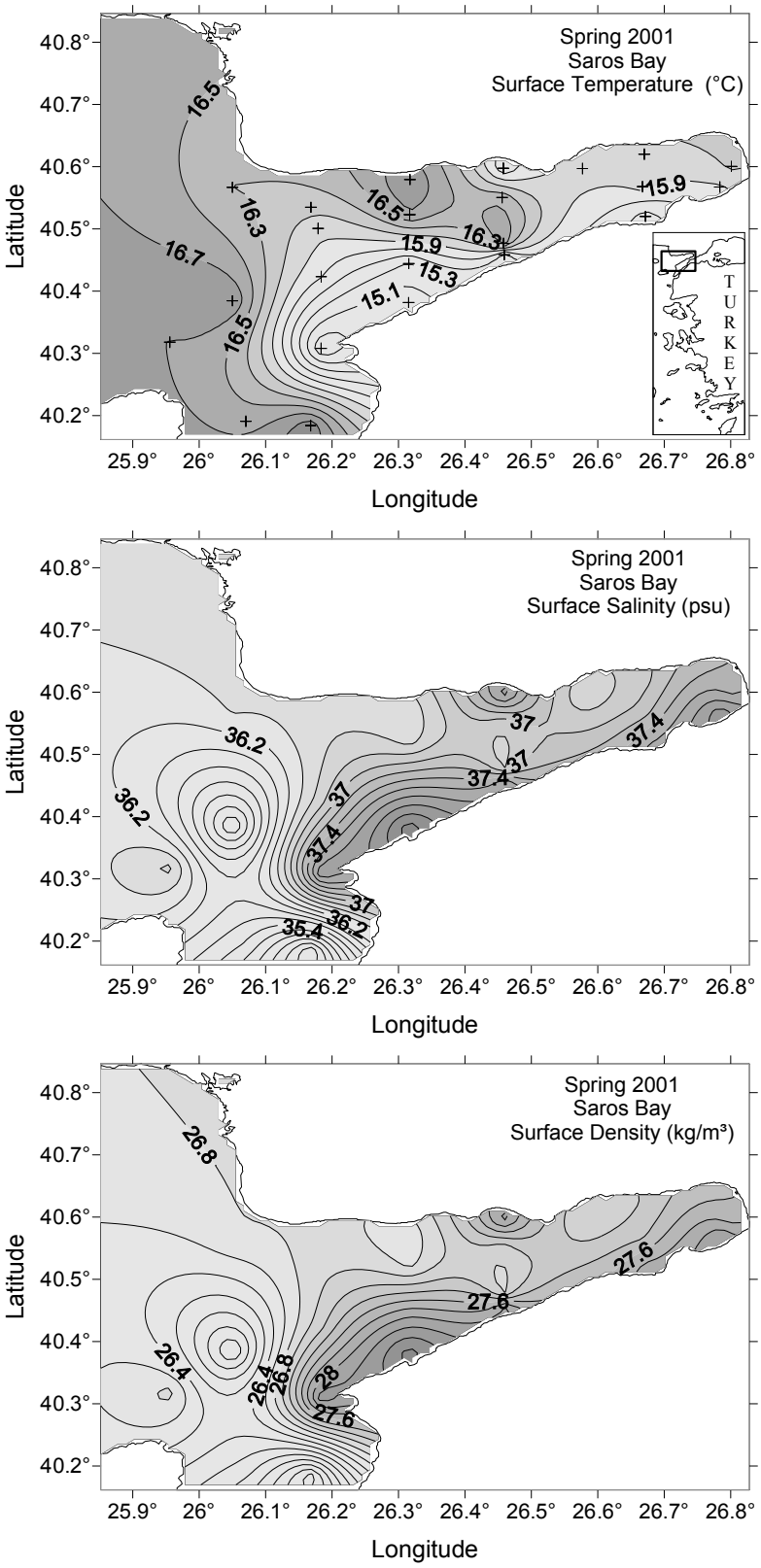

Figure 3.13 Horizontal temperature, salinity and density distributions in the Saros bay. The location of stations are shown on the map above upper left corner.

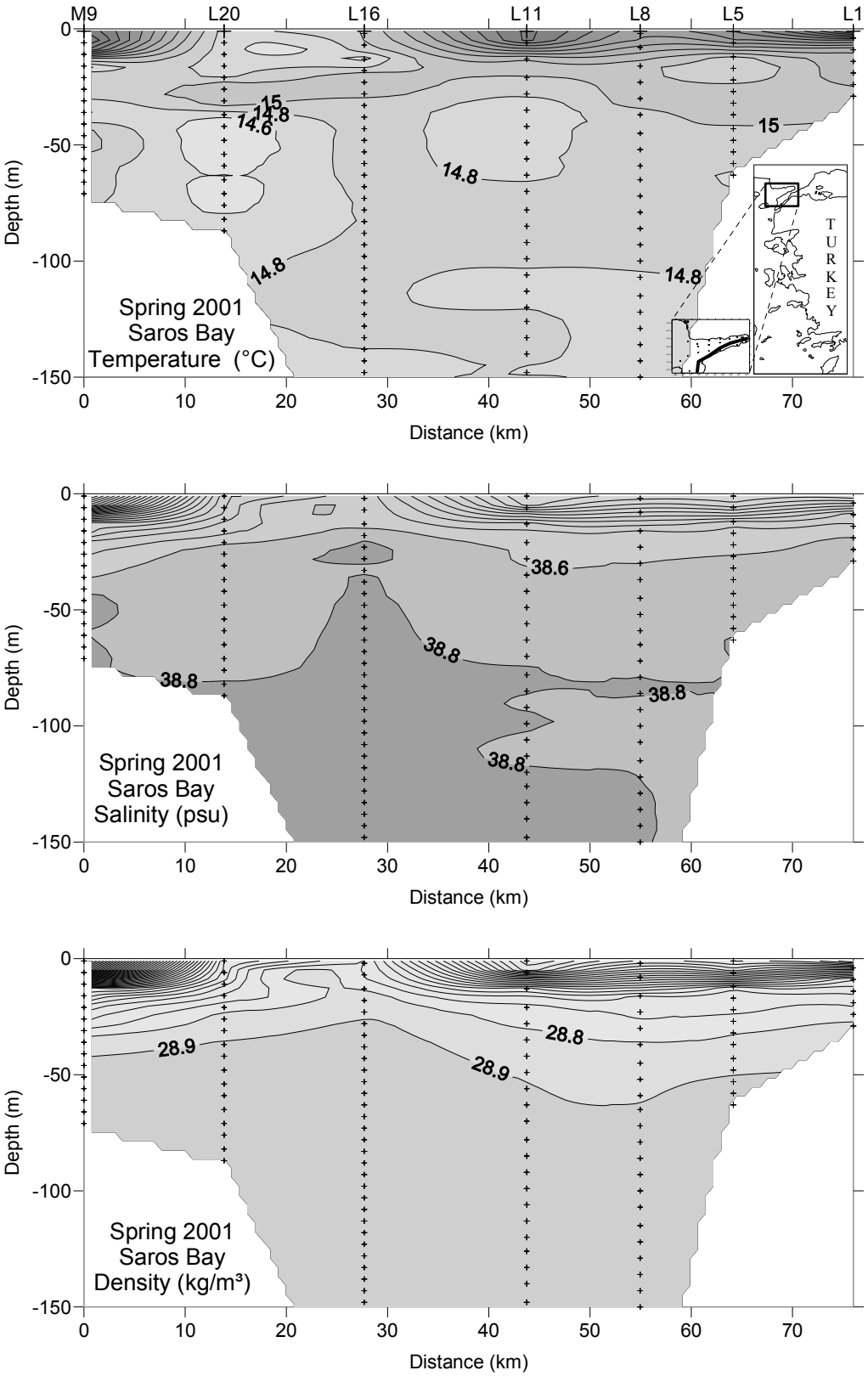

Figure 3.14 The temperature, salinity and density vertical section (0-150 m) of Saros Bay in spring 2001.

3.1.6.2 Winter 2002

The data obtained from 25 CTD stations during winter 2002 cruise (18-29.02.2002) have been examined (Figure 3.15-3.18).

BSW is identified by its very low salinity and, consequently, low density. Colder and less saline BSW from the Çanakkale Strait propagates to the north. It occupies the northern part of the Gallipoli Peninsula (not shown). The increasing buoyancy through the BSW results in the increase of stratification and decrease of vertical diffusion in the Saros area.The thickness of the BSW in the Saros Bay is about 15 m (Figure 3.18). It increases on the way to the north and mixes with the subsurface Levantine Sea water mass. Although it is slightly detectable the Levantine water reaches Saros Bay and exists between BSW and SIW. The Levantine water replaces with the subsurface Saros Bay water mass more in the direction to the north (Velaoras and Lascaratos, 2010).

The wind condition was variable during cruise time in winter 2002. A lasting northeasterly wind is needed in order to maintain an upwelling process in the north of the Gelibolu Peninsula near the Büyükkemikli Cape. Because of any lasting wind during cruise winter 2002, BSW was able to fill the area of northern side of Gelibolu Peninsula. The topographic slope makes it easier for BSW to flow to the north. BSW is thus accumulated, at the southwest corner of the Bay and cannot go any further to the inner part.

The surface temperature is slightly lower than the subsurface temperature. The difference between the surface and subsurface layer temperatures is about 2-3 ºC. NAgDW existed in the Saros Bay is only 0.35 ºC cooler than the North Aegean Sea Intermediate Water (NAgIW). The density value of 29.4 kg/m^3 found at 573 m deep is more close to the entrance.

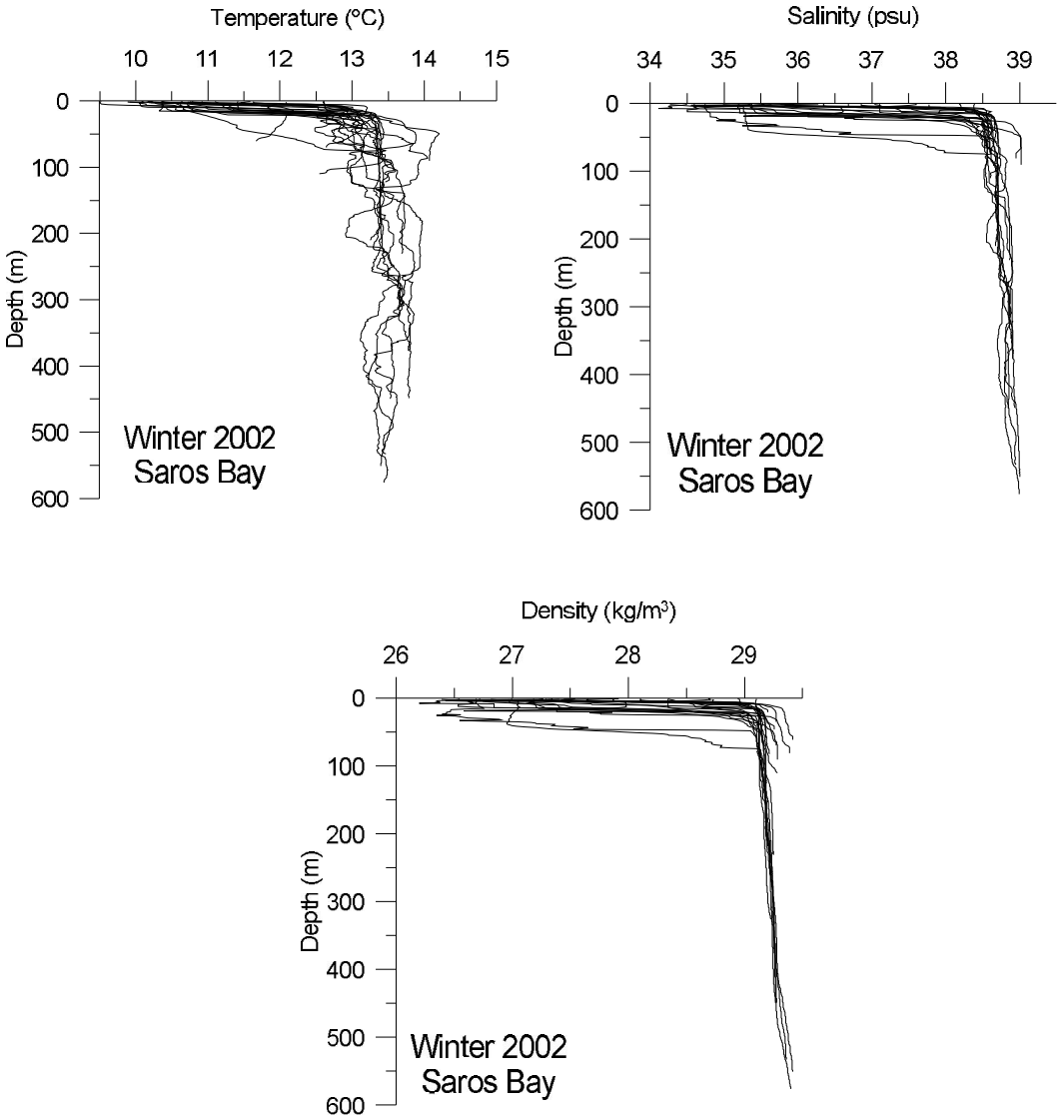

Figure 3.15 Temperature, salinity and density profiles of Saros bay in winter 2002.

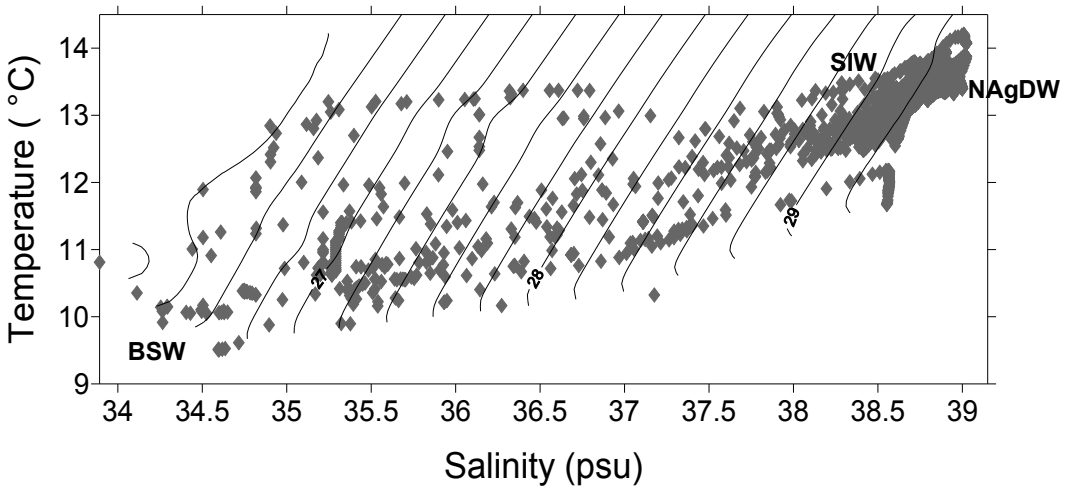

Figure 3.16. θ-S diagram of winter 2002 (Saros Bay).

Table 3.2. The water masses existing in the Saros bay and their range in winter 2002.

		Winter 2002		
	Water mass	Temperature (°C)	Salinity (psu)	Density (kg/m³)
SAROS BAY	SUW	----	----	----
	SIW	13.26-13.94	38.67-38.9	29.18-29.27
	NAgDW	13.39	39.0	29.41
	BSW	9.52-10.10	34.26-34.64	26.36-26.75
	LIW	----	----	----

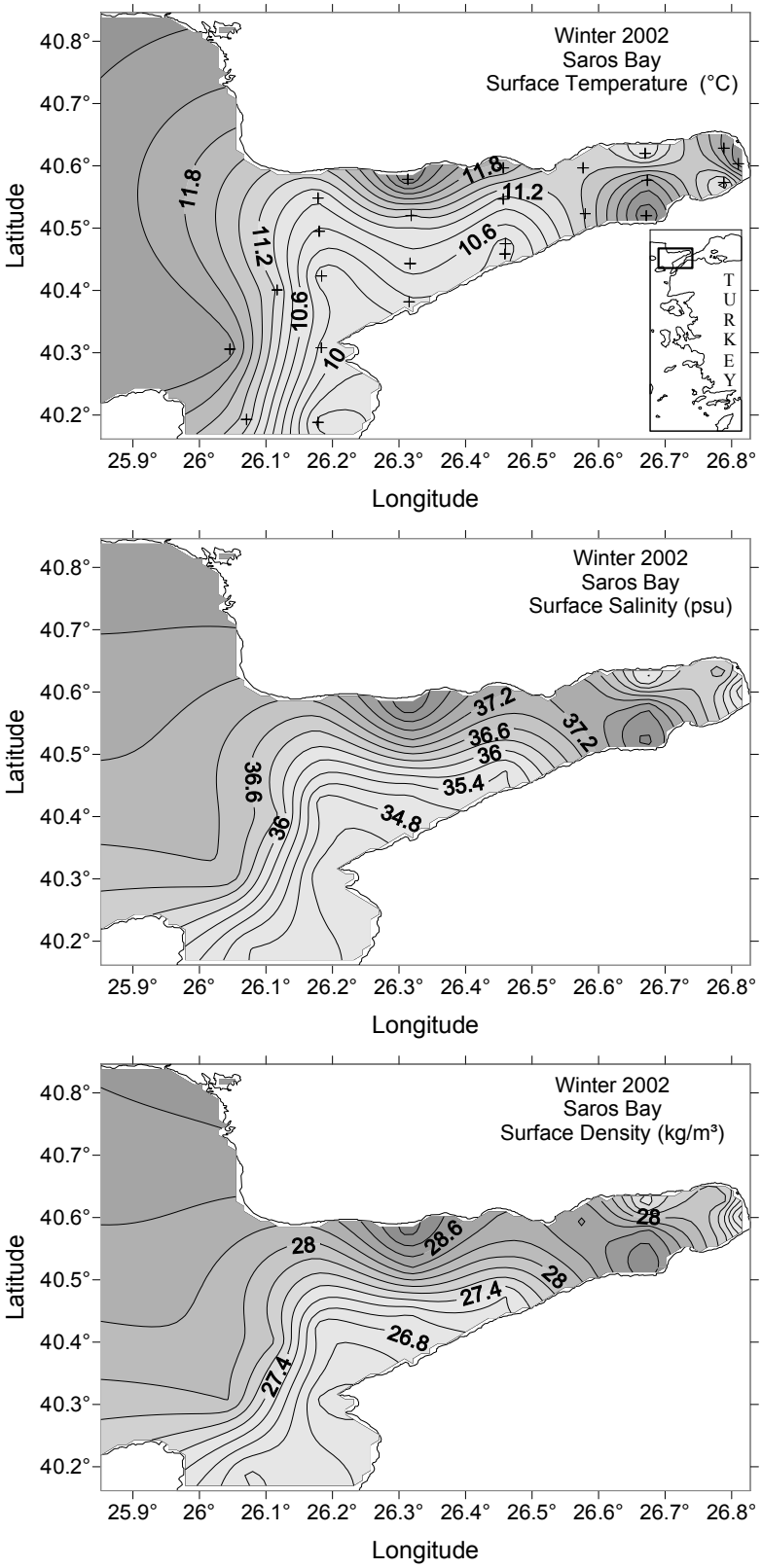

Figure 3.17 Winter 2002 surface (5 m) (upper panel) temperature, salinity and density field.

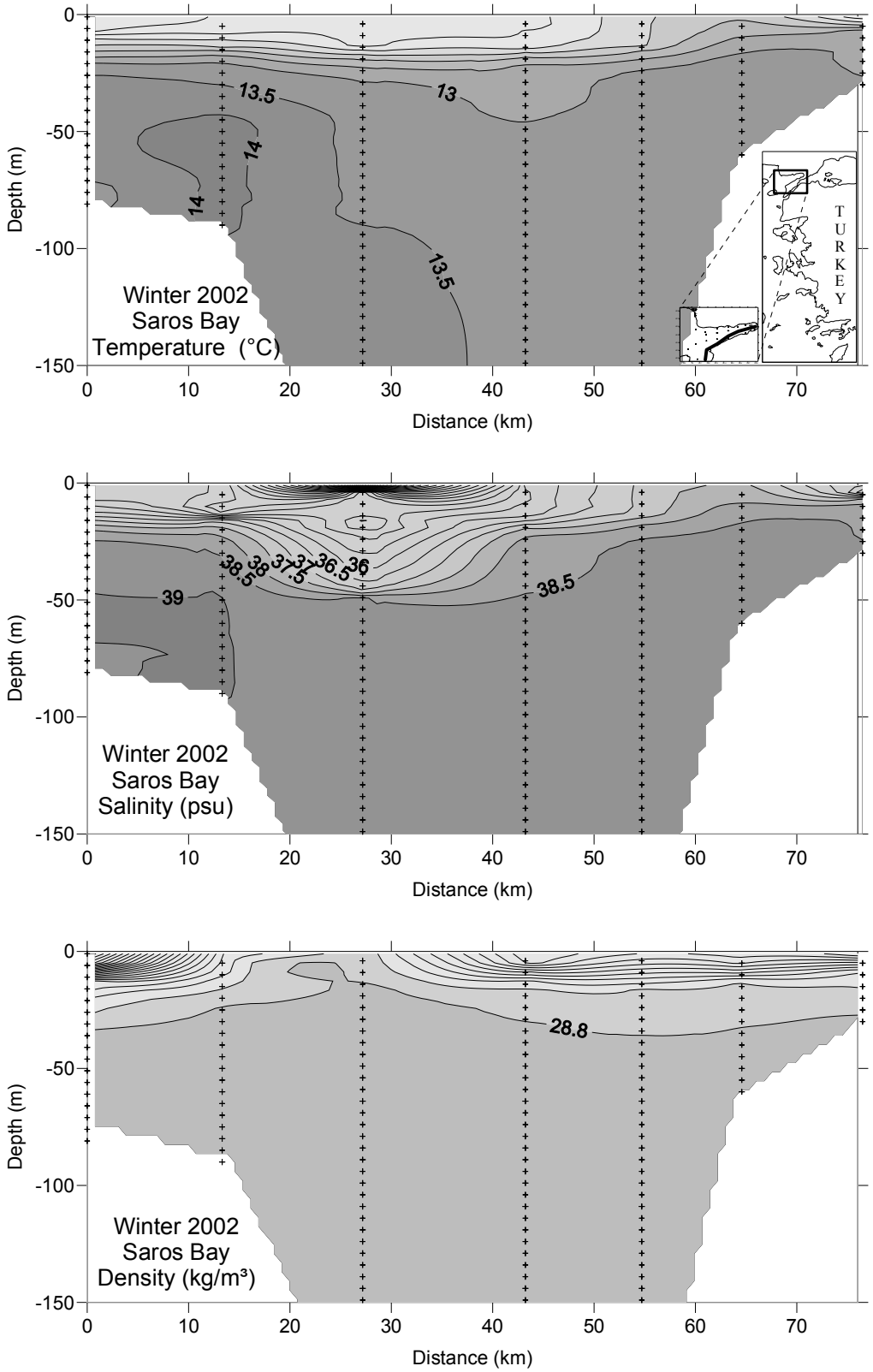

Figure 3.18 The temperature, salinity and density vertical section (0-150 m) of Saros Bay in Winter 2002.

3.2 Edremit Bay

3.2.1 Study Area

Edremit Bay, which is located on the northern Aegean part of the western Anatolia, is connected to the Aegean Sea with Müsellim Strait to the west and Dikili Strait (or Midilli Strait) to the south (Figure 3.19).

Edremit has got the Mediterranean climate, the summers are hot and dry, and winters are warm and rainy. However, at higher elevations from the coast line it changes in to Mediterranean-like mountain climate.

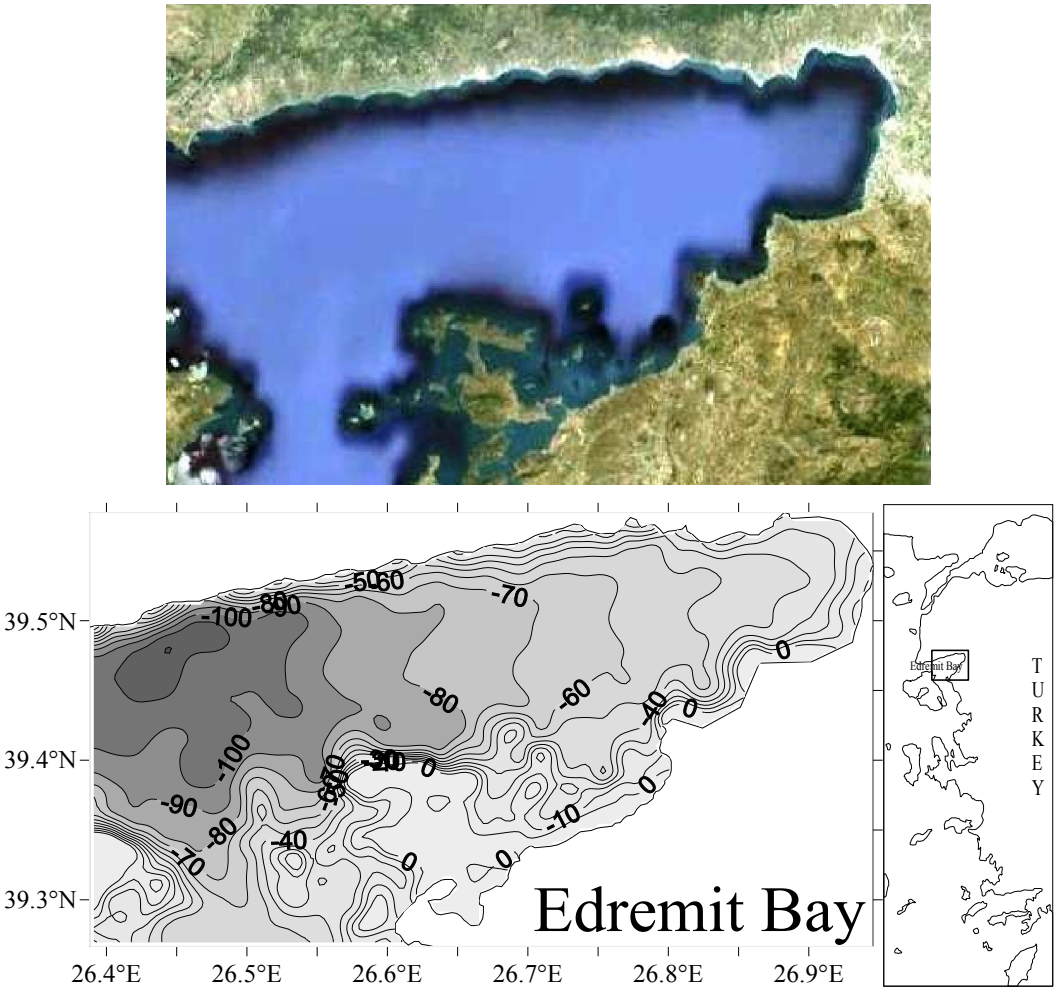

Figure 3.19 The view from Google Earth, bottom topography (from GEBCO, 2008 grided data) and location of the Edremit Bay.

3.2.2 Meteorological Conditions

We assume that the meteorological data obtained from Edremit Meteorological Center is representative for the Edremit Bay region. Hourly weather data including wind speed, wind direction, air temperature, precipitation, evaporation, relative humidity and air pressure were retrieved. Figure 3.20-3.27 show the weather measurements in the Edremit Bay, Turkey.

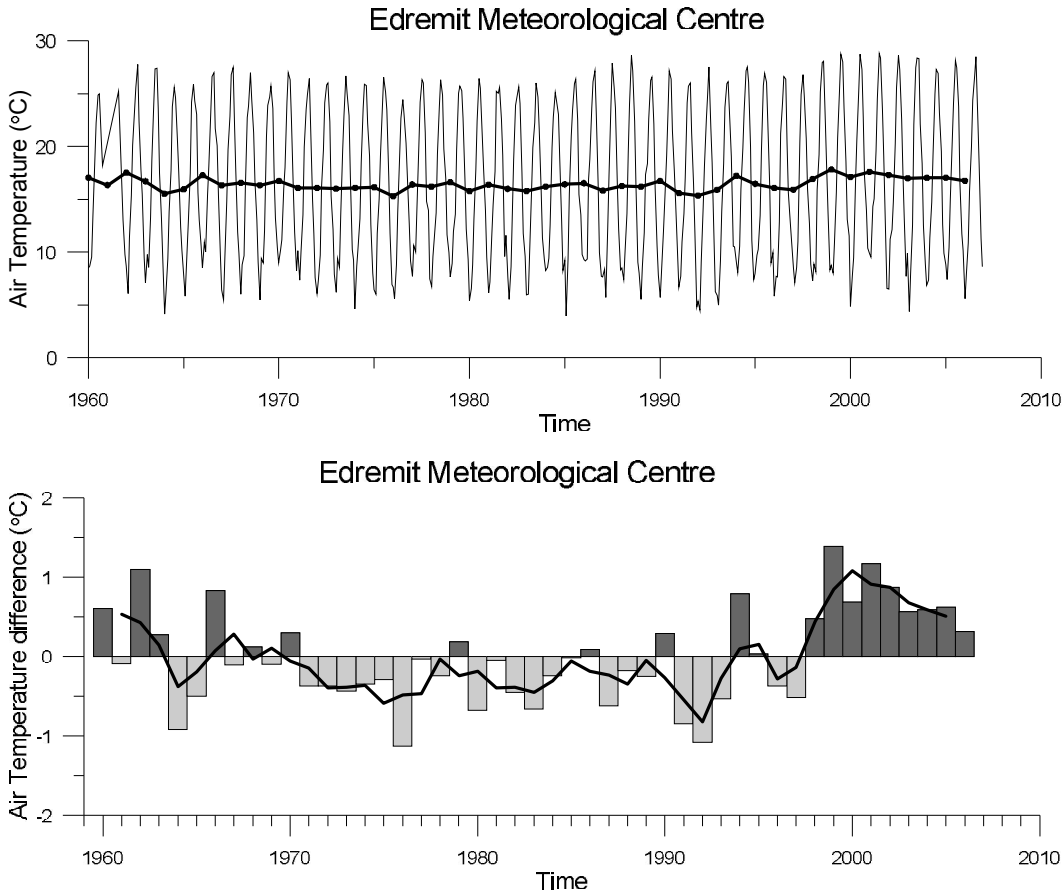

Figure 3.20 Time series of monthly average (thin line) and annual mean (thick line) air temperature (°C) (top), and yearly anomaly time series (bars) with moving averages (thick line) (bottom) for the Edremit Bay.

The annual mean temperature ranges from 15,5°C (in 1976) to 18°C (in 2009). The temperature difference reaches approximately 20 °C between the summers and winters (Figure 3.20). The maximum value ever measured in hourly data is 42.8 °C

in July 2000 and minimum value is -8.0 °C in January 1973. The average over 46 year (between 1960 and 2006) is 16.43 °C.

The time series of yearly averaged data (Figure 3.20 bottom panel) shows slight positive air temperature anomalies before late 1970s and after negative anomalies up to 1998. Air temperature anomaly gradually increases after 1998 as a result of global warming. The air temperature has negative anomalies again in the years of around major dense water formation period and before (1991,1992 and 1993).

Hourly precipitation data is retrieved from Edremit Meteorological Center. Monthly averaged precipitation data for the years 1959-2010 is shown in Figure 3.21. The maximum value ever measured in hourly data is 134.10 mm in October 2008. The average over 51 year is 7.31 mm. The rainfall is minimum in the months of late summer and early fall according to monthly averaged values.

The precipitation anomalies (Figure 3.21 bottom) show similar trend as air temperature with an exception in the last years after 2005. Less precipitation is expected for the years starting from 1988 till 1994. Figure 3.21 shows negative anomalies between the years 1988 and 1991. Starting from 1991 the precipitation indicates slightly positive anomalies till the beginning of the relaxation period of 1995.

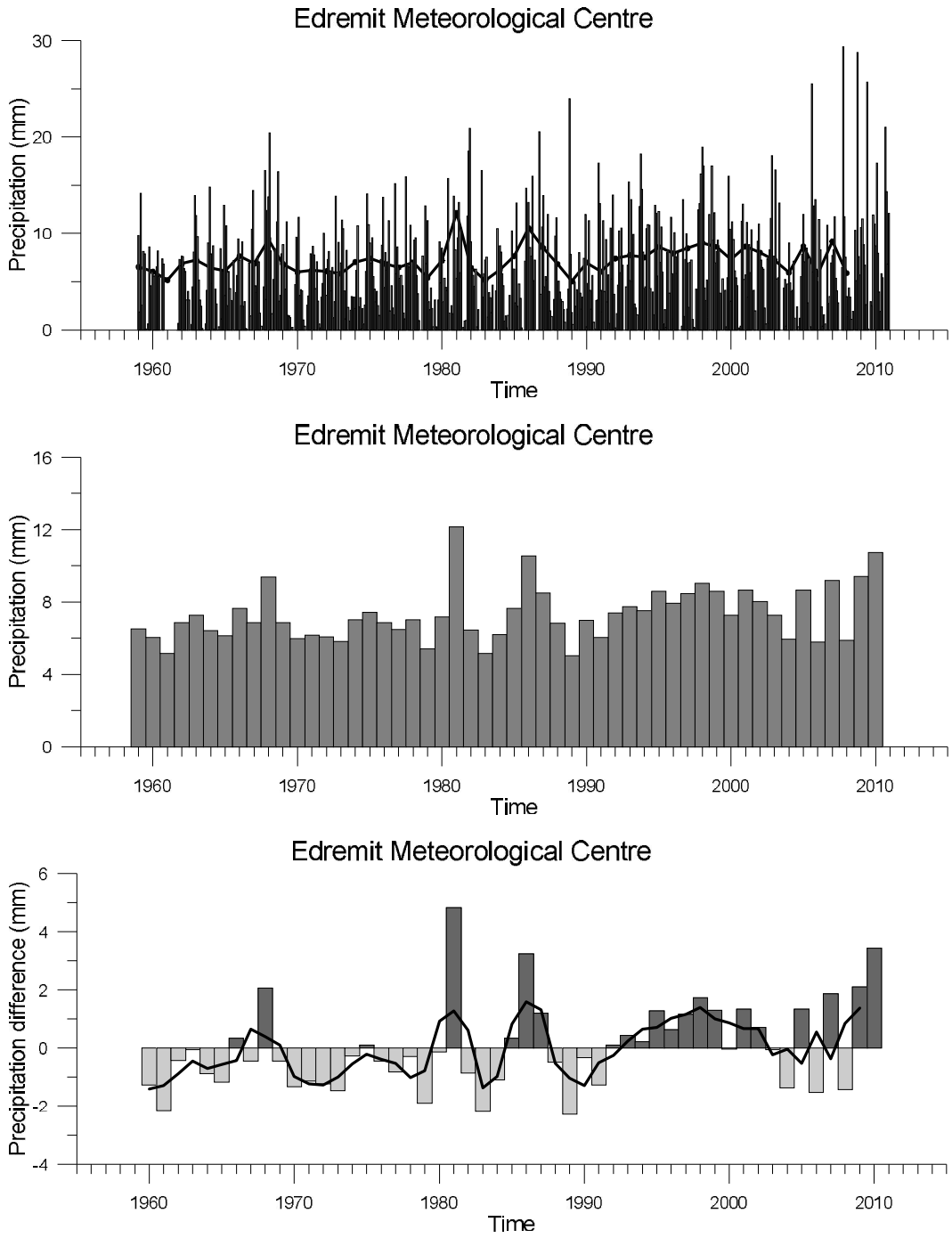

Figure 3.21 Time series of monthly averaged (top), annual mean precipitation (center) and yearly anomaly time series (bars) with moving averages (thick line) (bottom) for the Edremit Bay.

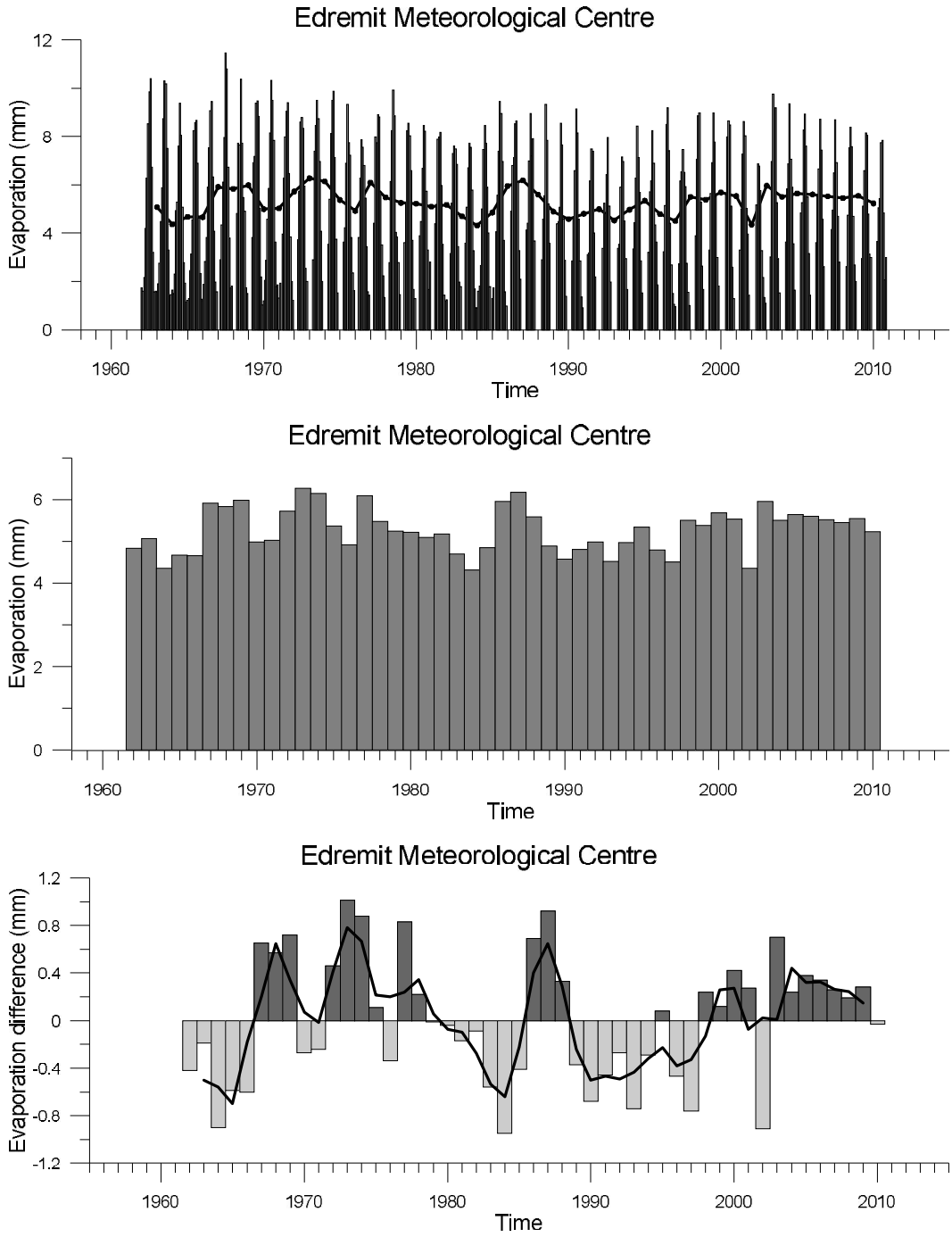

Figure 3.22 Time series of monthly averaged (top), annual mean evaporation (center) and yearly anomaly time series (bars) with moving averages (thick line) (bottom) for the Edremit Bay.

Hourly evaporation data is retrieved from Edremit Meteorological Center for the years 1961-2010. Monthly averaged values are shown in figure 3.22. The maximum evaporation value ever measured in hourly data is 17.6 mm in July 1972. The average over 49 year is 5.26 mm. The evaporation is minimum (0.9 mm) in winter and the maximum (11.46 mm) is in summer according to monthly averaged values.

Time series are used to see long-term trend in the evaporation data. Anomaly time series was used the time series of deviations of a quantity from mean of the all data (Figure 3.22 bottom). Evaporation data shows negative anomalies during major peak time before and after between the years 1989 and 1994. Because of the warming air temperature positive anomalies by evaporation data are observed with an exception in 2005.

Hourly humidity data is retrieved from Edremit Meteorological Center for the years 1959-2010. Monthly averaged humidity time series is shown in figure 3.23. The average relative humidity over 51 year is % 60.27 mm. The humidity is minimum (% 35.1) in summer and the maximum (% 83.36) is in winter according to monthly averaged values.

The anomaly time series of humidity shows 20 years period oscillations making negative peak values around 1980 and 2000 (Figure 3.23, bottom panel).

The highest pressure value ever recorded in hourly data in Edremit area is 1038.8 mbar in January 1989 and lowest value is 979.0 mbar in January 1968. The average over 45 year (between 1965 and 2010) is 1012.81 mbar (Figure 3.24).

The anomaly time series of yearly averaged pressure data (Figure 3.24, bottom panel) show very interesting evolution of high positive pressure anomalies during the years from 1989 until 1994 as seen by Saros Bay time series. Positive pressure anomalies can be related to air-sea interactions changing mainly in the deep water formation period in the Aegean Sea.

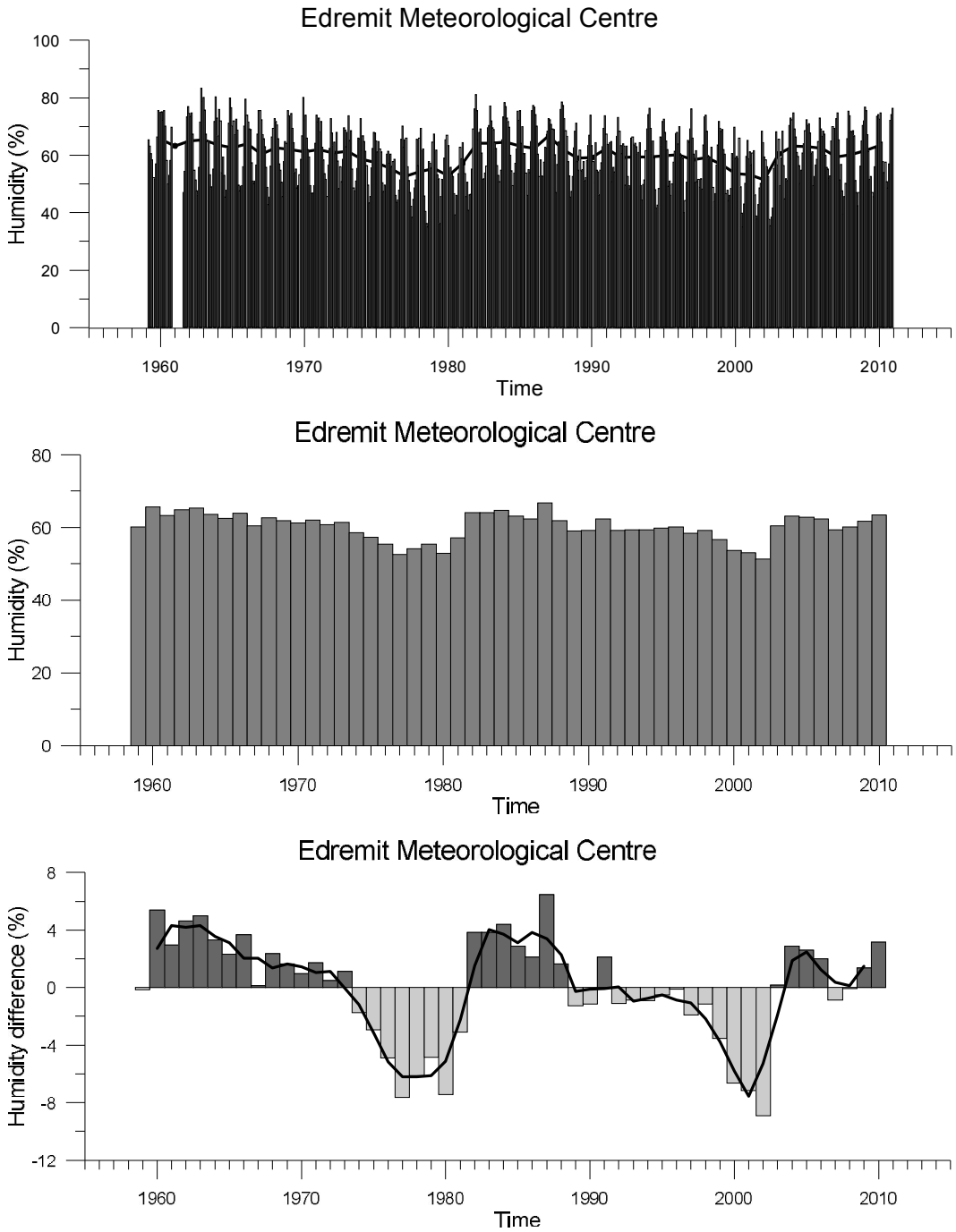

Figure 3.23 Time series of monthly averaged (top), annual mean humidity (center) and yearly anomaly time series (bars) with moving averages (thick line) (bottom) for the Edremit Bay.

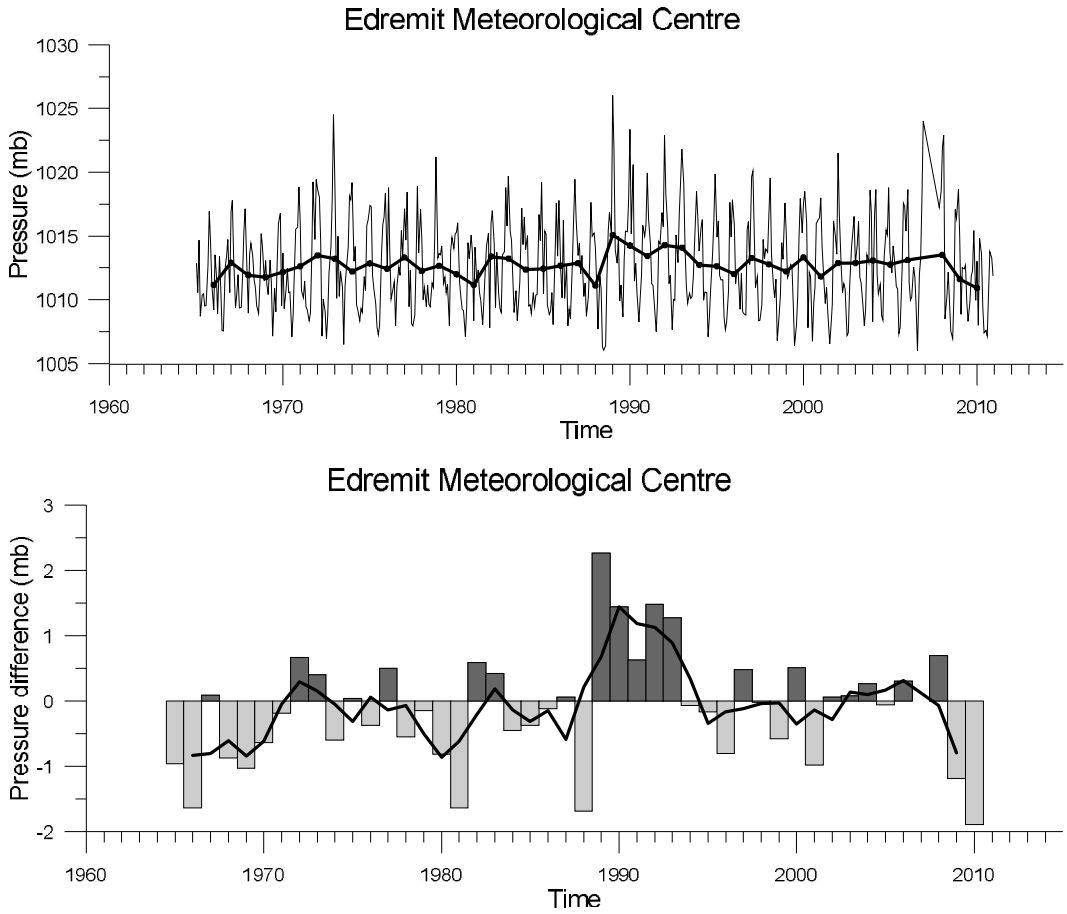

Figure 3.24 Time series of monthly average (thin line) and annual mean (thick line) pressure (mb) (top), and yearly anomaly time series (bars) with moving averages (thick line) (bottom) for the Edremit Bay.

3.2.3 Wind Analysis

In the region, wind from ENE direction dominates throughout the years with an average speed of 2.76 m/s is shown in Figure 3.25.

The prevailing wind over the Edremit area is ENE direction shown in the wind-rose map in Figure 3.25. Wind vectors of the monthly time series of wind speed and direction anomalies for 1966-2010, depending on the availability of the data, were constructed from hourly wind measurements in the Edremit Meteorological Centre. The wind vectors of the monthly prevailing wind with average wind speed values for Edremit Bay data from Edremit Meteorological Centre is shown in Figure 3.26. The

wind vectors show that the wind direction changes around the year 1966-1969, 1978-1983 and after 2006.

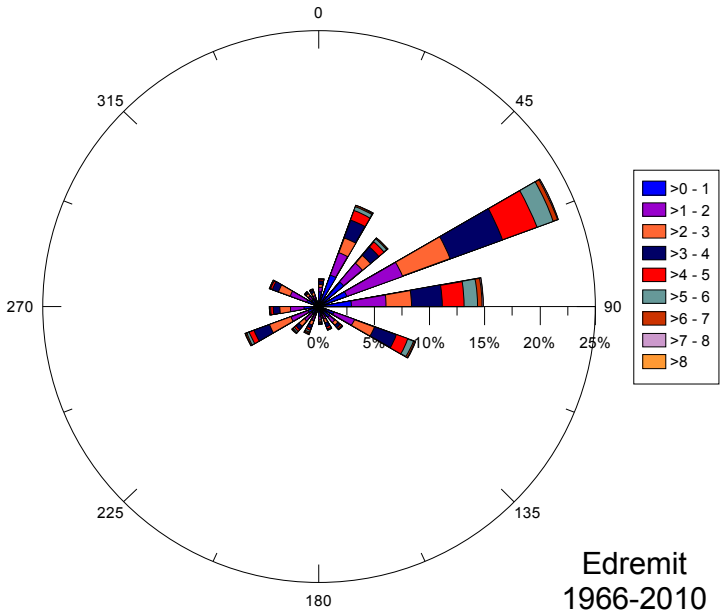

Figure 3.25 Wind chart of the prevailing wind for Edremit Bay data from Edremit Meteorological Centre.

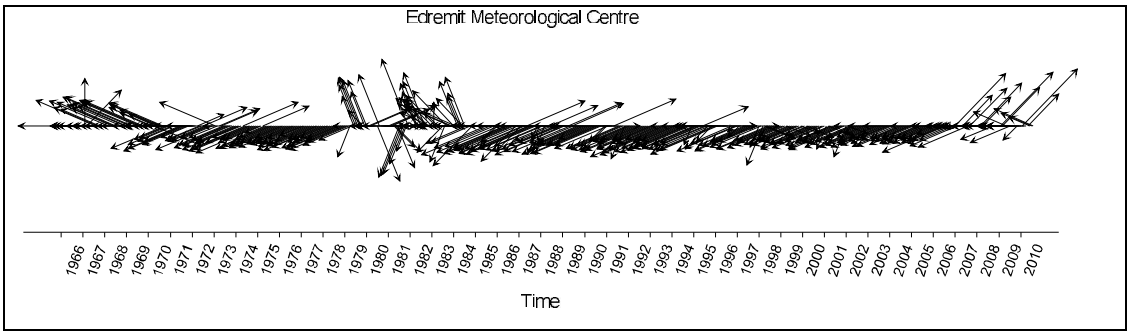

Figure 3.26 Wind vectors of the monthly prevailing wind with average wind speed values for Edremit Bay data from Edremit Meteorological Centre. (V_{max}=12.1 m/s).

The long duration (more than 12 hours) wind directions and speeds are selected for Edremit region and shown in Figure 3.27. The prevailing wind direction is also dominant characteristics by the long duration wind. The lasted wind direction is more or less same and indicate NNE during the period which the dense water formation takes place.

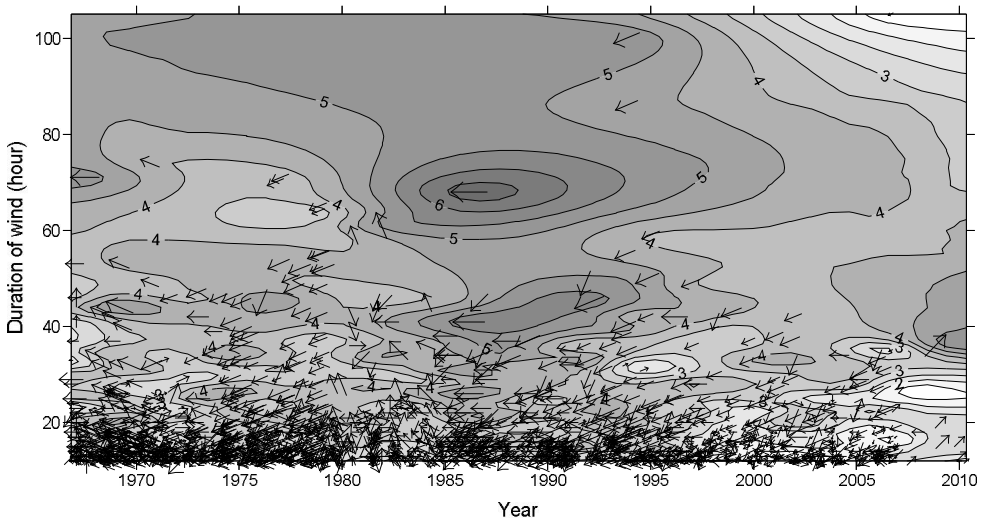

Figure 3.27 The wind vectors for the wind blowing more than 12 hours drawn on the average wind field.

3.2.4 Time Series of the Edremit Bay

Time series are analyzed by profiles of temperature, salinity and density from several cruises in the Edremit bay extending from 1991 to 2009.

The prevailing wind over the Edremit area is ENE direction (Figure 3.28). Not only the excess evaporation in summer but also the frequently taking place upwelling process is responsible to find the very high density values in Edremit bay. The prevailing wind from ESE direction is suitable to trigger the upwelling process near the east and north coast of the Lesvos Island in all seasons.

The water exchange between the Aegean Sea and the Levantine Basin starts before 1990 and major dense deep water formation and the maximum exchange period is in winter 1993. After peak period the exchange decreases gradually (relaxation period) with an exception in 1996. It stops around the year 2000.

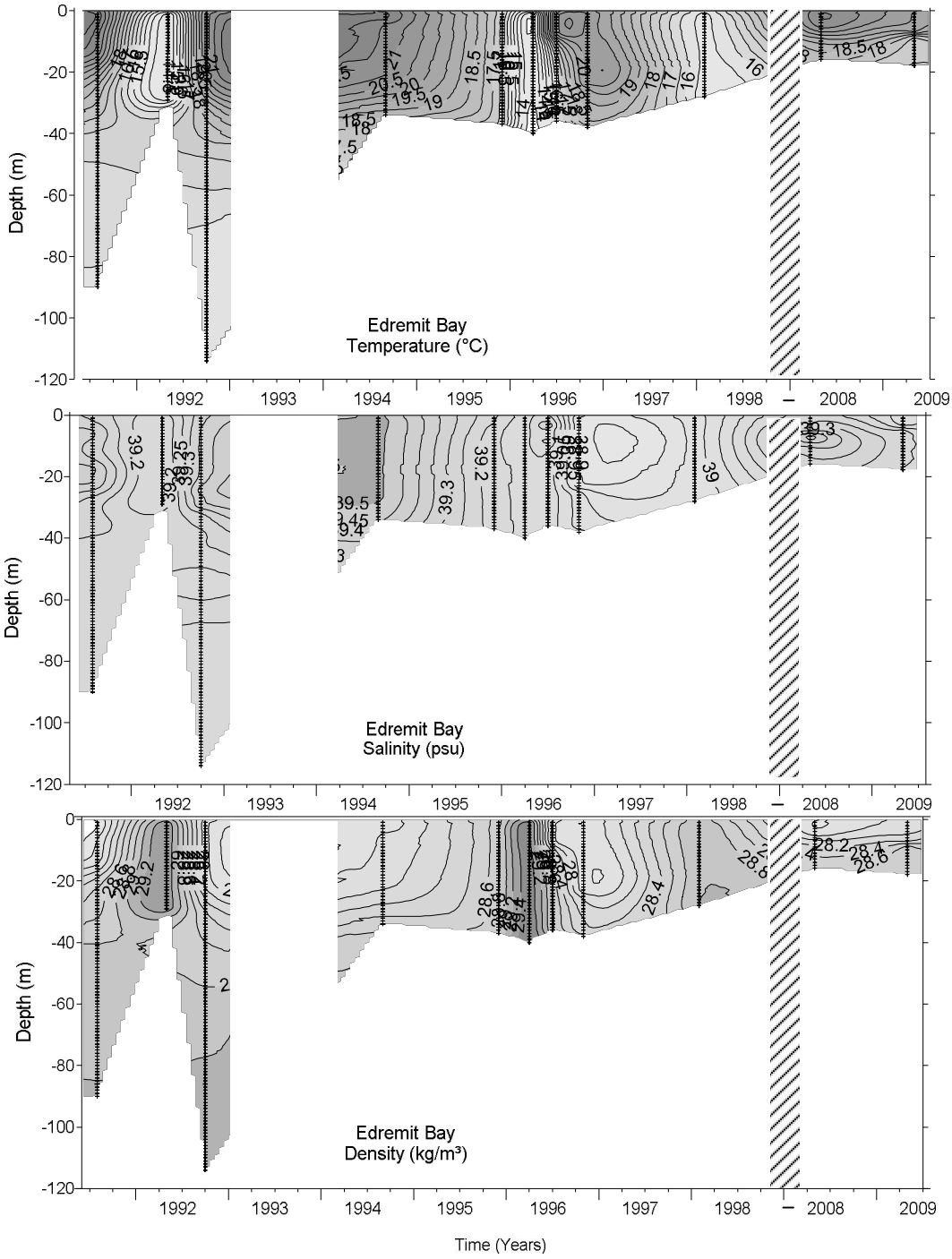

Figure 3.28 Temporal evaluations of temperature, salinity and density fields of Edremit region starting from summer 1991 up to spring 2009. The areas in white represent where data was not collected.

The scarce data of Edremit Bay makes not available to follow all the water mass development in the Bay during the periods explained above. Because of the cold winter event, cold and dense water can be observed even at the surface in spring 1992 (14.5 °C and 29.2 kg/m^3) and in spring 1996 (13.5 °C and 29.4 kg/m^3). More dense water mass can not be detected after 1996 until spring 2009. Besides the upwelling process occurring in all seasons any relation was found between wind event and forming water mass in the Bay from time evolution. The water is denser in the Edremit Bay than the water in Saros Bay in comparison. The upwelling process could be the reason for the existing denser water in the Edremit Bay.

3.3 Çandarlı Bay

3.3.1 Study Area

The Çandarlı Bay, known in antiquity as the Elaitic Gulf, is a bay on the Aegean Sea, with its inlet between the cities of Çandarlı and Foça (Figure 3.29). Around it were located the chief cities of the Aeolian confederacy. The bay is located just north of İzmir on the western coast of Turkey in water depths ranging from 0-80 metres.

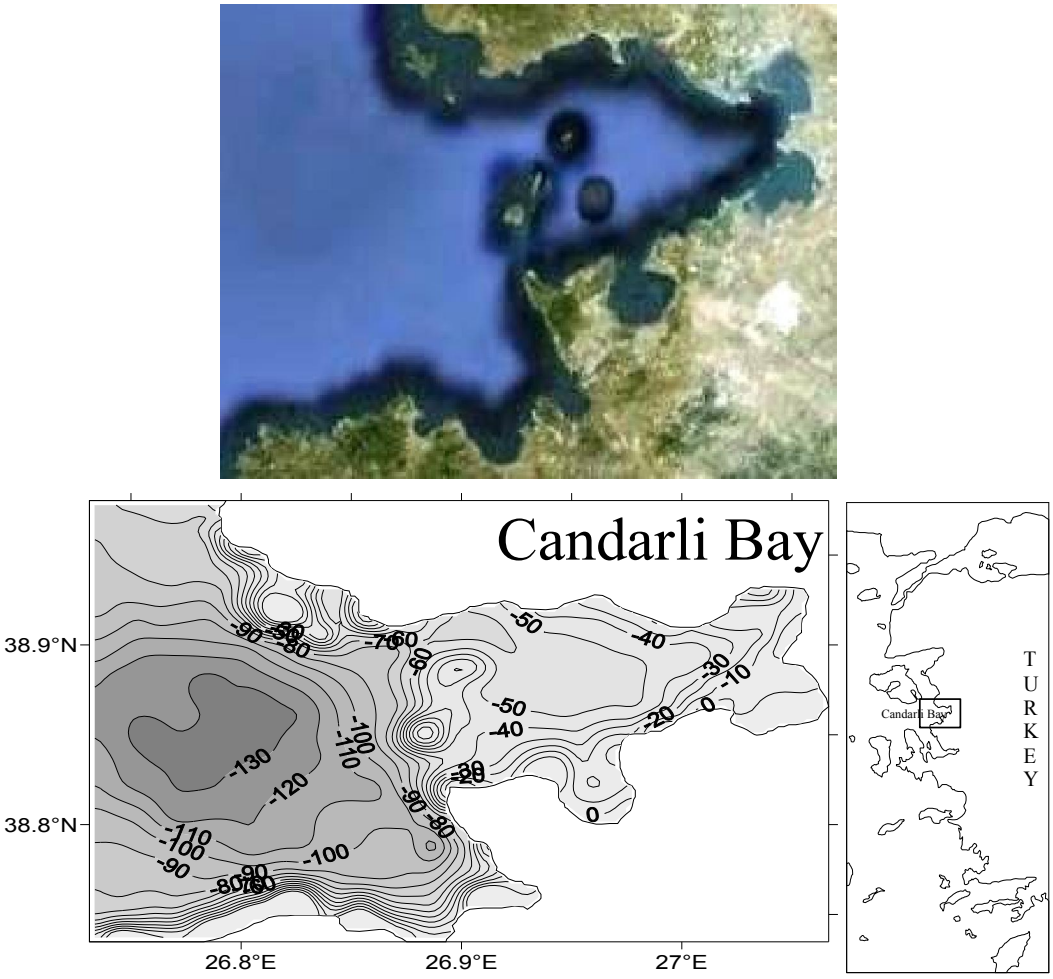

Figure 3.29 The view from Google Earth, bottom topography (from GEBCO, 2008 grided data) and location of the Çandarlı Bay.

3.3.2 Meteorological Conditions

The meteorological data from Dikili Meteorological Centers for Çandarlı Bay area were recorded as hourly and include wind speed, wind direction, air temperature, precipitation, evaporation, relative humidity and air pressure. Figure 3.30-3.37 shows the weather condition in the Çandarlı Bay, Turkey.

The annual mean temperature ranges from 15,5°C (in 1976) to 18°C (in 2009). The temperature difference reaches approximately 20 °C between the summers and winters (Figure 3.30). The maximum value ever measured in hourly data is 41.2 °C in July 1988 and minimum value is -7.7 °C in January 1968. The average over 50 year (between 1960 and 2010) is 16.48 °C.

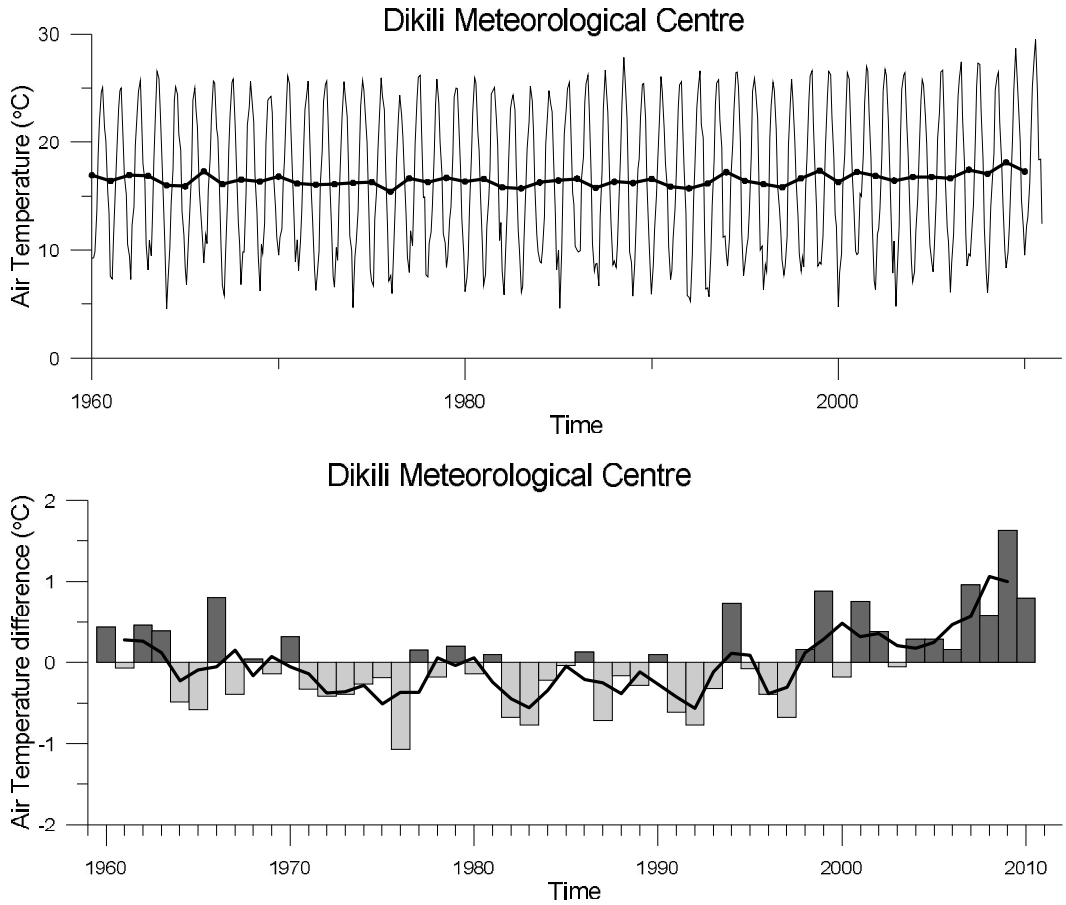

Figure 3.30 Time series of monthly average (thin line) and annual mean (thick line) air temperature (°C) (top), and yearly anomaly time series (bars) with moving averages (thick line) (bottom) for the Çandarlı Bay.

The time series of yearly averaged data (Figure 3.30 bottom panel) shows slight positive air temperature anomalies before late 1960s and after negative anomalies up to 1994. Air temperature anomaly gradually increases after 1995 as a result of global warming. The very dense water formation period in the Aegean Sea is between 1990 and 1994. It means the beginning of relaxation period from 1995 to 2000 is not incidence. High excess air temperature could be one of the reasons for the relaxation of forming dense water in the Aegean Sea. Air temperature decline ~1 °C between 1963 and 1997.

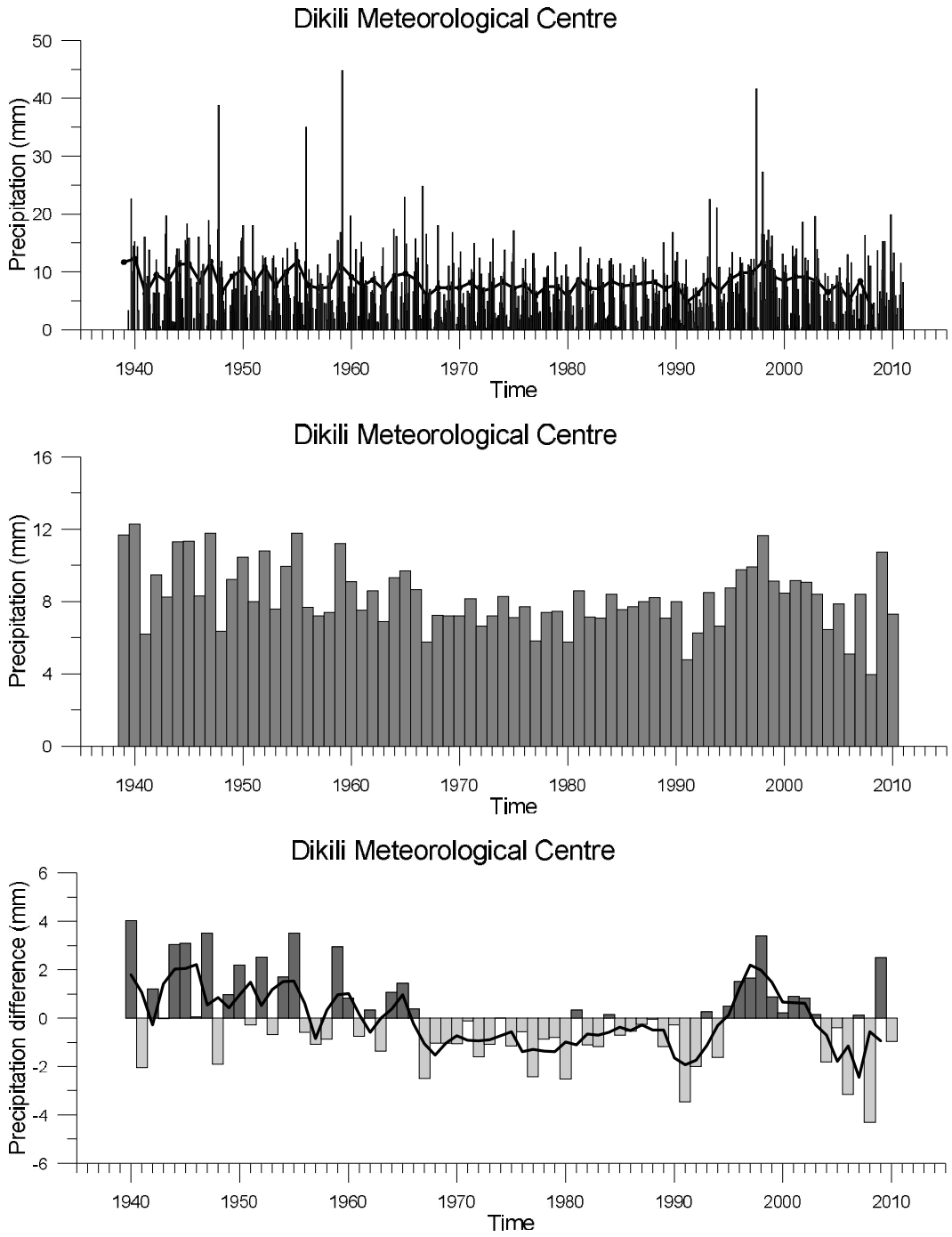

Figure 3.31. Time series of monthly averaged (top), annual mean precipitation (center) and yearly anomaly time series (bars) with moving averages (thick line) (bottom) for the Çandarlı Bay.

Hourly precipitation data is retrieved from Dikili Meteorological Center. Monthly averaged precipitation data for the years 1939-2010 is shown in Figure 3.31. The maximum value ever measured in hourly data is 183.10 mm in October 1947. The

average over 71 year is 8.26 mm. The rainfall is minimum in the months of early summer according to monthly averaged values.

The precipitation anomalies (Figure 3.31 bottom) show similar trend as air temperature with an exception in the last years after 2005. The precipitation values are greater than the averaged one until late 1960s. The data shows negative anomalies after. Negative anomalies continue until 1995. Precipitation gradually increases after 1995. The positive air temperature anomalies might be the reason for the increasing of precipitation after 1995. Again the negative anomalies can be seen in the last years due to warm and dry air.

Hourly evaporation data is retrieved from Dikili Meteorological Center for the years 1978-2010. Monthly averaged values are shown in Figure 3.32. The maximum evaporation value ever measured in hourly data is 20.0 mm in September 2009. The average over 32 year is 4.31 mm. The evaporation is minimum (0.9 mm) in winter and the maximum (9.18 mm) is in summer according to monthly averaged values.

Time series are used to see long-term trend in the evaporation data. Evaporation anomaly shows negative anomalies extending from 1978 to 1998 with exception in late 1980s and in the middle 1990s. The salinity values had an increasing trend during late 1980s in the Aegean Sea (V & L, 2005). As a result of the increasing air temperature the positive anomalies were observed in the last years after 1998 with an exception in 2005.

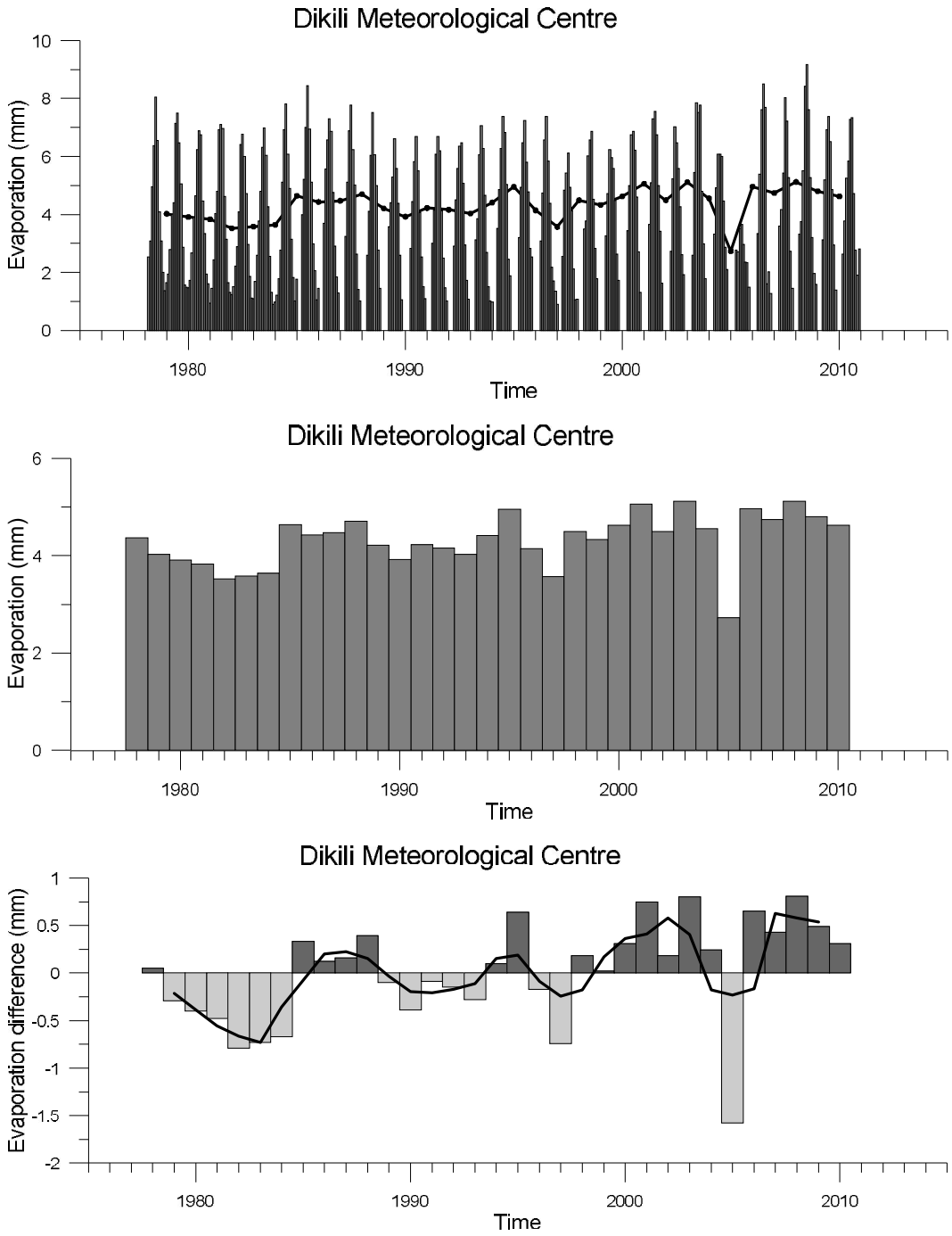

Figure 3.32 Time series of monthly averaged (top), annual mean evaporation (center) and yearly anomaly time series (bars) with moving averages (thick line) (bottom) for the Çandarlı Bay.

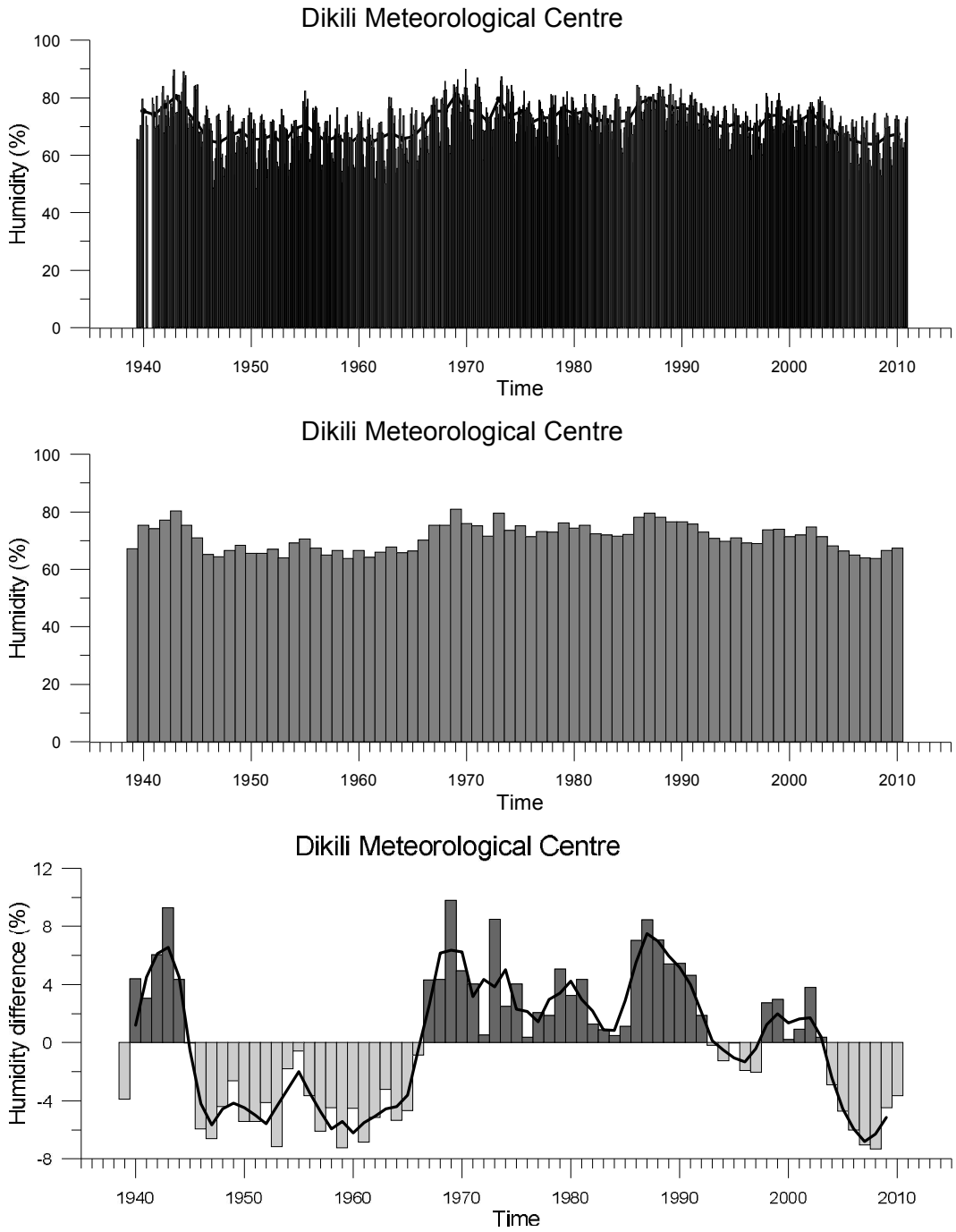

Figure 3.33 Time series of monthly averaged (top), annual mean humidity (center) and yearly anomaly time series (bars) with moving averages (thick line) (bottom) for the Çandarlı Bay.

Hourly humidity data is retrieved from Dikili Meteorological Center for the years 1939-2010. Monthly averaged humidity time series is shown in Figure 3.33. The average relative humidity over 71 year is % 71.03. The humidity is minimum (% 48.46) in summer and the maximum (% 89.92) is in winter according to monthly averaged values.

The time series of yearly averaged humidity data (Figure 3.33, bottom panel) shows negative humidity anomalies before late 1960s and after positive anomalies up to 1994. Humidity anomaly oscillates in a short time after 1995 in the relaxation period. The negative anomaly values are observed after 2002 probably affected by warm air.

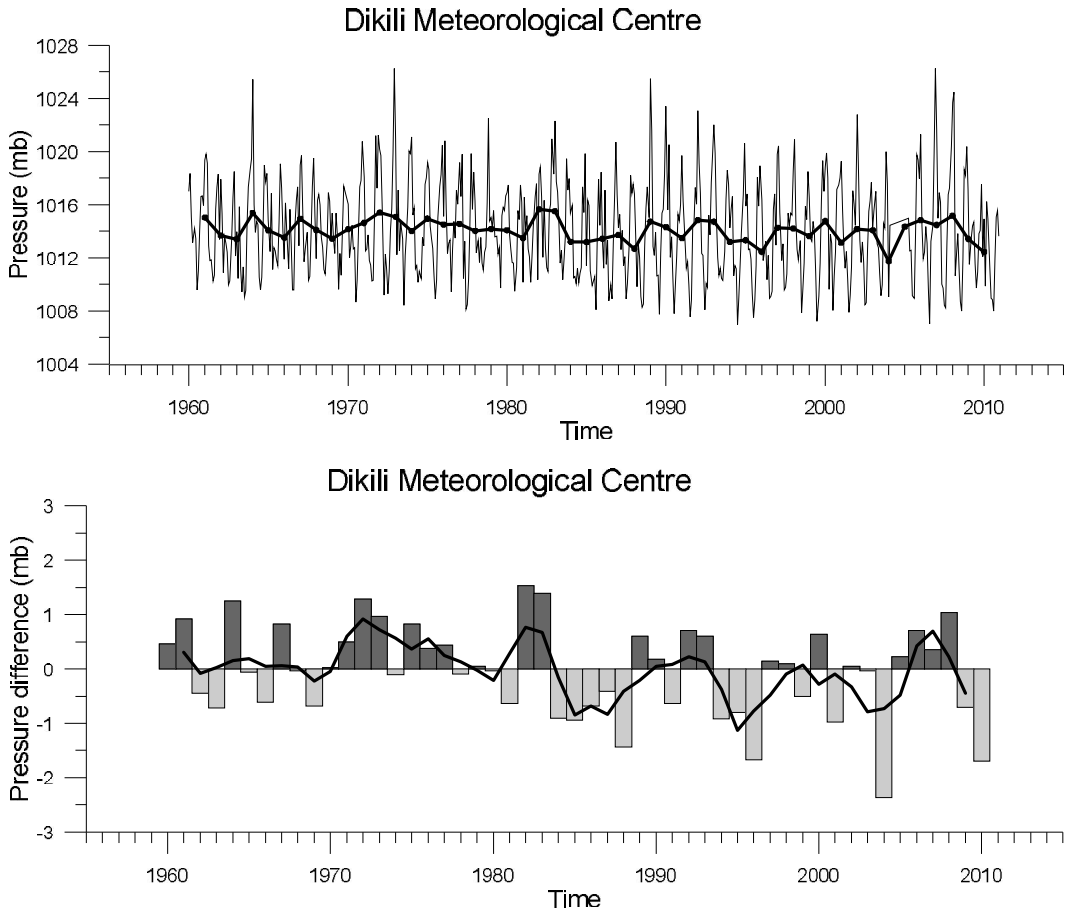

Figure 3.34 Time series of monthly average (thin line) and annual mean (thick line) pressure (mb) (top), and yearly anomaly time series (bars) with moving averages (thick line) (bottom) for the Çandarlı Bay.

The highest pressure value ever recorded in hourly data in Çandarlı area is 1040.1 mbar in January 1973 and lowest value is 783.0 mbar in May 2007. The average over 50 year (between 1960 and 2010) is 1013.23 mbar.

The anomaly time series of yearly averaged pressure data (Figure 3.34, bottom panel) show very interesting evolution of high positive pressure anomalies during the years from 1989 until 1994. These are the years that the big amount of Aegean Deep Water (ADW) flowed over the sills of the Creatan Arc into the Levantine Basin. This time span covers the deep water formation period in the Aegean Sea.

3.3.3 Wind Analysis

In the region, wind from ESE direction dominate throughout the years with an average speed of 2.19 m/s is shown in Figure 3.35.

The prevailing wind over the Çandarlı area is ESE direction shown in the wind-rose map in Figure 3.35. Wind vectors of the monthly time series of wind speed and direction anomalies for 1963-2006, depending on the availability of the data, were constructed from hourly wind measurements in the Dikili Meteorological Centre. The wind vectors of the monthly prevailing wind with average wind speed values for Çandarlı Bay data from Dikili Meteorological Centre is shown in Figure 3.36. The wind vectors show that the wind direction changes around the year 1983. ENE direction is dominant short before 1987 and variable after 1987. The intensity of wind increases over average and the wind direction turns to SSE in the period which very dense water formation takes place (1993).

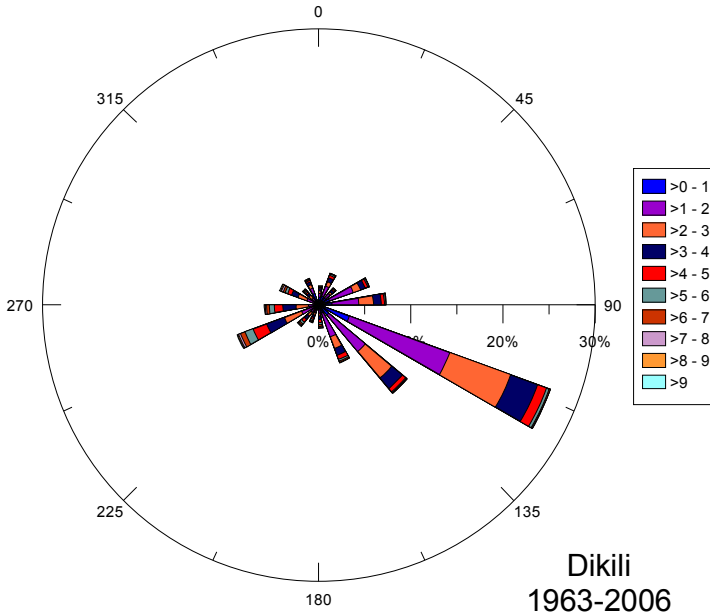

Figure 3.35 Wind chart of the prevailing wind for Çandarlı Bay data from Dikili Meteorological Centre.

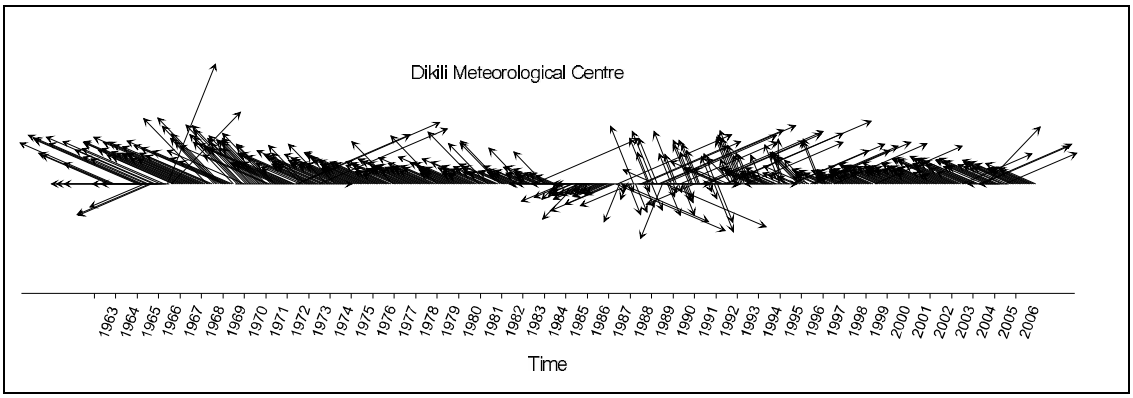

Figure 3.36 Wind vectors of the monthly prevailing wind with average wind speed values for Çandarlı Bay data from Dikili Meteorological Centre (V_{max}=11.1 m/s).

The wind speed and direction are usually variable, so the currents are also variable. The currents need sufficient time to be established towards a certain direction. If the wind blows more than 12 hours, the establishing current will be the same direction as wind direction and the speed of current will be proportional to wind intensity for wind-driven circulation. The long duration (more than 12 hours) wind directions and speeds are selected for Çandarlı region and shown in Figure 3.37. The prevailing wind direction is dominant characteristics by the long duration wind. The number of the lasting wind event decreases and is limited to about 20

hours during the period which the dense water formation takes place and wind direction more or less in a line SSE-NNW.

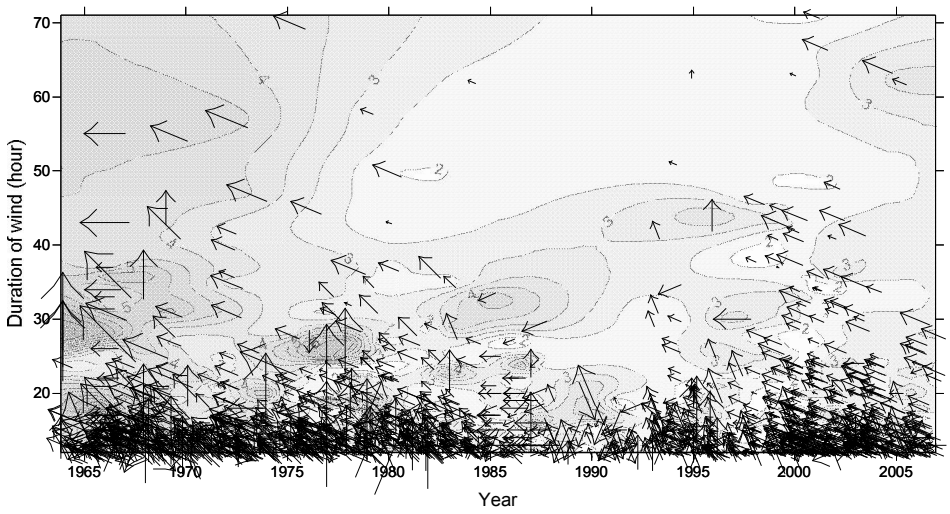

Figure 3.37 The wind vectors for the wind blowing more than 12 hours drawn on the average wind field.

3.3.4 Time Series of the Çandarlı Bay

Time series are analyzed by profiles of temperature, salinity and density from several cruises in the Çandarlı bay extending from 1991 to 2009.

The off-shore side of Çandarlı Bay is one of the deep water formation site (not shown) in the Aegean Sea. But on-shore part of the Çandarlı Bay differs not much from Edremit Bay. The time evolution of density field Çandarlı Bay (Figure 3.38, lower panel) shows that even isopycnal of 29.5 kg/m3 can be detected in winter 1993 at the depth of 70m. The level of the isopynal in Çandarlı Bay is lower in comparison to the level found in Edremit Bay in spring 1992 just before major peak period. The isopycnal level during spring 1992 is higher campared to the level in spring 1996 in Çandarlı Bay contrary to the evolution in Edremit Bay. High densities (29.4 kg/m3) were observed near surface in Edremit Bay during spring 1996. In spite of existing high salinities, the level of densities are not high because of warm water near surface during period from 2003 to 2009. The increasing air temperature heats the water

from surface in the last years as a result of global warming. Only the isopycnal of 29.0 kg/m3 can be detectable at the depth of 30 m in spring 1994.

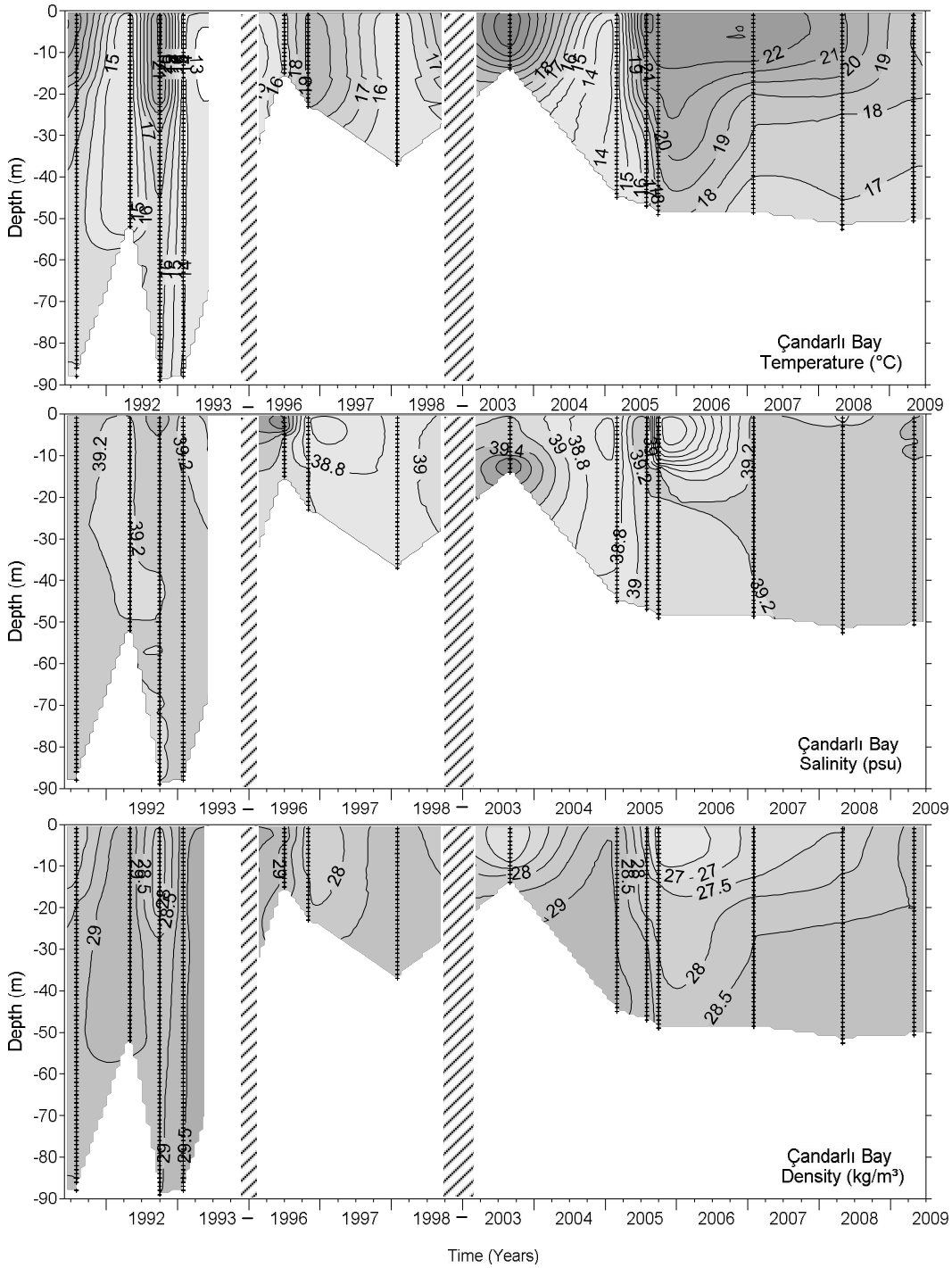

Figure 3.38 Temporal evaluations of temperature, salinity and density fields of Çandarlı region starting from summer 1991 up to spring 2009. The areas in white represent where data was not collected.

3.4 İzmir Bay

3.4.1 Study Area

İzmir Bay is one of the great natural bays of the Eastern Aegean Sea, which is an "L" shaped geometry with the leg of the "L" about 20 km wide and 40 km long, and the base of the "L" about 5 to7 km wide and 24 km long (Figure 3.39). It's total surface area is over 500 square kilometers and a water capacity of 11.5 billion cubic meters. The İzmir Bay, formerly known as the Gulf of Smyrna, is between the peninsula of Karaburun and the mainland area of Foça. The city of İzmir, an important Turkish seaport, surrounds the end of this bay. Levent Marina is the only marina inside the city of İzmir.

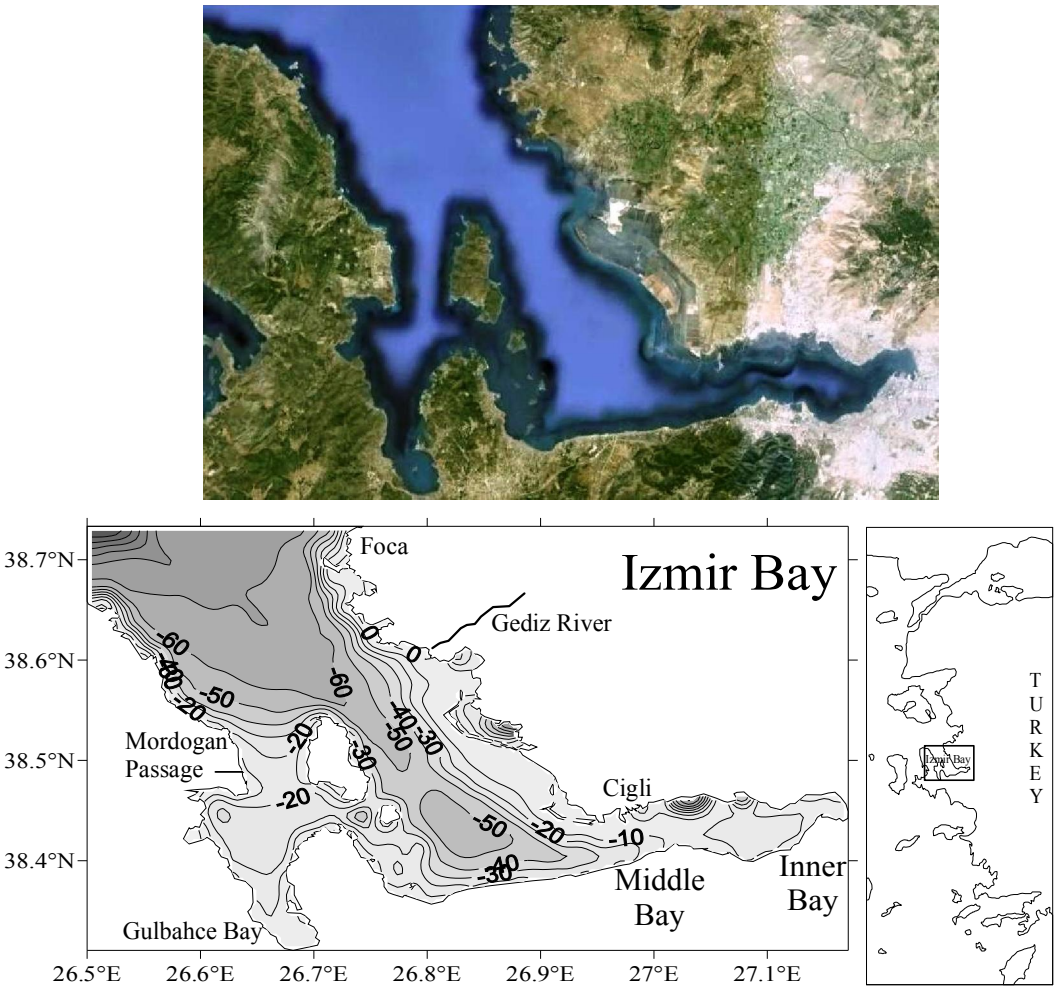

Figure 3.39 The view from Google Earth, bottom topography (from GEBCO, 2008 grided data) and location of the İzmir Bay.

İzmir Bay has been studied in three areas according to their physical characteristics: outer, middle and inner Bays. The outer Bay is further divided into three sub-regions, outer I, outer II and outer III. Outer Bay receives discharge from the Gediz River. The Gediz River is the second-largest river in Anatolia flowing into the Aegean Sea. The drainage area and annual average discharge rate of Gediz River are 15617 km^2 and 85.1 m^3/s (Yasar, 1994) respectively The water properties of the bay were analyzed generally using the data from these different regions.

3.4.2 Meteorological Conditions

The meteorological data obtained from Çiğli and İzmir Meydan Meteorological Center is representative for the İzmir Bay region. Hourly weather data including wind speed, wind direction, air temperature, precipitation, evaporation, relative humidity and air pressure were retrieved. Figure 3.40-3.47 show the weather measurements in the İzmir Bay, Turkey.

The temperature difference reaches approximately 20 °C between the summers and winters. The maximum value ever measured in hourly data is 30.1 °C in July 1988 and minimum value is 5.6 °C in February 2003. The average over 34 year (between 1974 and 2008) is 17.74 °C.

The time series of yearly averaged data (Figure 3.40 bottom panel) shows slight negative air temperature anomalies before 1993 and positive after anomalies up to 1994. The very dense water formation period in the Aegean Sea is between 1990 and 1994. The negative anomalies during 1991, 1992 and 1993 are common characteristics in all bays. It is not coincidence. Very dense water is formed mainly in severe weather condition in winter time. The very dense water formation period in the Aegean Sea is between 1990 and 1994.

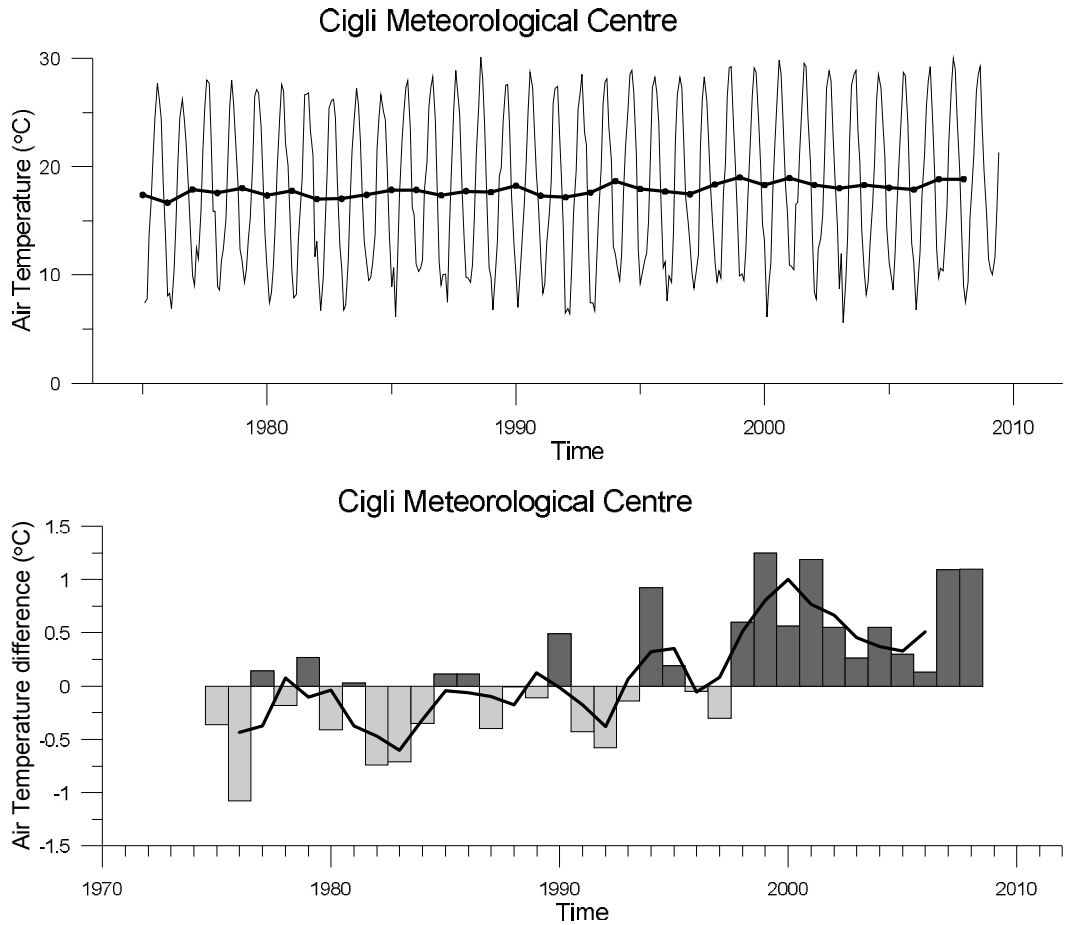

Figure 3.40 Time series of monthly average (thin line) and annual mean (thick line) air temperature (°C) (top), and yearly anomaly time series (bars) with moving averages (thick line) (bottom) for the İzmir Bay.

Monthly averaged precipitation data in İzmir Bay for the years 1938-2010 is shown in Figure 3.41. The maximum value ever measured in hourly data is 145.30 mm in September 2006. The average over 72 year is 7.89 mm. The rainfall is minimum in the months of late summer and early fall according to monthly averaged values.

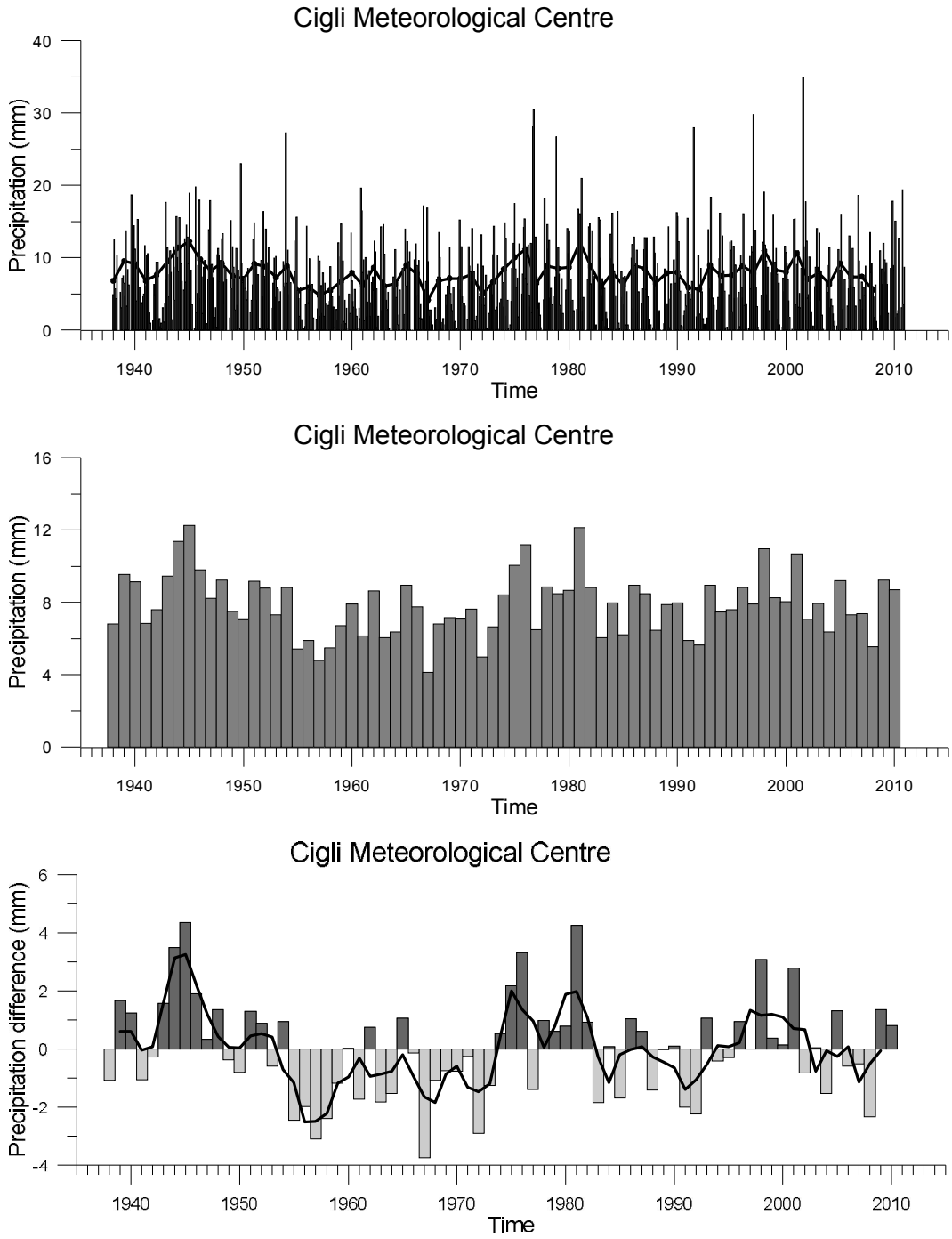

Figure 3.41 Time series of monthly averaged (top), annual mean precipitation (center) and yearly anomaly time series (bars) with moving averages (thick line) (bottom) for the İzmir Bay.

Precipitation time series and anomalies of İzmir Bay (Figure 3.41 bottom) are not much different than the other Bays along the eastern Aegean cost. More precipitation means the more isolation of sea from the air interactions. It is expected that less

precipitation is in the main EMT period. Precipitation data (Figure 3.41 bottom) shows negative anomalies around the year 1990.

İzmir Bay hourly evaporation data is retrieved for the years 1950-2010. Monthly averaged values are shown in Figure 3.42. The maximum evaporation value ever measured in hourly data is 98.50 mm in August 1962. The average over 60 year is 5.46 mm. The evaporation is minimum (1.07 mm) in winter and the maximum (16.25 mm) is in summer according to monthly averaged values. Evaporation anomaly (Figure 3.42 bottom) shows negative anomalies until 1960s. The surface salinity can be calculated proportional to precipitation minus evaporation in middle latitude regions. There is slight decrease in salinity values starting from 1994. But it is not considerable amount. It means we expect low evaporation values when low precipitation is observed. Figure 3.42 shows low evaporation anomalies during the main EMT period.

Hourly humidity data is retrieved for İzmir Bay for the years 1938-2010. Monthly averaged humidity time series is shown in Figure 3.43. The average relative humidity over 72 year is % 61.57 mm. The humidity is minimum (% 38.1) in summer and the maximum (% 82.22) is in winter according to monthly averaged values.

Anomaly time series (Figure 3.43, bottom panel) shows positive humidity anomalies before late 1945 and after negative anomalies up to 1970s. The negative anomaly values are observed after 2002 probably affected by warm air.

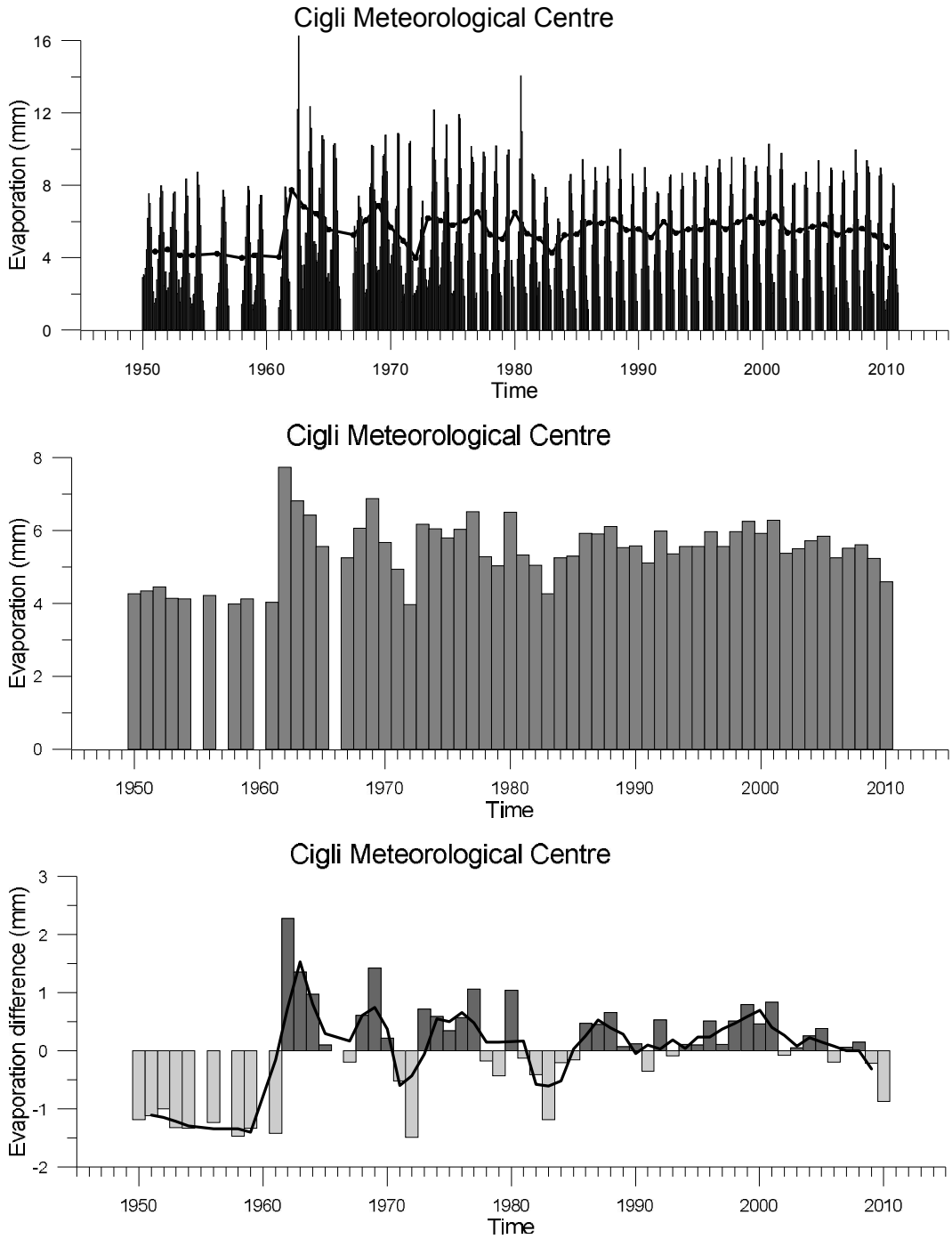

Figure 3.42 Time series of monthly averaged (top), annual mean evaporation (center) and yearly anomaly time series (bars) with moving averages (thick line) (bottom) for the İzmir Bay.

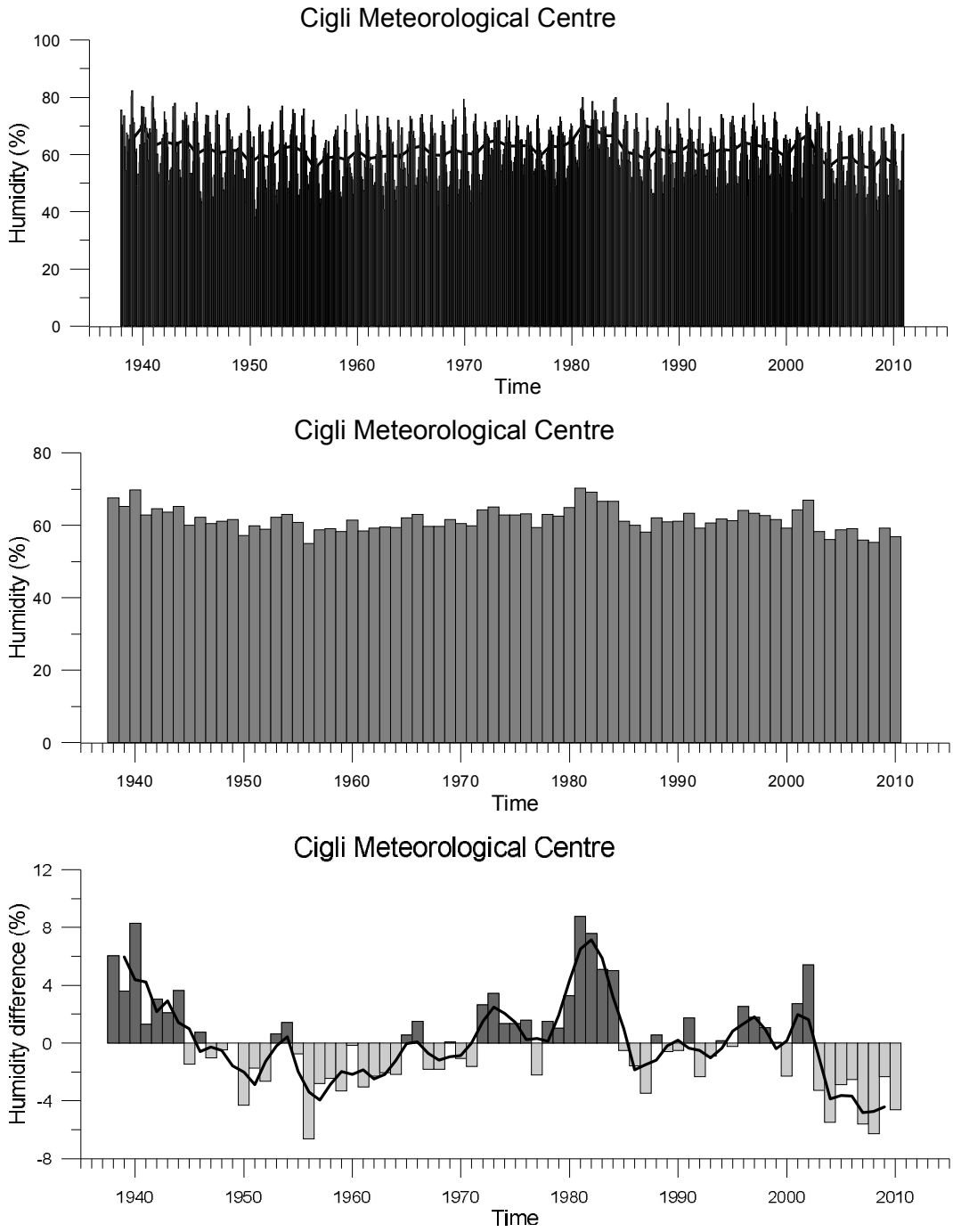

Figure 3.43 Time series of monthly averaged (top), annual mean humidity (center) and yearly anomaly time series (bars) with moving averages (thick line) (bottom) for the İzmir Bay.

The highest pressure value ever recorded in hourly data in İzmir area is 1036.4 mbar in February 2008 and lowest value is 878.6 mbar in January 2004. The average over 50 year (between 1960 and 2010) is 1011.08 mbar.

Anomaly time series of pressure data (Figure 3.44, bottom panel) shows high positive pressure anomalies observed similar in almost all bays during the years from 1989 until 1994.

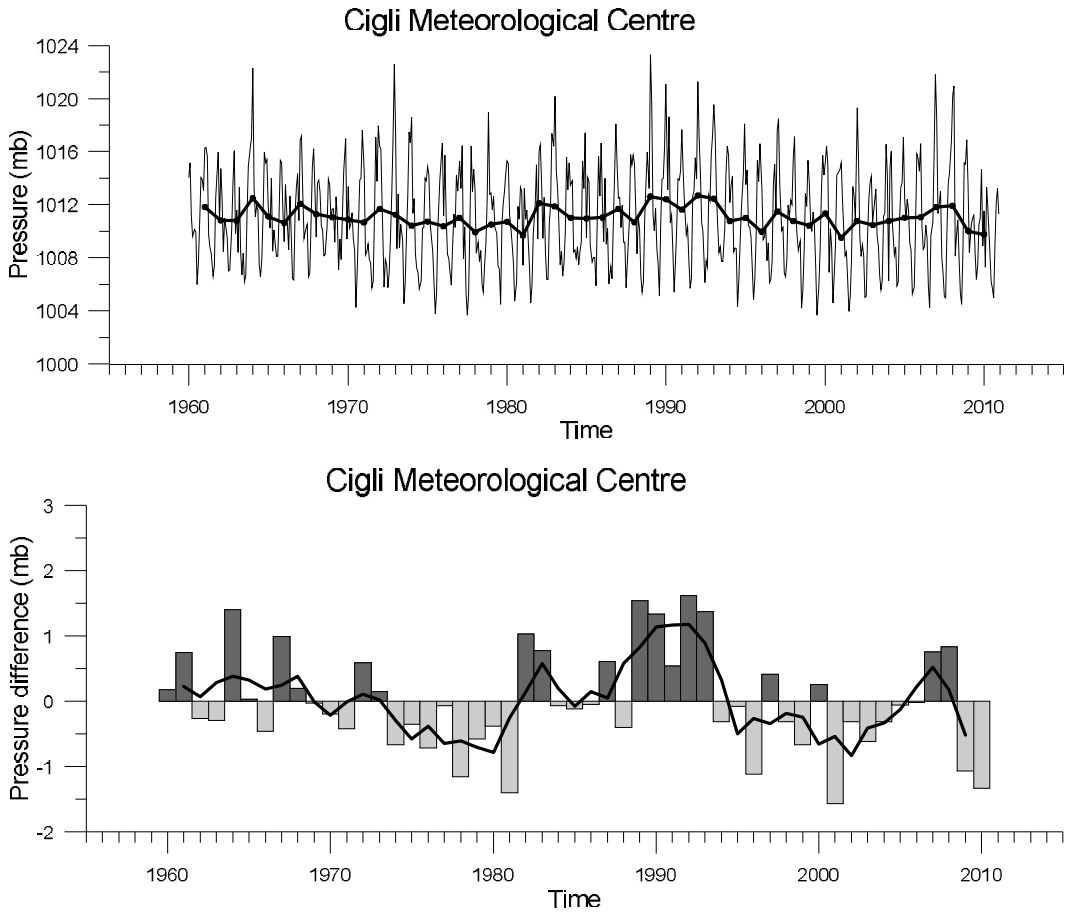

Figure 3.44 Time series of monthly average (thin line) and annual mean (thick line) pressure (mb) (top), and yearly anomaly time series (bars) with moving averages (thick line) (bottom) for the İzmir Bay.

3.4.3 Wind Analysis

In the region, wind from N direction dominates throughout the years with an average speed of 4.71 m/s is shown in Figure 3.45.

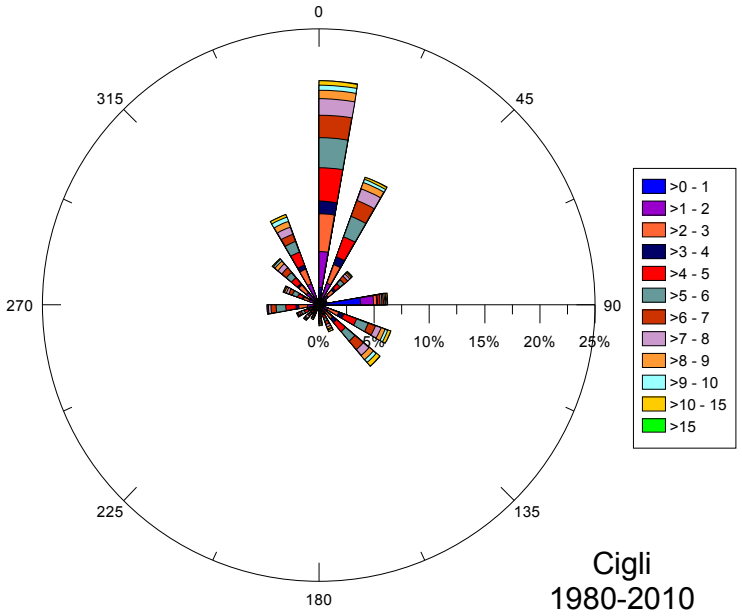

Figure 3.45 Wind chart of the prevailing wind for İzmir Bay data from Çiğli Meteorological Centre.

The prevailing wind over the İzmir area is N direction shown in the wind-rose map in Figure 3.45. Wind vectors of the monthly time series of wind speed and direction anomalies for 1980-2010, depending on the availability of the data, were constructed from hourly wind measurements in the Çiğli Meteorological Centre. The wind vectors of the monthly prevailing wind with average wind speed values for İzmir Bay data from Çiğli Meteorological Centre is shown in Figure 3.46.

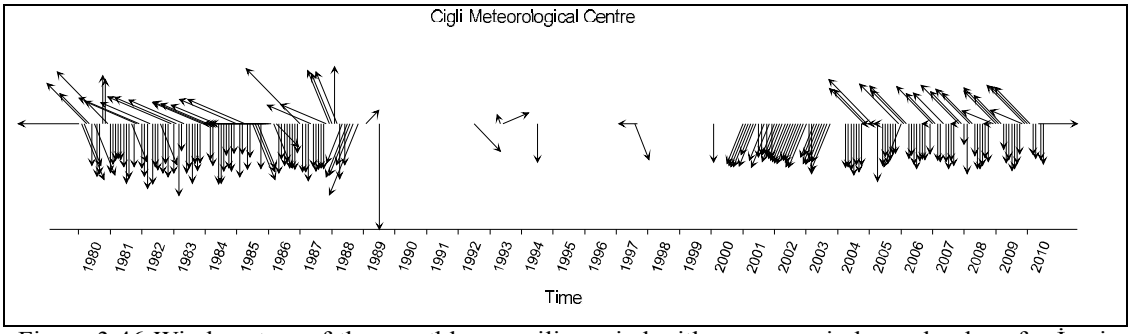

Figure 3.46 Wind vectors of the monthly prevailing wind with average wind speed values for İzmir Bay data from Çiğli Meteorological Centre. (V_{max}=43.2 m/s).

3.4.4 İzmir Bay General Circulation Pattern

As a result of wind analysis it is found that the prevailing wind direction of the İzmir Bay (N) coincides circumstantially with the dominant wind direction in the winter cruise time. Therefore the model runs were conducted using the prevailing wind intensity and direction in order to obtain general water movements in the Bay. The circulation is based on the basin wide net current flowing along the water column.

The general circulation pattern that are frequently seen in the İzmir bay under the influence of prevailing wind (N) are shown schematically. Figure 3.47 shows the İzmir Bay circulation pattern. After entering the bay near the coast of Karaburun, of Aegean origin (after Sayin et al., 2006) follow the path along the coast up to the Mordoğan Passage. The water that cannot enter the Mordoğan Passage makes a cyclonic gyre in the Outer Bay. Outflow occurs mainly near the coast of Foca as a result of compensating flow against the coastal flows leaving an anticyclonic gyre in the middle of the Bay. Acording to the direction of the wind a cyclonic gyre can be seen from time to time in stead of anticyclonic one (Sayin et al. 2006)..

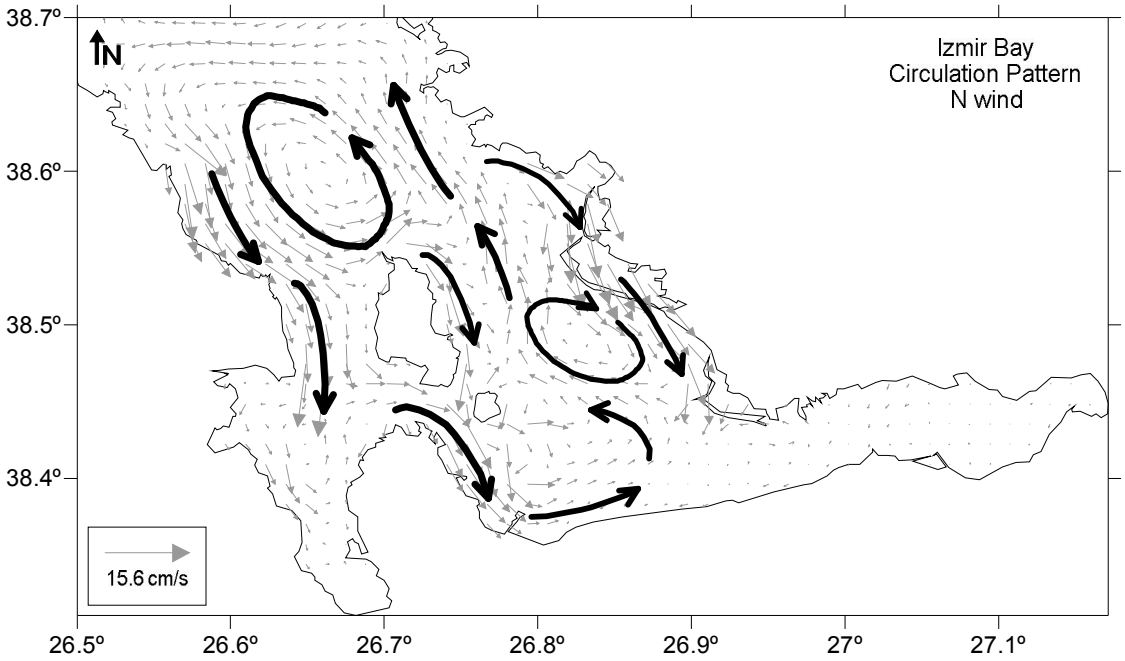

Figure 3.47 General circulation patterns of İzmir Bay.

According to the calculated values, the recycle time is the shortest for the Izmir Bay with 15 days; it was found as one month by Sayin (2003) before who takes the vertical section more inside the bay. The other reasons for such small difference could be the strength of forming stratification in the bay and the intensity of the blowing wind.

3.4.5 Time Series of the İzmir Bay

İzmir Bay is chosen to represent Central Aegean shallow area. The monitoring studies have begun after 1991 in the bay and 56 cruises have been conducted. The data covers whole bay. We concentrate on the Outer Bay (hereafter OB) and Middle Gyre area (hereafter MG). The relaxation episode of EMT was very clear in Saros and Gökova Bays where the collected data was just after the last major deep-water formation episode in the Aegean Sea (1993) and after. İzmir Bay is the shallowest one of three bays. Therefore, the air sea interactions are more effective over the İzmir area. Especially the local wind force is the main mechanism for the bay. The middle part of the İzmir Bay produces its own water mass (IBW). Although the water properties are different in the bay than those in the Aegean Sea, they show similar interanual variability to the Aegean Sea according to the evolution of water masses influenced by the rising isopycnals. It seems that MG area is a suitable place for the occurrence of dense water in the core of forming cyclonic gyre. The relaxation period could be resolved with the data collected during many cruises in the OB area where Aegean Sea Water (ASW) enters the bay. Therefore this data gives detailed information about the major deep-water formation episode and the EMT post-peak period. The same information can be obtained from the MG area. It means that the Aegean Sea and the bays show similar characteristics in the point of view of interannual variability of water masses. The water of Aegean Sea can be influenced by the water masses of such shallow bay through temperature or salt controlled dense water cascading. The EMT relaxation period continued and the isopycnal level decreased gradually until April 2000 making an exceptional anomaly in January 1996 in both time evolutions of two regions in the bay (Figure 3.48). The decreases can be evaluated from the isopycnal levels σ_θ = 28.8 kg/m^3 and σ_θ = 29.0 kg/m^3

easily in the region OB and MG respectively. In other words the Aegean Sea and the bay seem to be interconnected during the EMT period. But MG region contains more dense water inside. After April 2000 the isopycnal levels started to increase. The isopycnal level σ_θ = 28.8 kg/m^3 was approximately 70 m during the year 2000. It reached up to 10m in July 2007 in the region OB. The level σ_θ = 29.0 kg/m^3 was not observed even in the bottom in the Middle Gyre region in 2000. It reached to 20m in March 2004 and outcropped at the surface in July 2007, mainly due to an observed salinity increase. Similar trend can be observed by the time evolution of temperature field in both regions. Both regions contained saline water inside after the EMT post-peak period around the year 2007. The slowly decreasing isopycnals took place after 2007 until 2010.

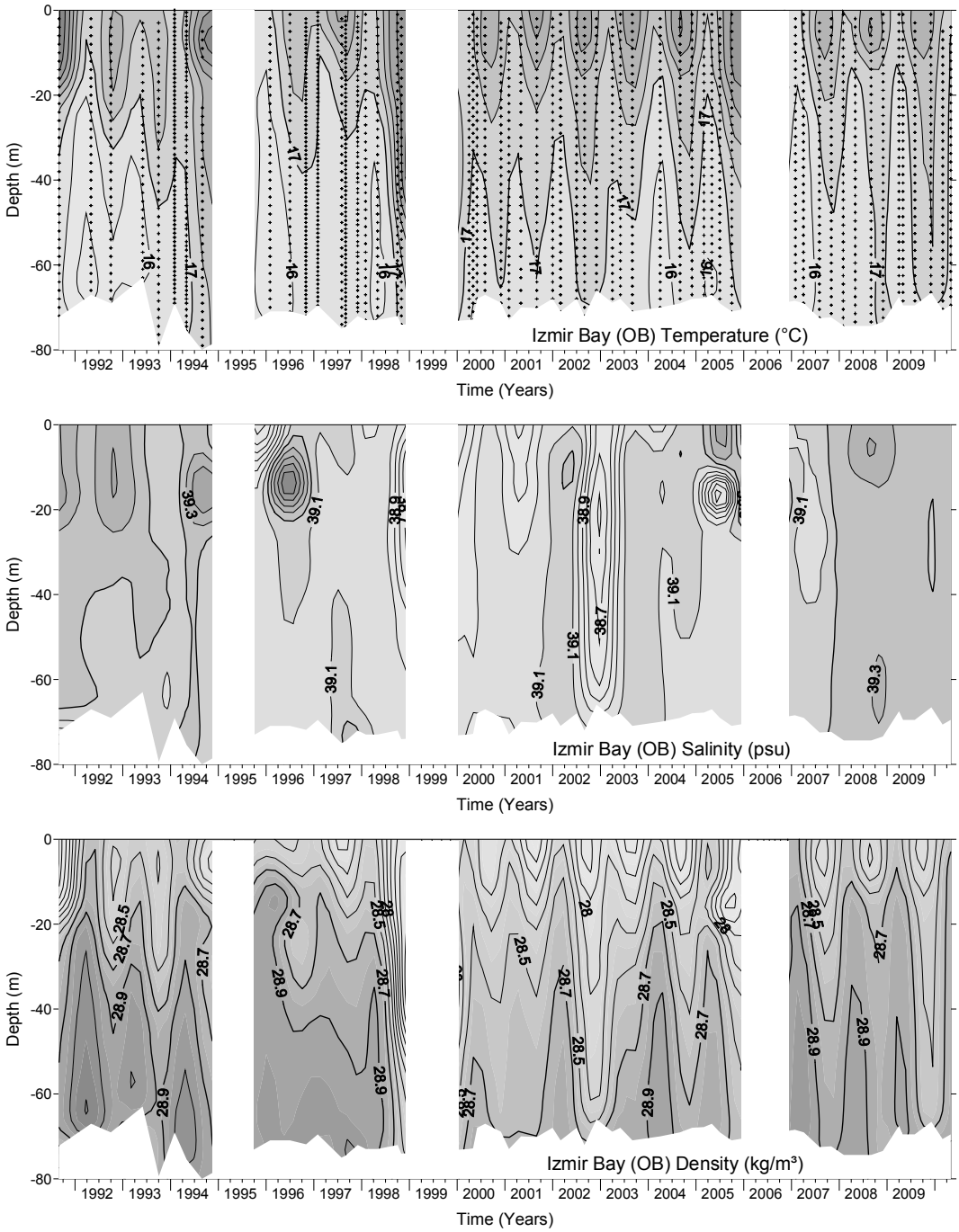

Figure 3.48 a Temporal evaluations of temperature, salinity and density fields of İzmir Outer Bay region starting from summer 1991 up to spring 2010. The areas in white represent where data was not collected.

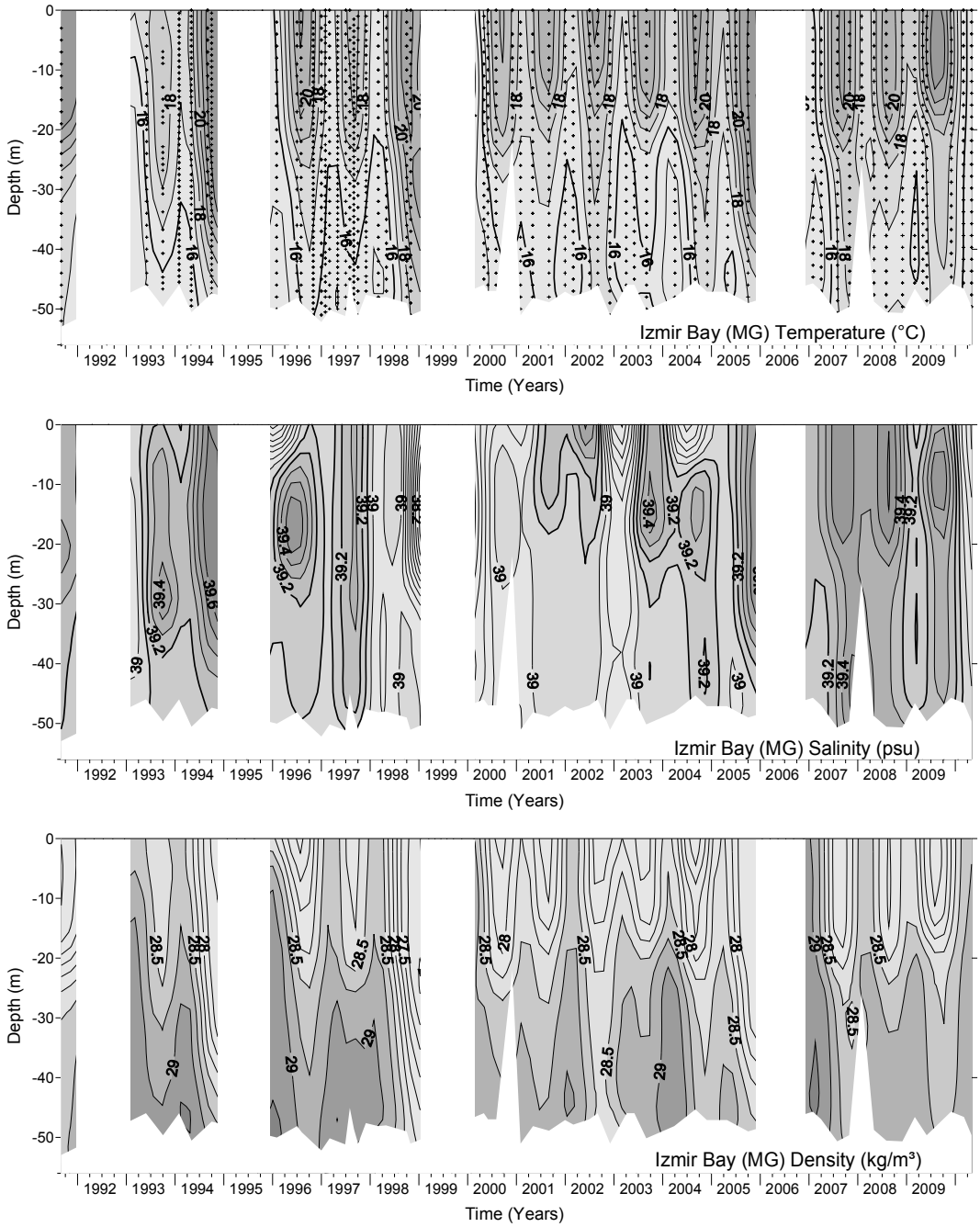

Figure 3.48 b Temporal evaluations of temperature, salinity and density fields of İzmir Middle Gyre region starting from summer 1991 up to spring 2010. The areas in white represent where data was not collected.

3.4.6 Hydrographic Characteristics of the İzmir Bay

3.4.6.1 Spring 2001

The water mass properties of the İzmir Bay are analyzed using the data obtained from the 31 stations during the spring 2001 cruise (10-12.04.2001) (Figure 3.49-3.52).

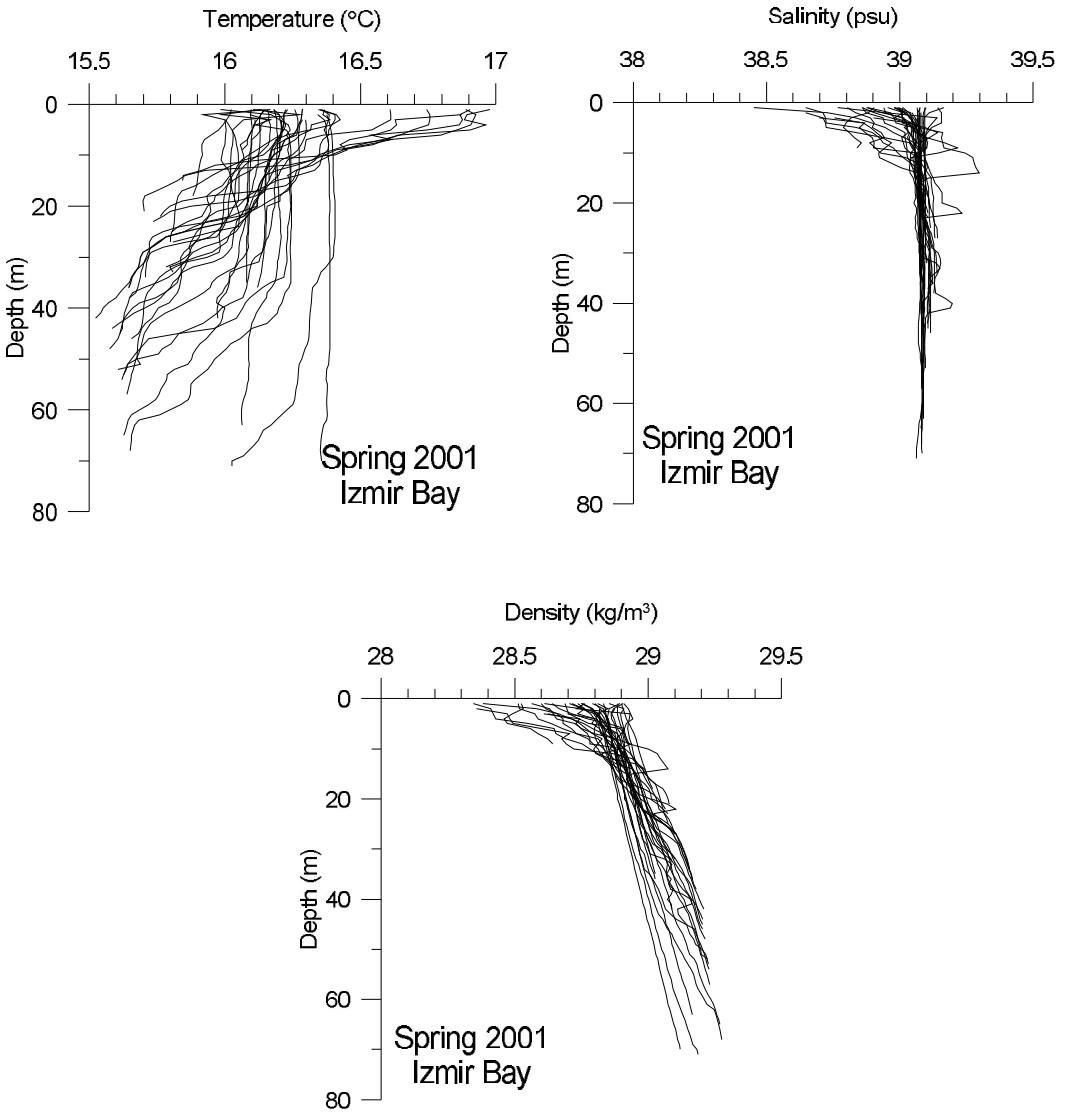

Figure 3.49 Temperature, salinity and density profiles of İzmir bay in spring 2001.

April and October are the transient months between winter and summer in the İzmir Bay. In April, the upper and lower layers show summer and winter characteristics, respectively, except for the surface water of Aegean origin. Because of its large volume, the water of Aegean origin preserves its winter character. In the late April, the stratifications start to be stronger, but gradually, horizontal homogeneity takes place in time (Sayin et al. 2006).

Three water masses are observed in the İzmir Bay in April 2001 as mentioned by Sayin et al., (2006) (Figure 3.50): Aegean Sea Water (ASW), İzmir Bay Water (IBW) and İzmir Bay Inner Water (IBIW). All these water masses are surface masses because of Izmir bay is a shallow area. IBIW is very distinct water with its low salinity, because of fresh water discharge discharge (with 7 m^3/s after Saner et. al. 1999) to the Inner Bay in spring. The temperature values increase towards the Inner Bay because of differential heating of land and sea by increasing air temperature in spring (Figure 3.51 and 3.52). IBW is formed in the region of Middle Gyre. IBW remains colder between the two warmer water masses IBIW and ASW. The bay is under the influence of southerly wind. It can be understood by the northward movement of IBW in the middle of the bay compensating the water mass (ASW) entering the bay near the coast of Karaburun and flowing through Mordoğan passage. It is noticed that the outflowing water, which is observed near the Aegean Sea, is originated from the middle gyre area as a result of detailed θ-S analysis. The inflowing ASW influences time to time the surface water of Gulbahce Bay and the intermediate water of Foca area.

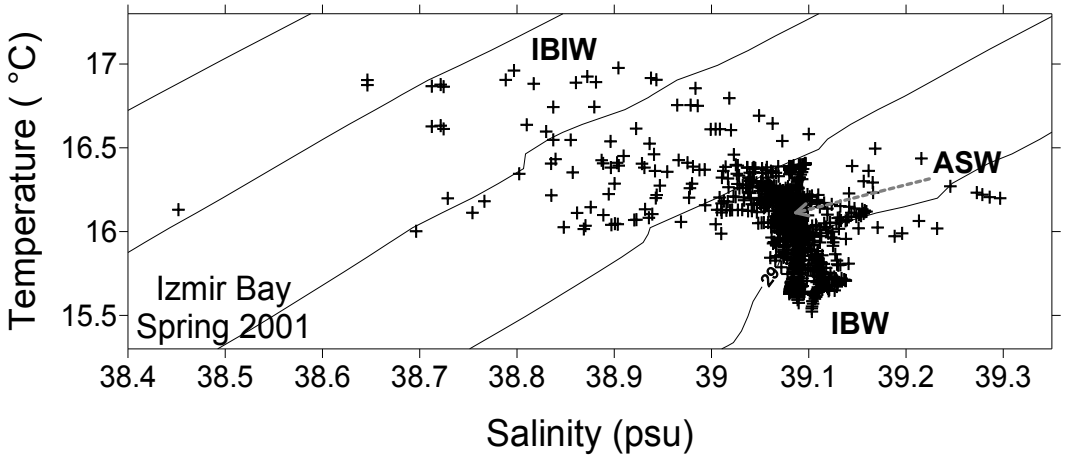

Figure 3.50 θ-S diagram of spring 2001 (İzmir Bay).

Table 3.3 The water masses existing in the İzmir bays and their range in spring 2001.

		Spring 2001			
		Water mass	Temperature (°C)	Salinity (psu)	Density (kg/m³)
IZMİR BAY		ASW	16.4	39.1	28.82 - 29.12
		IBW	15.5-15.8	39.09 – 39.12	29.2
		IBIW	> 16.5	< 38.9	< 28.7

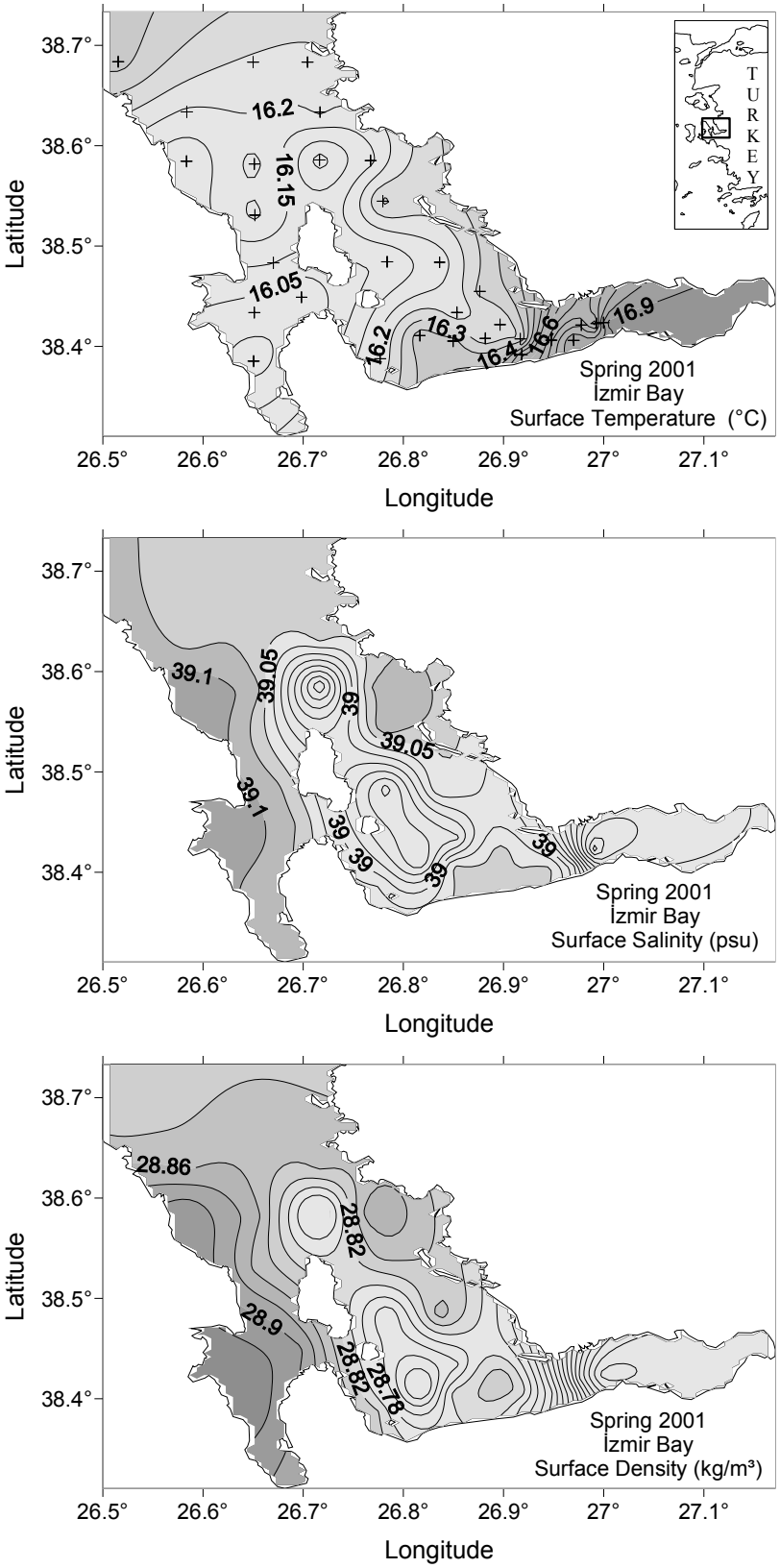

Figure 3.51 The horizontal distribution of surface temperature of İzmir bay in spring 2001.

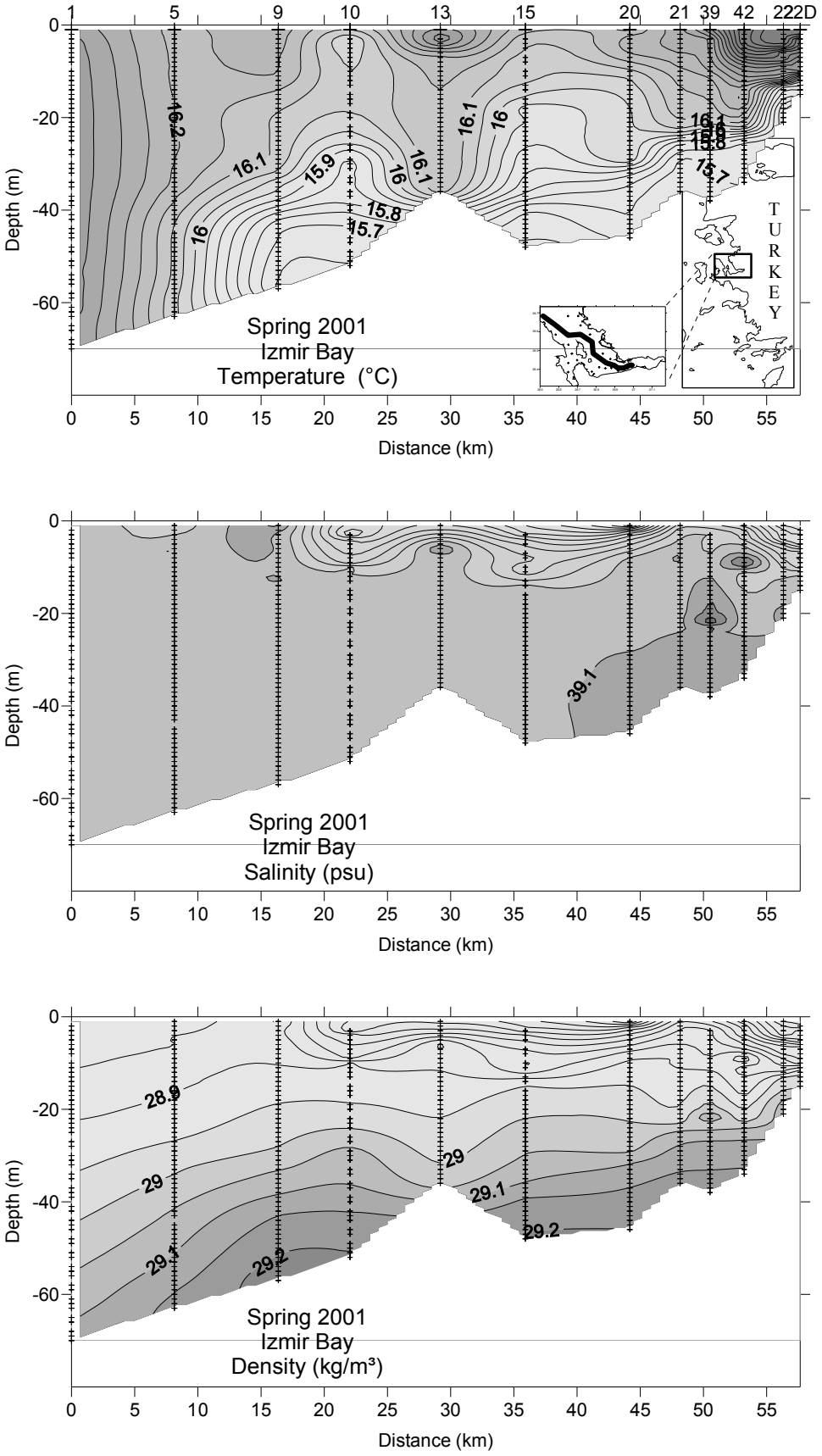

Figure 3.52 The temperature, salinity and density vertical section of İzmir Bay in Spring 2001.

3.4.6.2 Winter 2002

The water properties of the bay are analyzed using the data retrieved from 34 stations in a period of winter 2002 cruise (13-14.02.2002) (Figure 3.53-3.56). Although the prevailing wind is from the southerly direction, it does not blow consecutively more than six hours. Therefore, the Bay is not under the influence of the wind alone. It is under the influence of thermohaline and wind forces together. The middle part is relatively colder than the other part of the İzmir Bay. It could be due to the existance of cyclonic gyre seen frequently over the area in case of southerly winds. This cyclonic gyre is very important for the bay. Firstly, it brings nutrient rich water to the surface. Secondly, it is the source of the IBW water masses of the bay itself distinctively different than ASW and IBIW (Figure 3.54). Traces of the ASW can be observed even in the Middle Bay. The temperature decreases gradually from Outer Bay towards the Inner Bay (Figure 3.55 and 3.56).

The IBIW mass is colder and less saline than the other water masses and the ASW is warmer and more saline than the water masses of other regions. ASW and IBW show a homogenous vertical distribution due to the winter convection and wind mixing. IBIW is stratified due to fresh water discharges to the Inner Bay. Levantine waters are not observed in the bay in the winter 2002. The temperature values of the bay are low in comparison to the usual temperature values of Levantine. Another probable water mass, the Central Aegean Intermediate Water (CAgIW) mass does not seem to have an influence directly on the bay. This is obvious from the low density values of ASW.

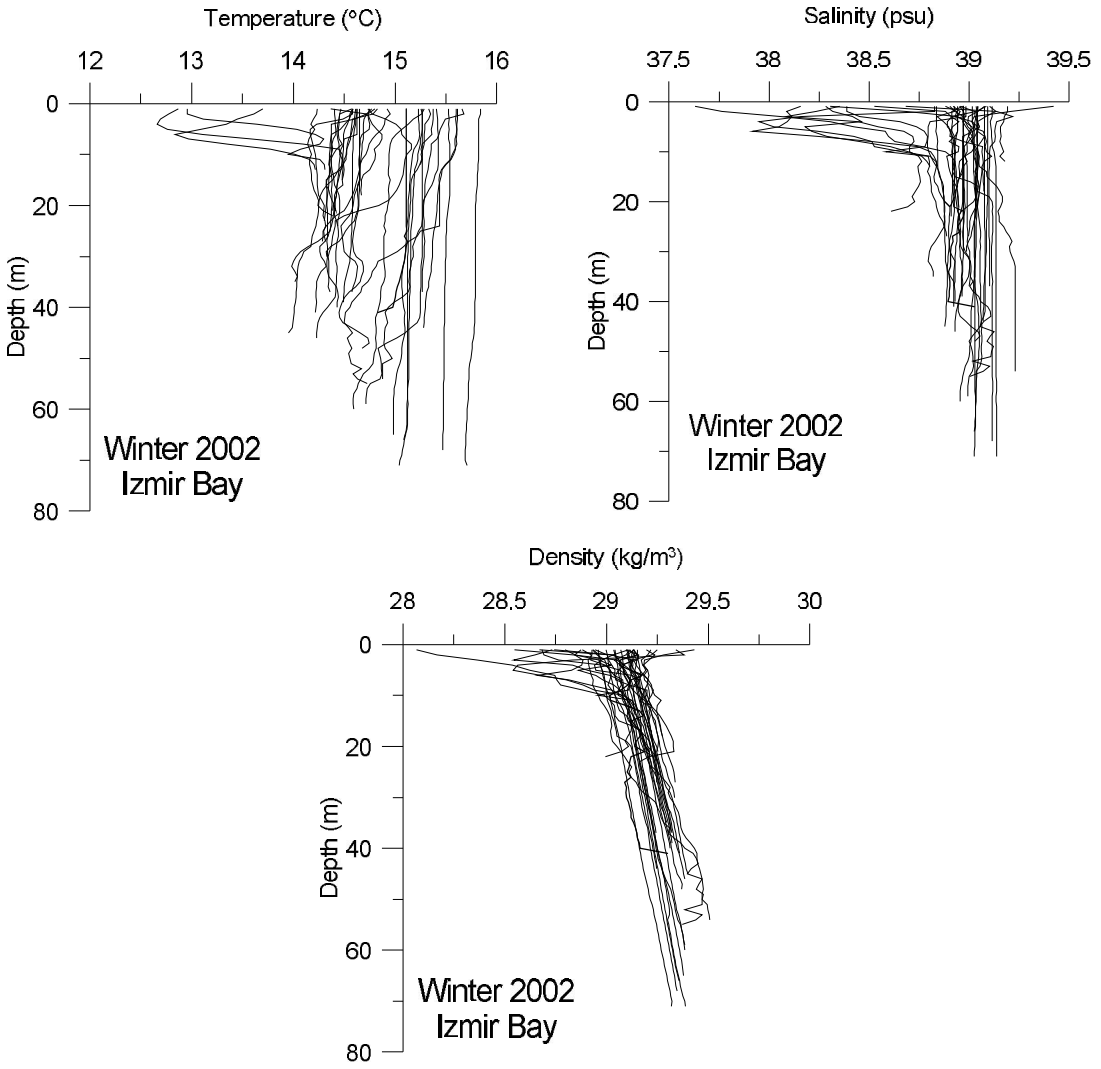

Figure 3.53 Temperature, salinity and density profiles of İzmir bay in winter 2002.

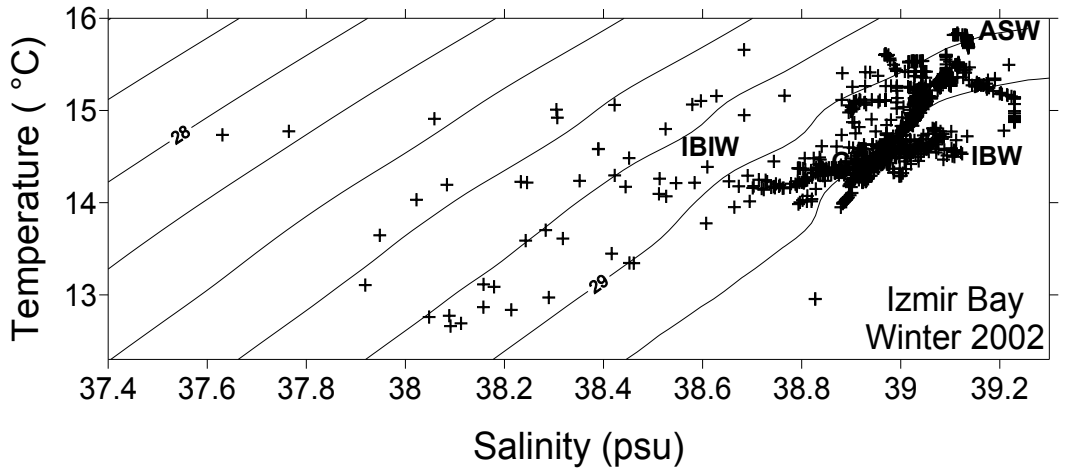

Figure 3.54 θ-S diagram of winter 2002 (İzmir Bay).

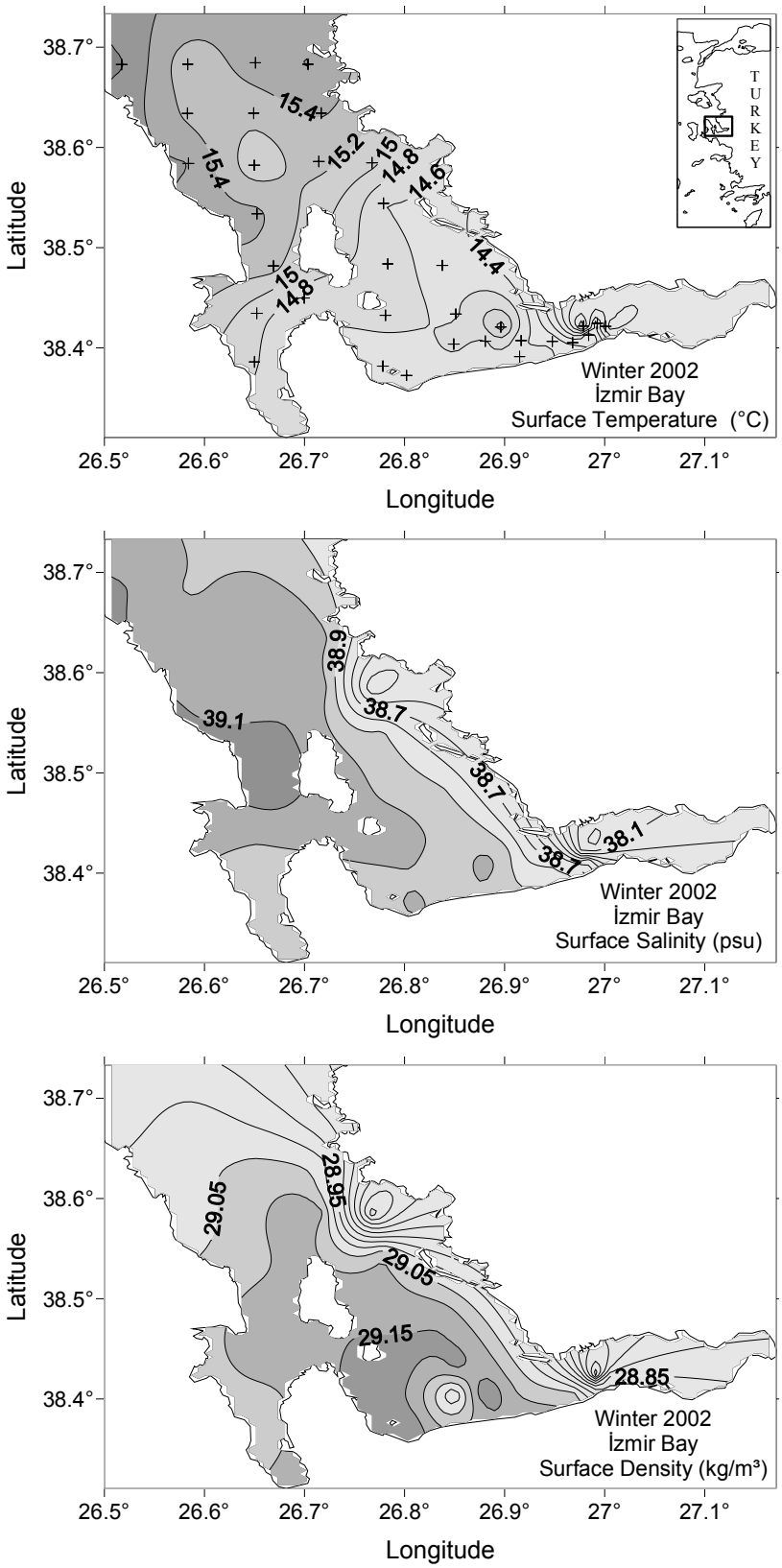

Figure 3.55 The horizontal distribution of surface temperature of İzmir bay in winter 2002.

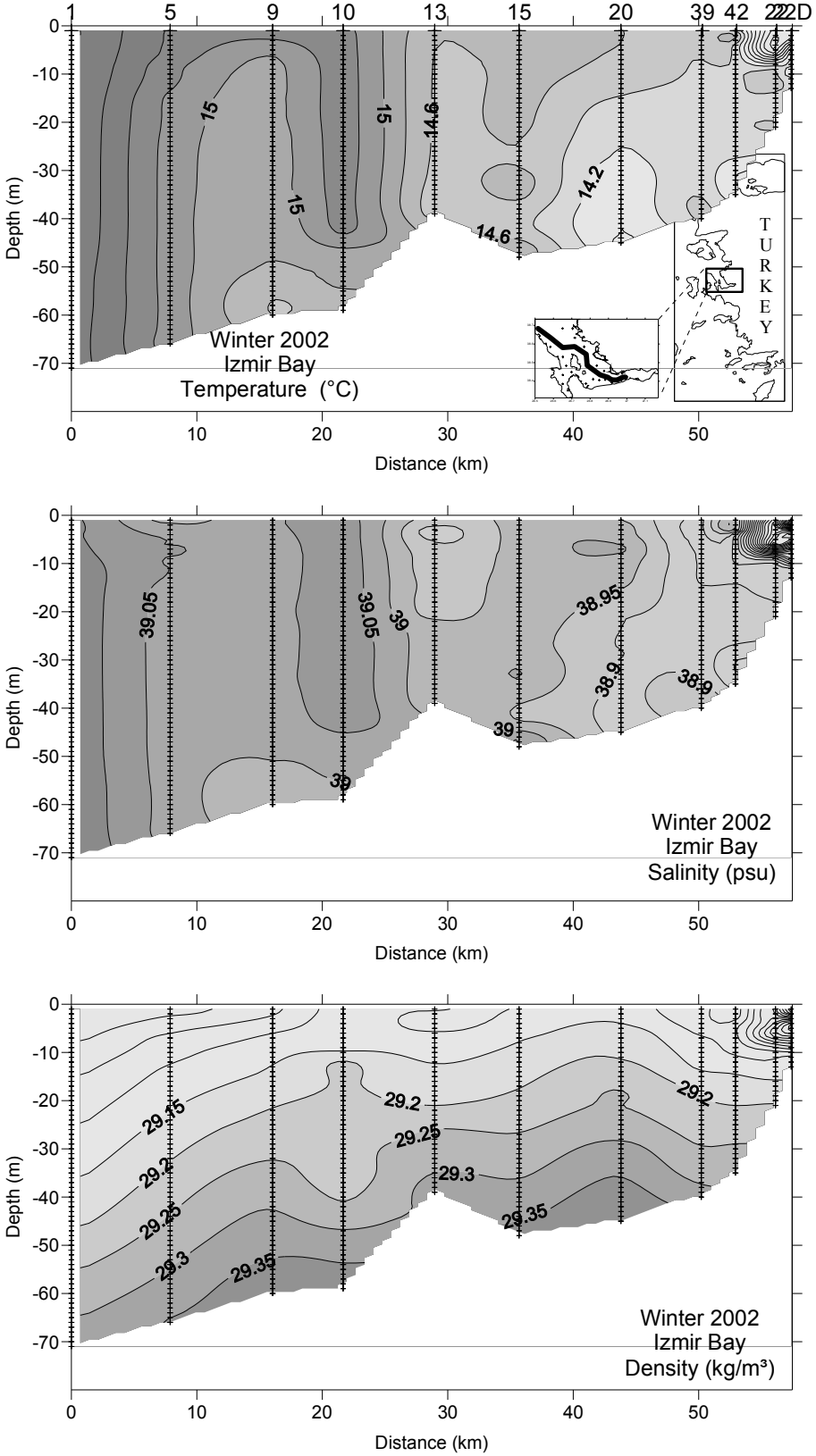

Figure 3.56 The temperature, salinity and density vertical section of İzmir Bay in Winter 2002.

Table 3.4. The water masses existing in the İzmir bay and their range in winter 2002.

		Winter 2002		
	Water mass	Temperature (°C)	Salinity (psu)	Density (kg/m³)
IZMİR BAY	ASW	> 15.7	39.14	29.32
	IBW	14.0	38.88	29.4
	IBIW	< 14.1	< 38.7	< 28.9

3.5 Kuşadası Bay

3.5.1 Study Area

The Kuşadası Bay is a small gulf and strait in the Aegean Sea, separating the Greek island of Samos from the mainland of Turkey (Figure 3.57).

3.5.2 Meteorological Conditions

The meteorological data from Kuşadası Meteorological Centers for Kuşadası Bay area were recorded as hourly and include wind speed, wind direction, air temperature, precipitation, evaporation, relative humidity and air pressure. Figure 3.58-3.65 show the weather condition in the Kuşadası Bay, Turkey.

The temperature difference reaches approximately 20 °C between the summers and winters (Figure 3.58). The maximum value ever measured in hourly data is 41.5 °C in August 2007 and minimum value is -8.4 °C in December 2007. The average over 46 year (between 1964 and 2010) is 16.95 °C.

The time series of yearly averaged data (Figure 3.58 bottom panel) shows negative air temperature anomalies before 1993 after positive anomalies up to 1994. Air temperature anomaly gradually increases after 1994 as a result of global warming. The very dense water formation period in the Aegean Sea is between 1990 and 1994. High excess air temperature could be one of the reasons for the relaxation of forming dense water in the Aegean Sea.

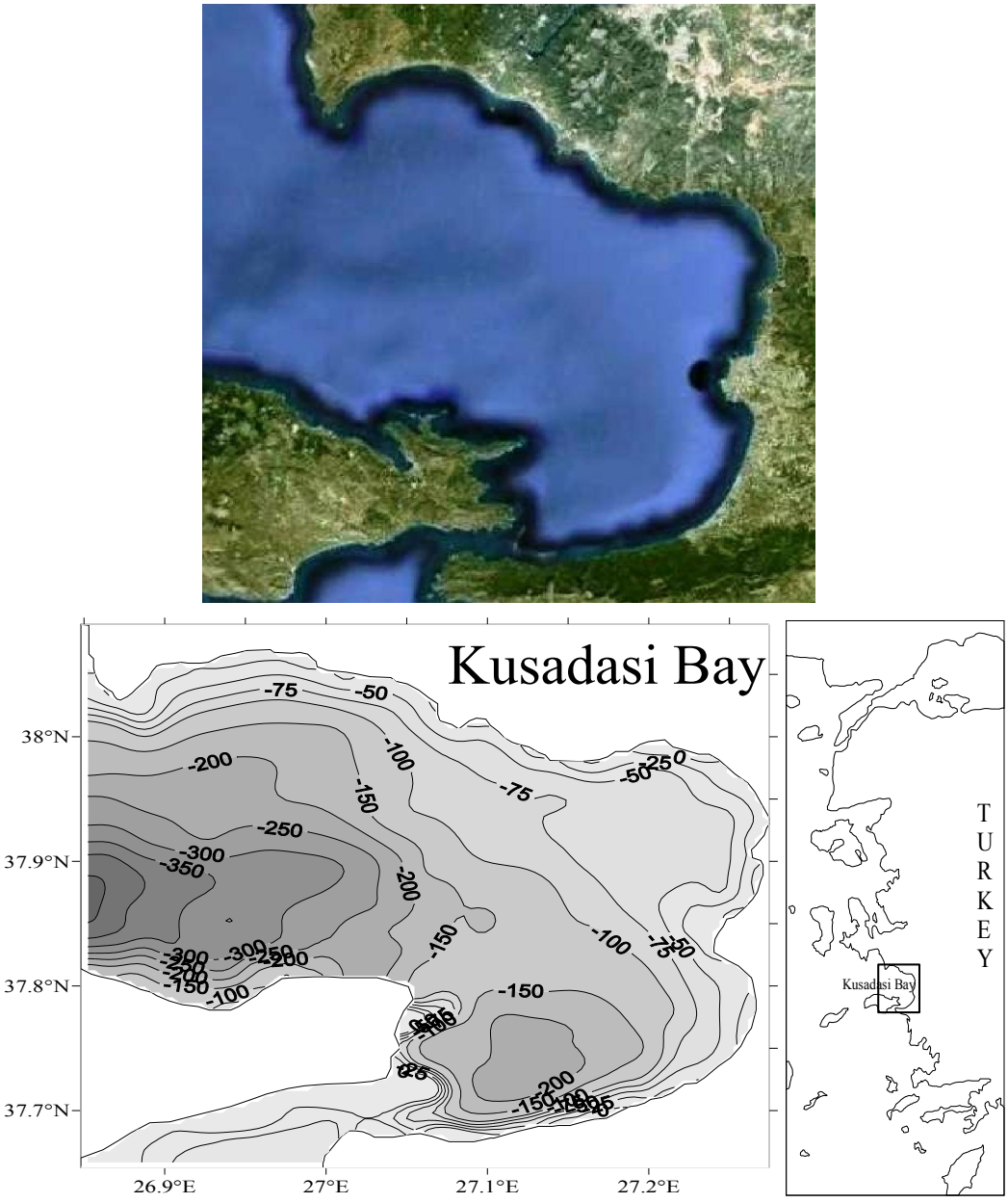

Figure 3.57 The view from Google Earth, bottom topography (from GEBCO, 2008 grided data) and location of the Kuşadası Bay.

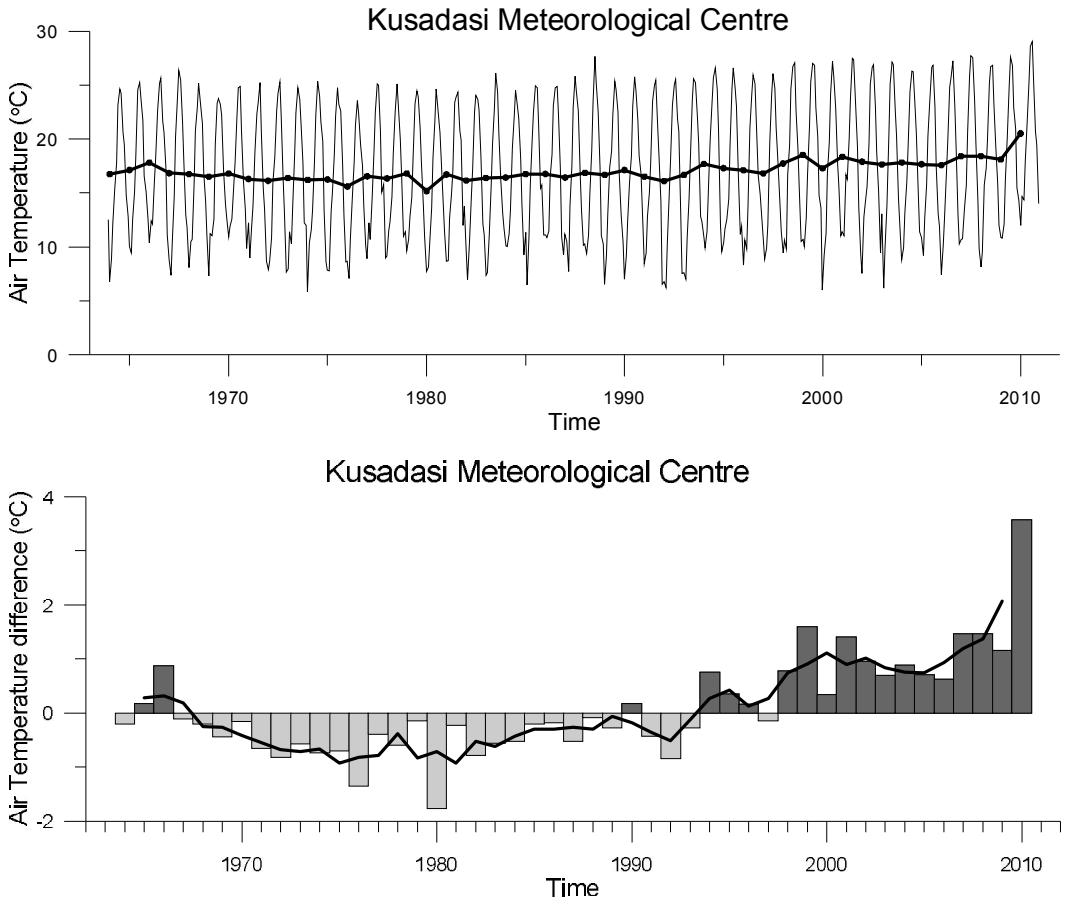

Figure 3.58 Time series of monthly average (thin line) and annual mean (thick line) air temperature (°C) (top), and yearly anomaly time series (bars) with moving averages (thick line) (bottom) for the Kuşadası Bay.

Hourly precipitation data is retrieved from Kuşadası Meteorological Center. Monthly averaged precipitation data for the years 1939-2010 is shown in Figure 3.59. The maximum value ever measured in hourly data is 113.80 mm in October 1977. The average over 71 year is 8.62 mm. The rainfall is minimum in the months of late summer and early fall according to monthly averaged values.

The precipitation anomaly values (Figure 3.59 bottom) are greater than the averaged one until late 1960s. The data generally shows negative anomalies after. Precipitation time series and anomalies of Kuşadası Bay are not much different than the other Bays along the eastern Aegean cost. Precipitation data (Figure 3.59 bottom) shows negative anomalies around the year 1990.

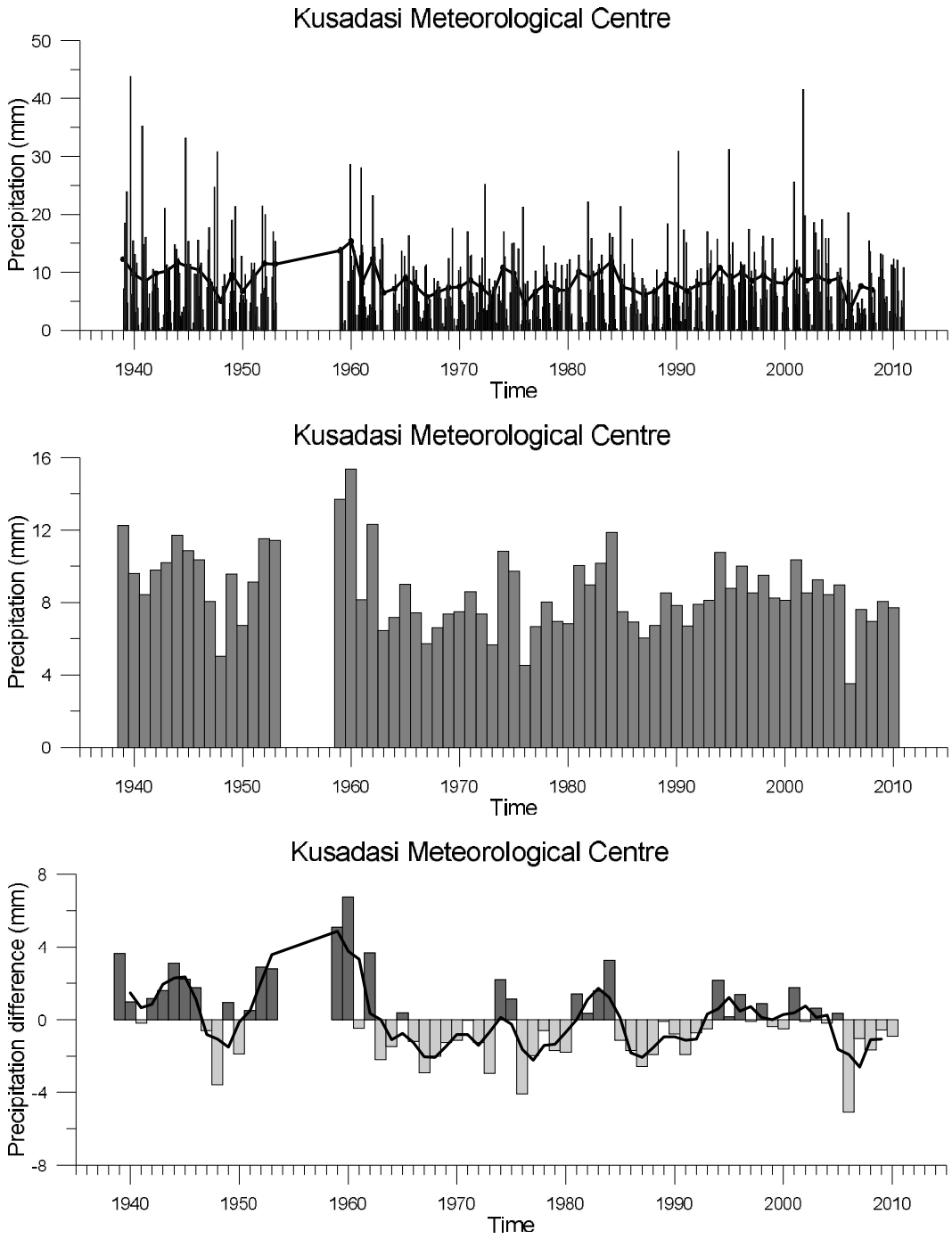

Figure 3.59 Time series of monthly averaged (top), annual mean precipitation (center) and yearly anomaly time series (bars) with moving averages (thick line) (bottom) for the Kuşadası Bay.

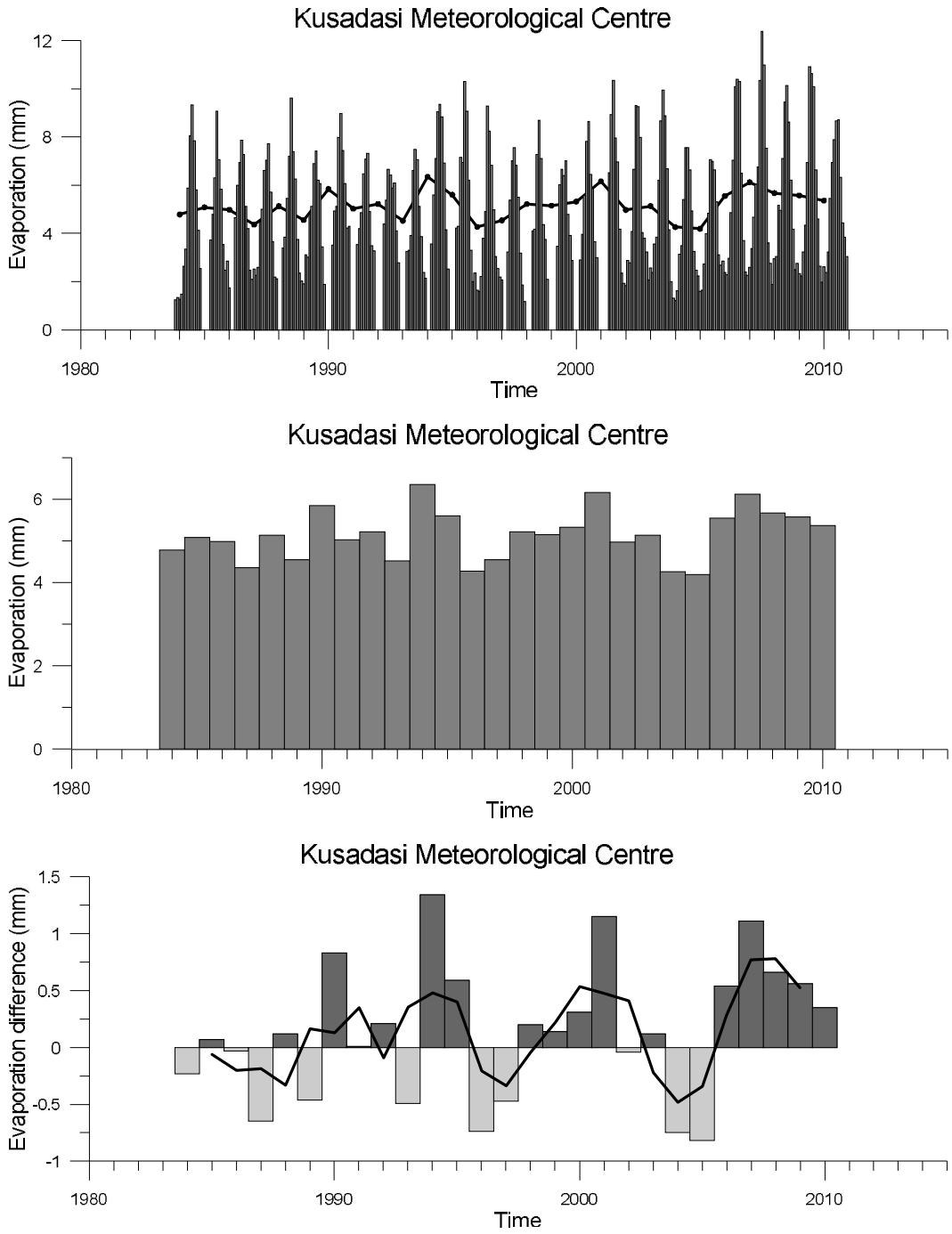

Figure 3.60 Time series of monthly averaged (top), annual mean evaporation (center) and yearly anomaly time series (bars) with moving averages (thick line) (bottom) for the Kuşadası Bay.

Hourly evaporation data is retrieved from Kuşadası Meteorological Center for the years 1984-2010. Monthly averaged values are shown in Figure 3.60. The maximum evaporation value ever measured in hourly data is 23.20 mm in August 2007. The

average over 26 year is 5.01 mm. The evaporation is minimum (1.18 mm) in winter and the maximum (12.37 mm) is in summer according to monthly averaged values.

Time series are used to see long-term trend in the evaporation data. Anomaly time series was usedthe time series of deviations of a quantity from mean of the all data (Figure 3.60 bottom). Evaporation anomaly does not show clear low values around 1990. Kusadası evaporation data set is not as long as the data of other bays are. This can be the reason that the negative anomalies can not be seen in the mean EMT time depending on the changing average value.

Hourly humidity data is retrieved from Kuşadası Meteorological Center for the years 1939-2010. Monthly averaged humidity time series is shown in Figure 3.61. The average relative humidity over 71 year is % 65.76 mm. The humidity is minimum (% 37.37) in summer and the maximum (% 84.88) is in winter according to monthly averaged values.

Anomaly time series (Figure 3.61, bottom panel) shows positive humidity anomalies before 1990s and after then negative anomalies. The negative anomalies make peak in 1999 and gradually increases after.

The highest pressure value ever recorded in Kuşadası area is 1035.1 mbar in February 2008 and lowest value is 843.0 mbar in February 2004. The average over 44 year (between 1966 and 2010) is 1011.36 mbar (Figure 3.62).

Anomaly time series of pressure data (Figure 3.62, bottom panel) shows similar evolution of high positive pressure anomalies observed in almost all bays during the years from 1989 until 1994. It is thought to be that it must have strong relation with EMT event effecting wind condition over the area.

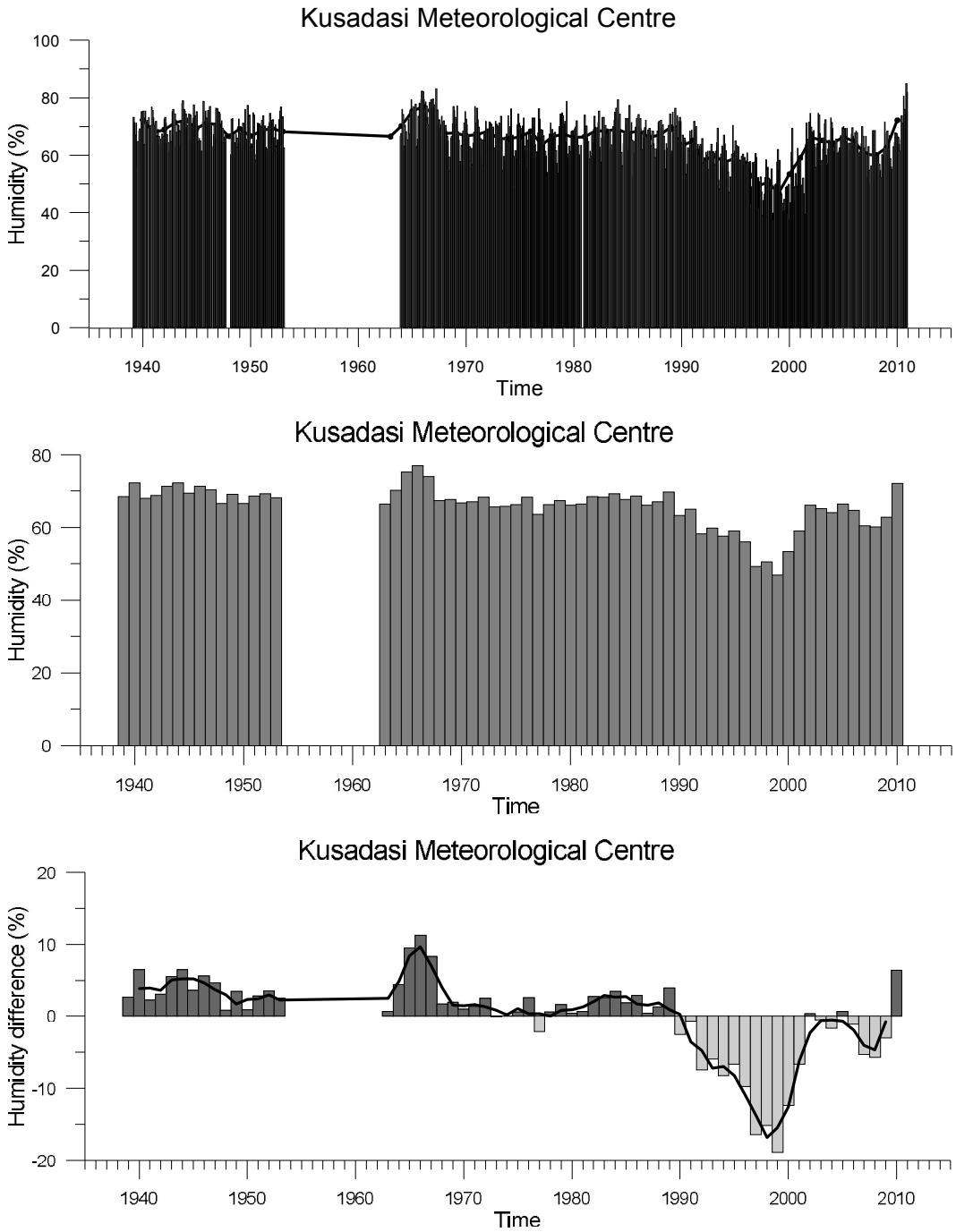

Figure 3.61 Time series of monthly averaged (top), annual mean humidity (center) and yearly anomaly time series (bars) with moving averages (thick line) (bottom) for the Kuşadası Bay.

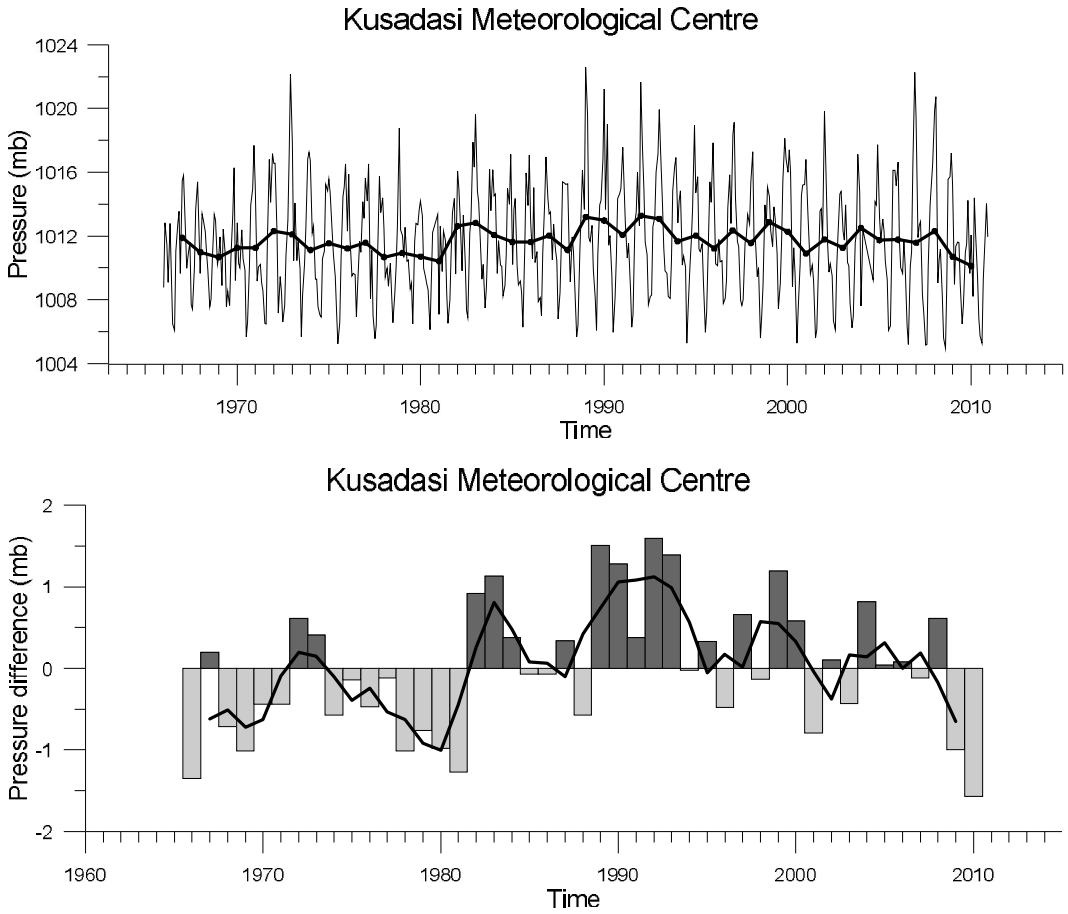

Figure 3.62 Time series of monthly average (thin line) and annual mean (thick line) pressure (mb) (top), and yearly anomaly time series (bars) with moving averages (thick line) (bottom) for the Kuşadası Bay.

3.5.3 Wind Analysis

In the region, wind from SE direction dominates throughout the years with an average speed of 2.37 m/s is shown in Figure 3.63.

The prevailing wind over the Kuşadası area is SE direction shown in the wind-rose map in Figure 3.63. Wind vectors of the monthly time series of wind speed and direction anomalies for 1967-2010, depending on the availability of the data, were constructed from hourly wind measurements in the Kuşadası Meteorological Centre. The wind vectors of the monthly prevailing wind with average wind speed values for Kuşadası Bay data from Kuşadası Meteorological Centre is shown in Figure 3.64. The wind intensities are low starting from 1985 until 1992. The frequently seen

direction is N in early 1990s. The wind vectors for the wind blowing more than 12 hours show also the N direction in the same period. Figure 3.65 indicates that the direction of the lasting wind most of time has no agreement with the prevailing wind direction seen over the Kuşadası region.

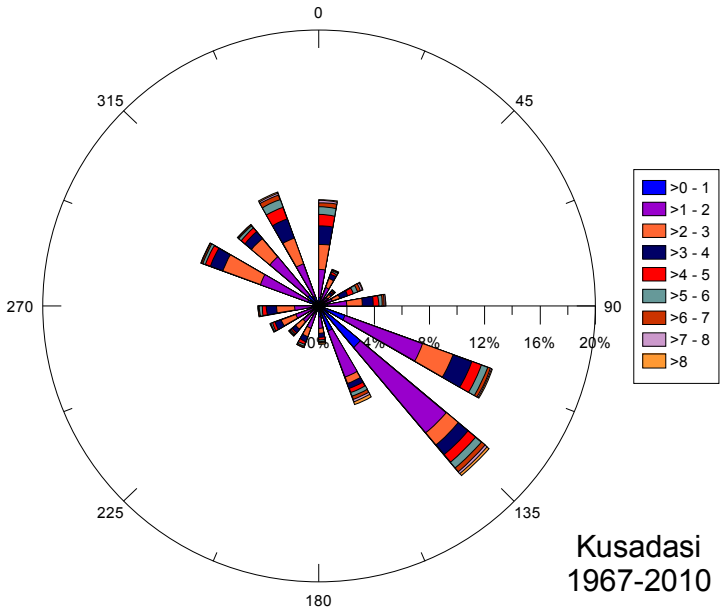

Figure 3.63 Wind chart of the prevailing wind for Kuşadası Bay data from Kuşadası Meteorological Centre.

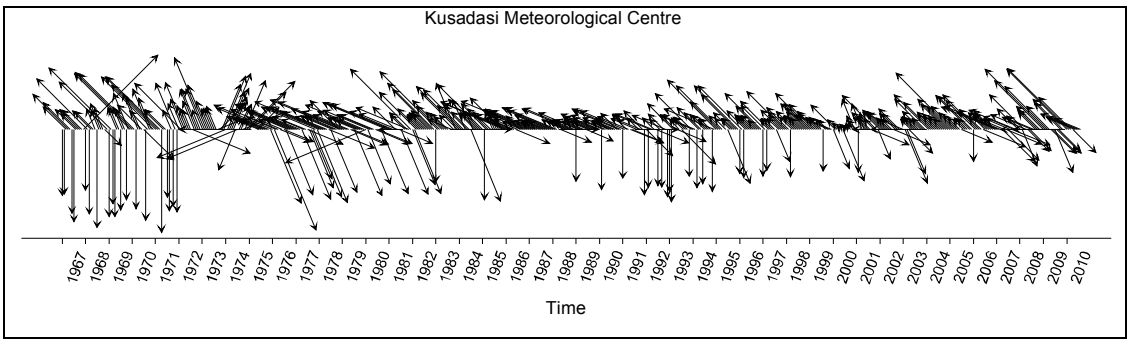

Figure 3.64 Wind vectors of the monthly prevailing wind with average wind speed values for Kuşadası Bay data from Kuşadası Meteorological Centre. (V_{max}=16.6 m/s).

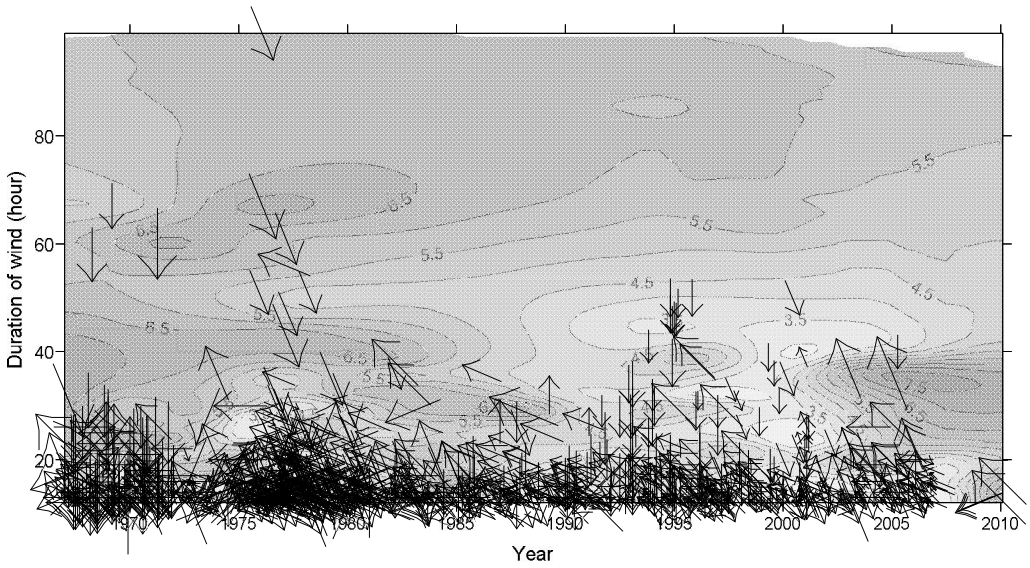

Figure 3.65 The wind vectors for the wind blowing more than 12 hours drawn on the average wind field.

3.5.4 Time Series of the Kuşadası Bay

Time series are analyzed by profiles of temperature, salinity and density from several cruises in the Kuşadası bay extending from 1991 to 2009.

The time evolution of water masses were analyzed using the data from the shallower and the deeper part of the Kuşadası Bay. The temperature and salinity values are higher in general in the shallower part compare to the temperature and salinity in the deeper part of the Kuşadası Bay. The temperature influence is more on the densities namely less dense water can be observed in the shallower area. The isopycnal of 28.6 kg/m3 shoals near surface in spring 1992 and deepens to the depth of 10m, 20m and 30m in the spring 1993, 1995 and 2007 respectively. Deepening of the isopycnals has one exception in spring 1996. Although the main water mass structure evolves, the scarce of data does not allow all EMT periods to present. It is difficult to recognize the major deep dense water formation and relaxation periods clearly in Kuşadası Bay.

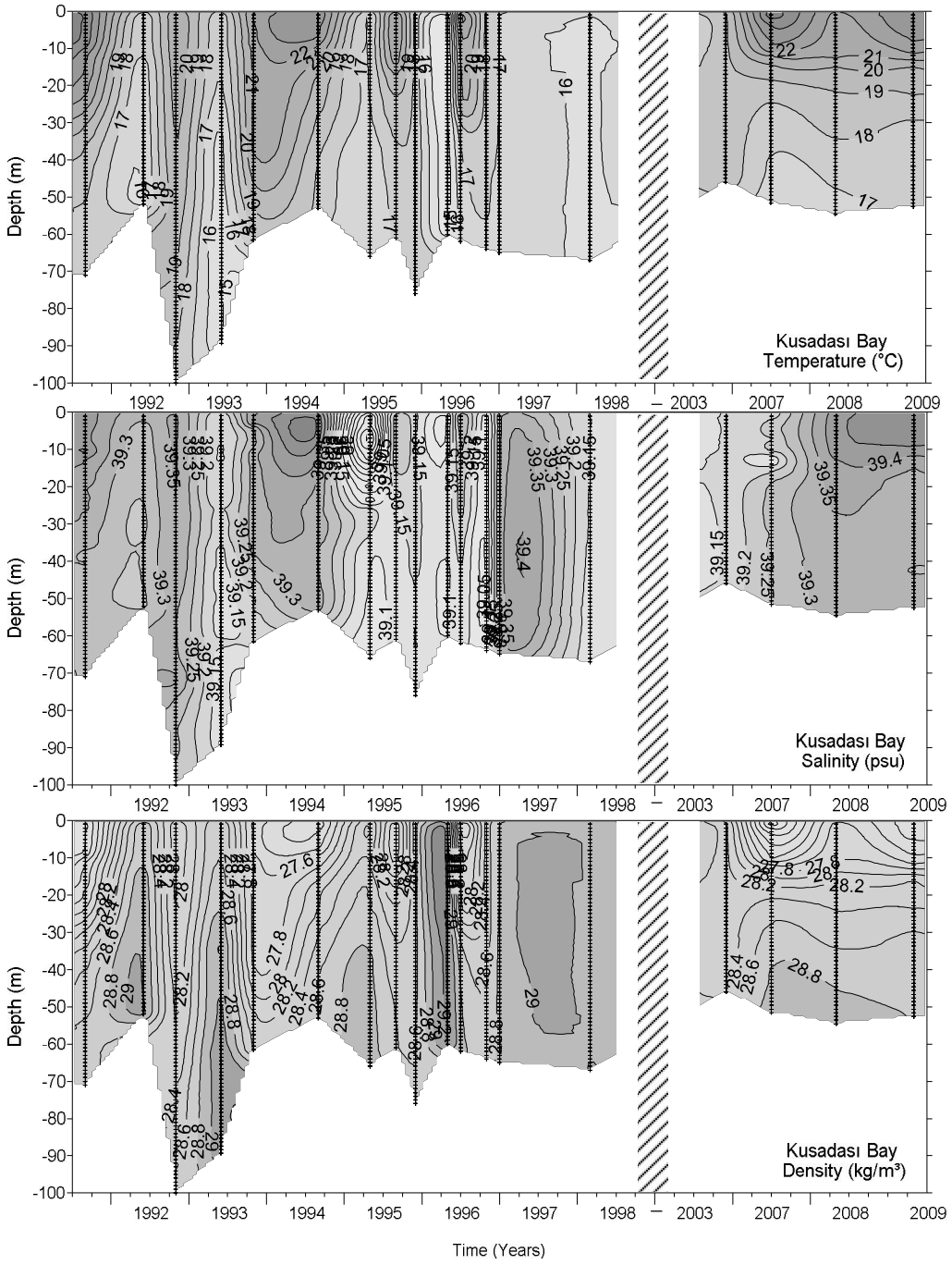

Figure 3.66 Temporal evaluations of temperature, salinity and density fields of Kuşadası region (Shallow part) starting from 1991 up to 2009. The areas in white represent where data was not collected.

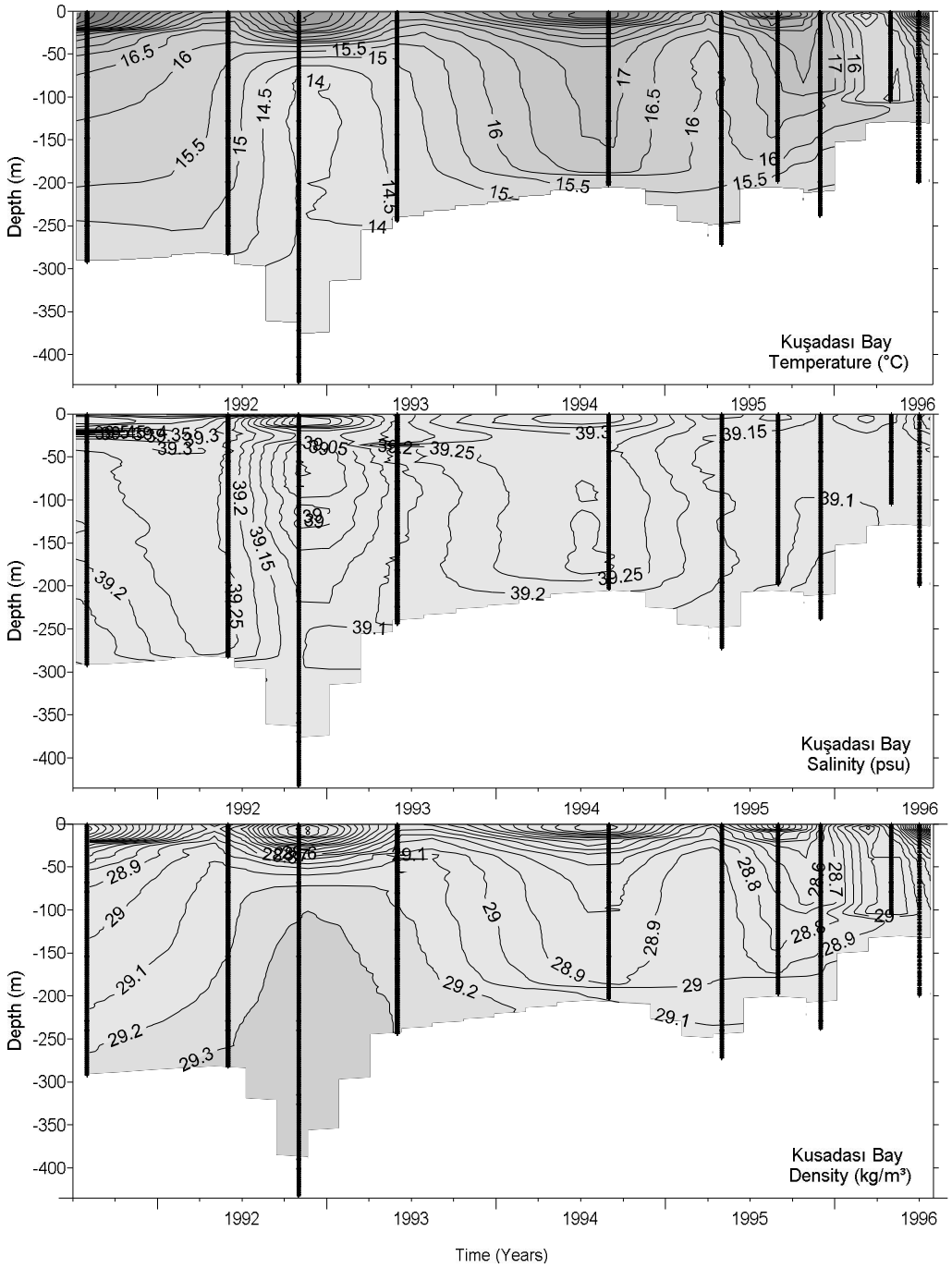

Figure 3.67 Temporal evaluations of temperature, salinity and density fields of Kuşadası region (Deeper part) starting from 1991 up to 2009. The areas in white represent where data was not collected.

LIW penetrates into the shallow area around peak period in the depth of greater than 50m with density more than 29.0 kg/m3. The LIW penetration is obvious at 50m for deeper part in spring 1992. It is seen that the CAgIW flows reverse direction towards south as a result of two-layered system. It can be understood from cold and

dense water mass produced in the Central Aegean Sea under LIW. This cold and dense water mass looses its influence in time. It can not be observed any more after the major dense water formation period (1993) in the deeper part of Kuşadası Bay. The surface temperature increases reducing the surface density because of increasing air temperature (Figure 3.66) at the same time the surface salinity increases due to the excess evaporation (Figure 3.67) in Kuşadası region in the last years especially for shallow part.

3.6 Güllük Bay

3.6.1 Study Area

The Güllük Bay which is a small bay in the Aegean Sea is shown in Figure 3.68

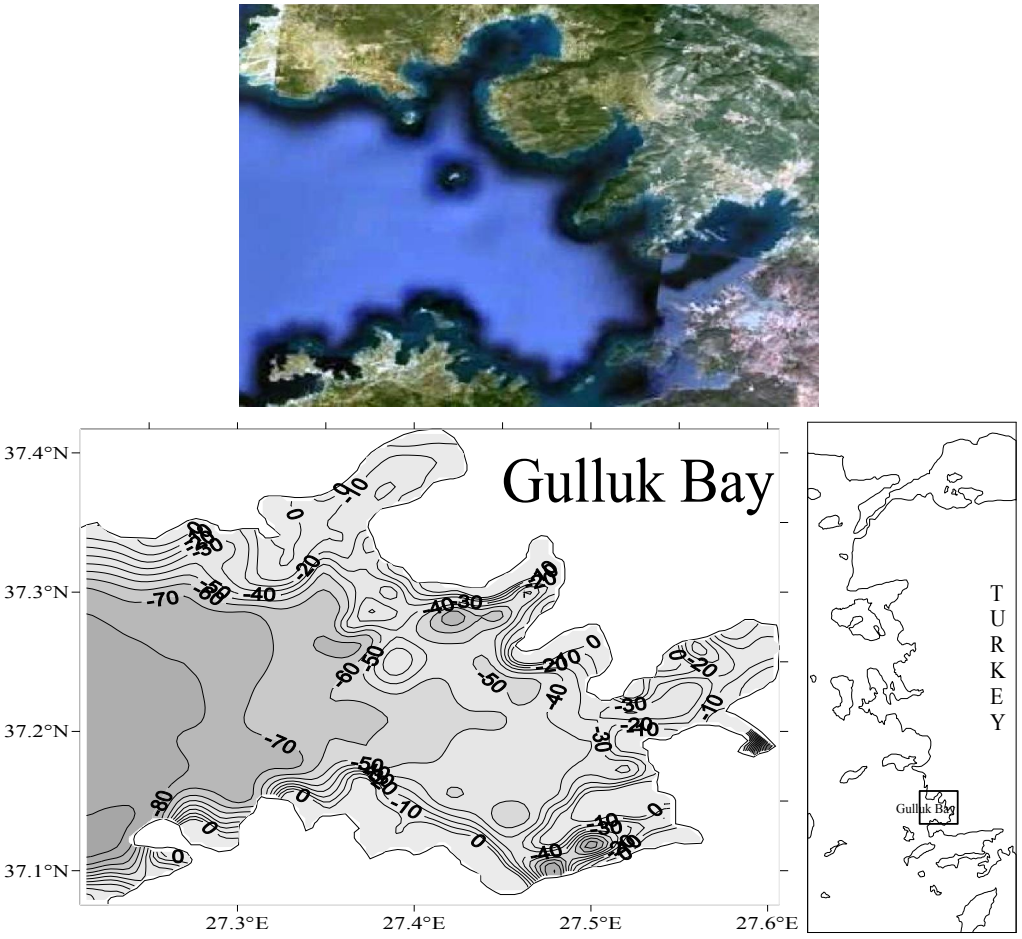

Figure 3.68 The view from Google Earth, bottom topography (from GEBCO, 2008 grided data) and location of the Güllük Bay.

3.6.2 Meteorological Conditions

Hourly weather data including wind speed, wind direction, air temperature, precipitation, evaporation, relative humidity and air pressure were retrieved from Didim Meteorological Center. Figs 3.69-3.74 show the weather measurements in the Güllük Bay, Turkey.

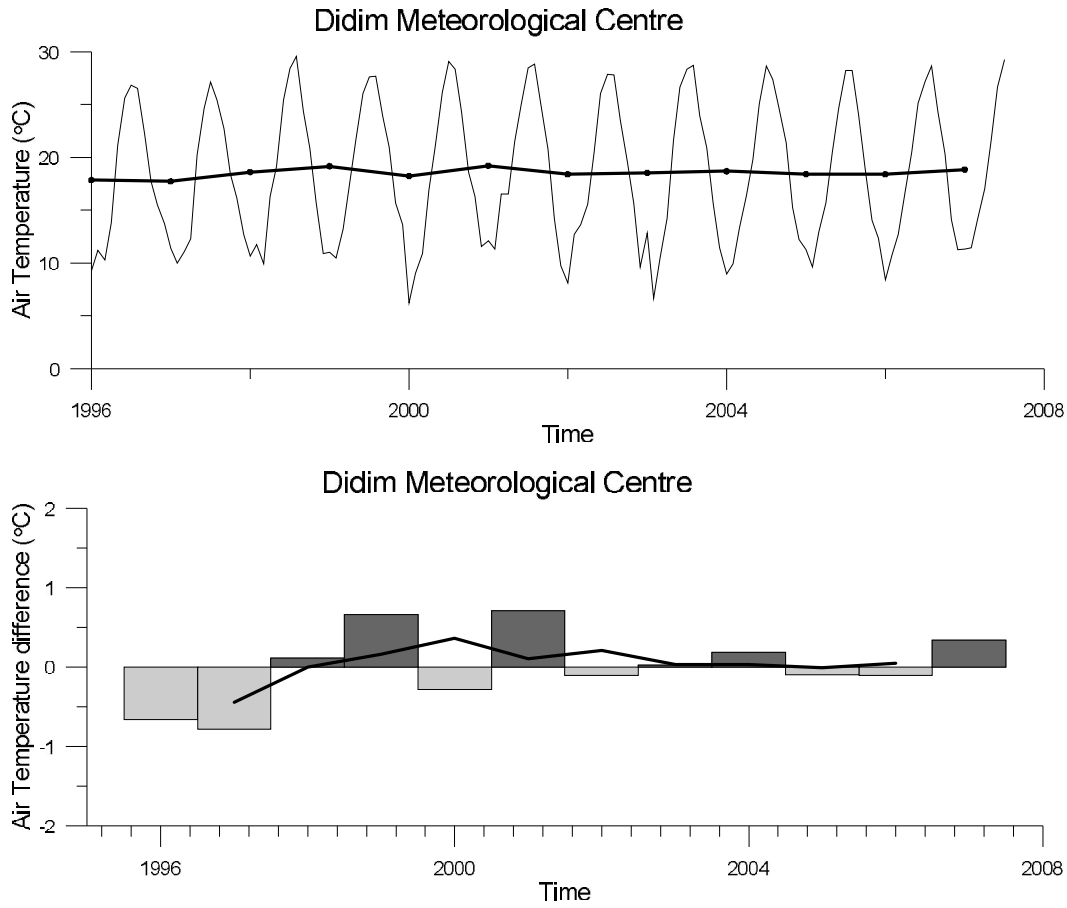

Figure 3.69 Time series of monthly average (thin line) and annual mean (thick line) air temperature (°C) (top), and yearly anomaly time series (bars) with moving averages (thick line) (bottom) for the Güllük Bay.

The temperature difference reaches approximately 20 °C between the summers and winters (Figure 3.69). The maximum value ever measured in hourly data is 43.4 °C in July 2007 and minimum value is -5.0 °C in February 2004. The average over 11 year (between 1996 and 2007) is 18.49 °C.

The time series of yearly averaged data (Figure 3.69 bottom panel) shows slight negative air temperature anomalies before late 1998 and after generally positive anomalies up to 2007.

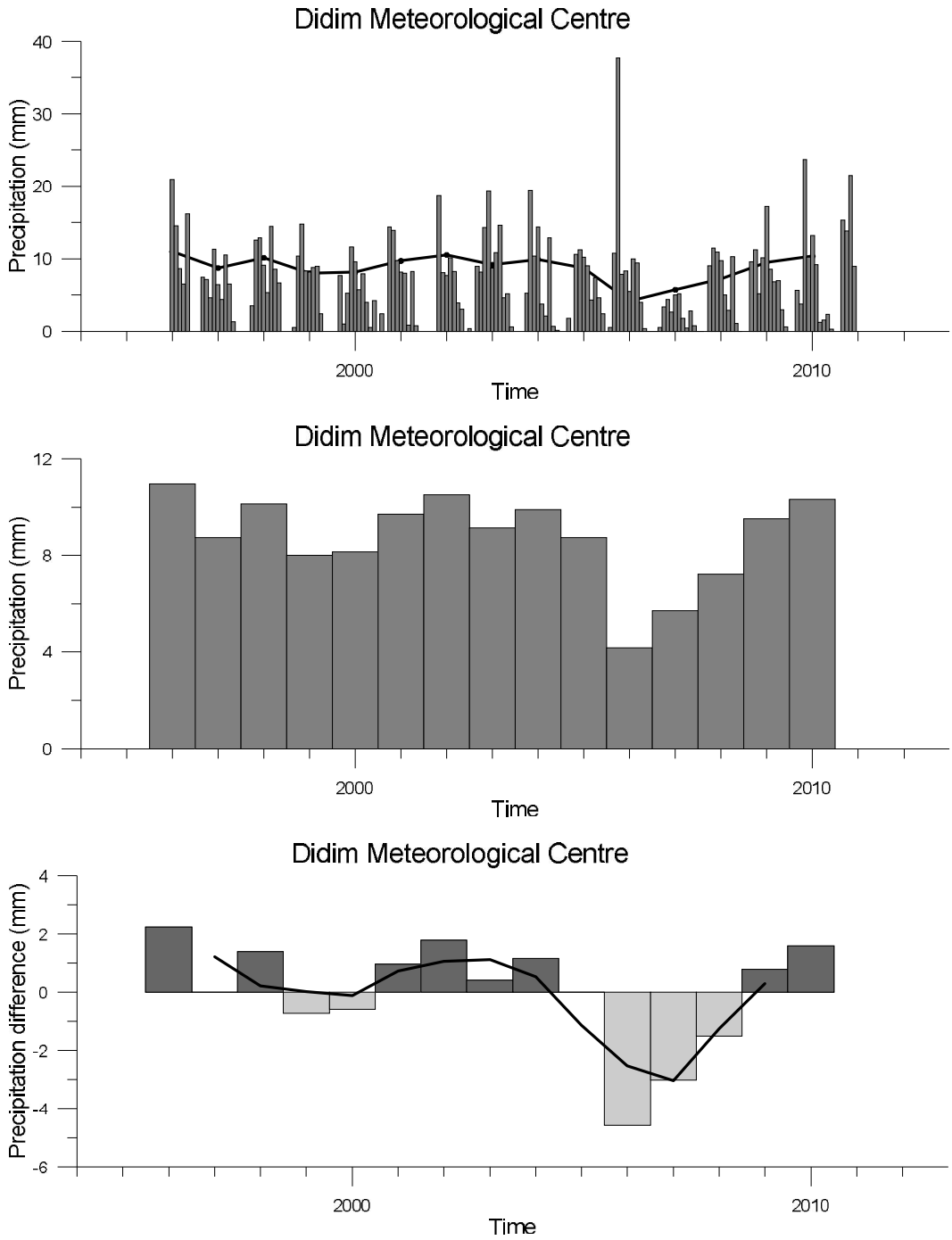

Figure 3.70 Time series of monthly averaged (top), annual mean precipitation (center) and yearly anomaly time series (bars) with moving averages (thick line) (bottom) for the Güllük Bay.

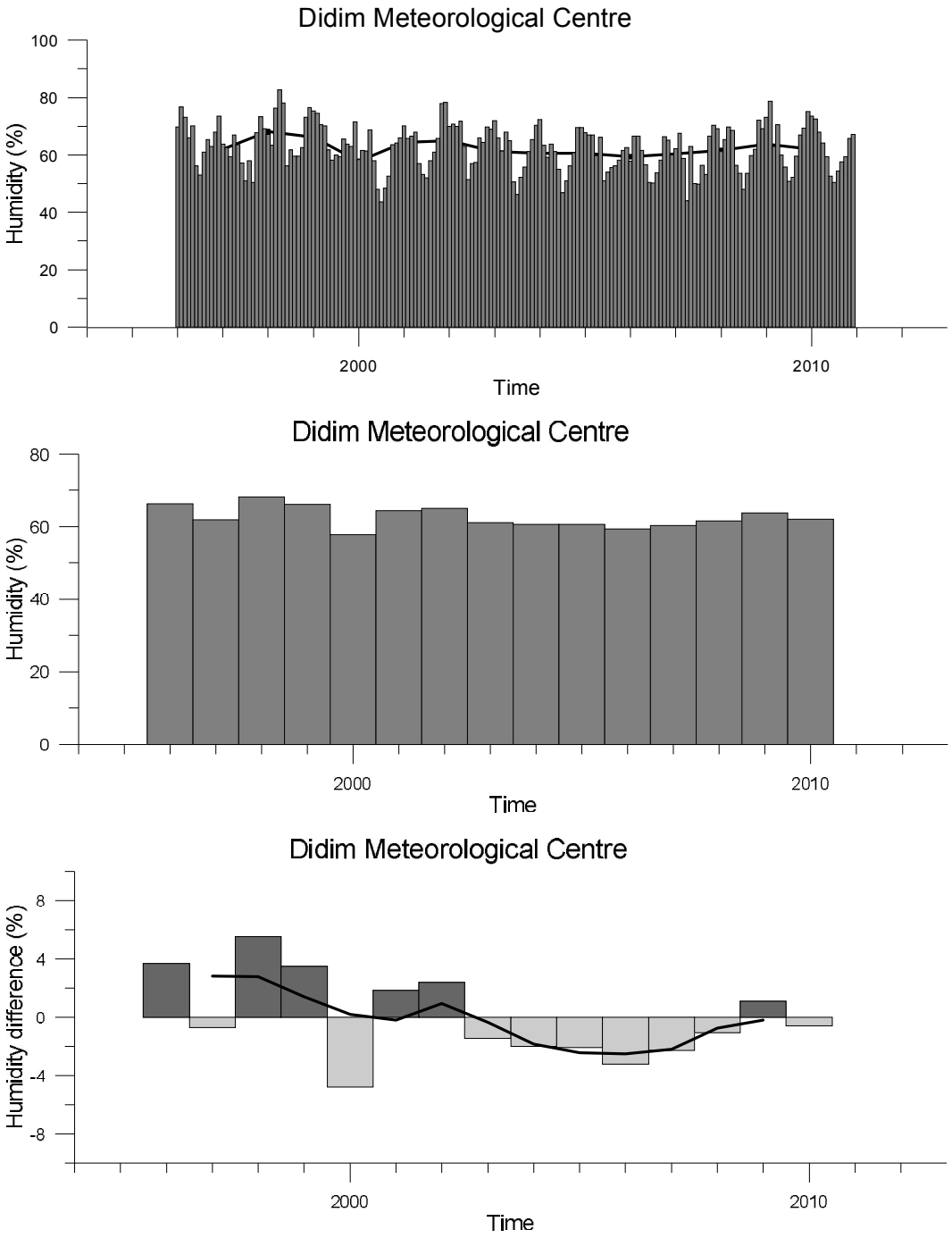

Figure 3.71 Time series of monthly averaged (top), annual mean humidity (center) and yearly anomaly time series (bars) with moving averages (thick line) (bottom) for the Güllük Bay.

Hourly precipitation data is retrieved from Didim Meteorological Center. Monthly averaged precipitation data for the years 1996-2010 is shown in Figure 3.70. The maximum value ever measured in hourly data is 116.20 mm in December 2002. The

average over 14 year is 8.73 mm. The rainfall is minimum in the months of late summer according to monthly averaged values.

Precipitation anomaly time series show peak negative anomaly in 2006 and the values increases gradually in the last years (Figure 3.70 bottom).

Hourly humidity data is retrieved from Didim Meteorological Center for the years 1996-2010. Monthly averaged humidity time series is shown in figure 3.71. The average relative humidity over 14 year is % 62.60. The humidity is minimum (% 43.69) in summer and the maximum (% 82.74) is in winter according to monthly averaged values.

Anomaly time series was used to see the deviations from the mean of the all data in time. The time series of yearly averaged data (Figure 3.71, bottom panel) shows positive humidity anomalies before 2002 and after negative anomalies up to 2010. The negative anomaly values are observed after 2002 probably affected by warm air.

The highest pressure value ever recorded in Güllük area is 1028.8 mbar in January 2007 and lowest value is 971.2 mbar in January 2004 (Figure 3.72). The average over 14 year (between 1996 and 2010) is 1009.55 mbar.

Anomaly time series was used to see the deviations from the mean of the all pressure data in time. The time series of yearly averaged pressure data (Figure 3.72, bottom panel) shows positive pressure anomalies during the years until 2004.

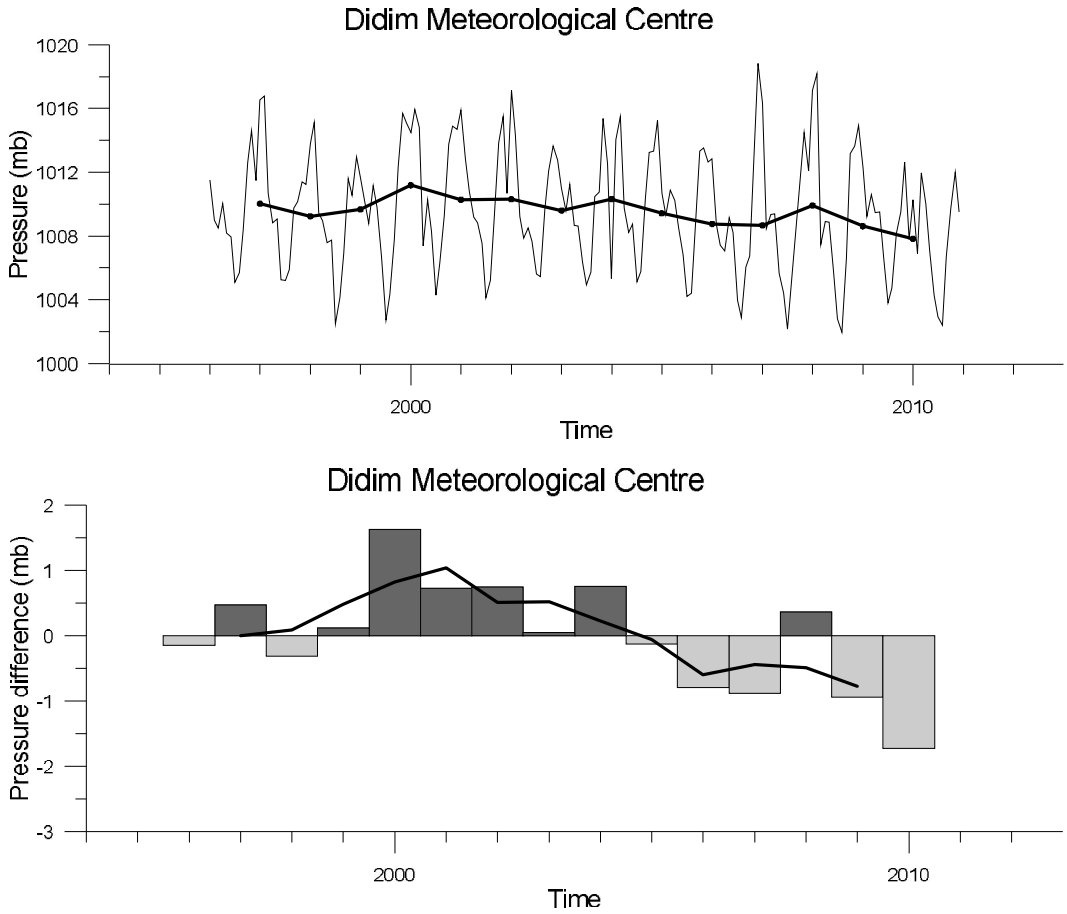

Figure 3.72 Time series of monthly average (thin line) and annual mean (thick line) pressure (mb) (top), and yearly anomaly time series (bars) with moving averages (thick line) (bottom) for the Güllük Bay.

3.6.3 Wind Analysis

In the region, wind from N direction dominates throughout the years with an average speed of 3.10 m/s is shown in Figure 3.73.

The prevailing wind over the Güllük area is N direction shown in the wind-rose map in Figure 3.73. Wind vectors of the monthly time series of wind speed and direction anomalies for 2007-2010, depending on the availability of the data, were constructed from hourly wind measurements in the Didim Meteorological Centre. The wind vectors of the monthly prevailing wind with average wind speed values for Güllük Bay data from Didim Meteorological Centre is shown in Figure 3.74.

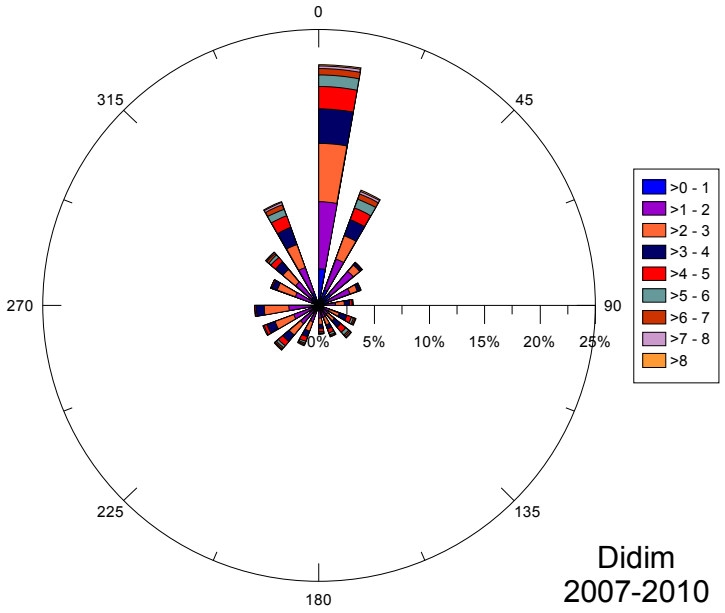

Figure 3.73 Wind chart of the prevailing wind for Güllük Bay data from Didim Meteorological Centre.

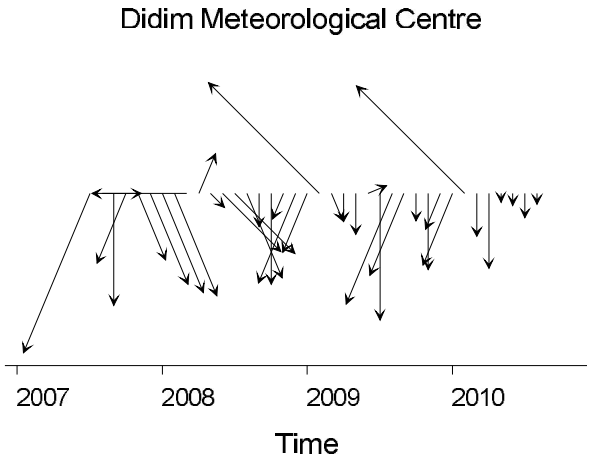

Figure 3.74 Wind vectors of the monthly prevailing wind with average wind speed values for Güllük Bay data from Didim Meteorological Centre. (V_{max}=8.07 m/s).

3.6.4 Time Series of the Güllük Bay

Time series are analyzed by profiles of temperature, salinity and density from several cruises in the Güllük bay extending from 1991 to 2009 (Figure 3.75).

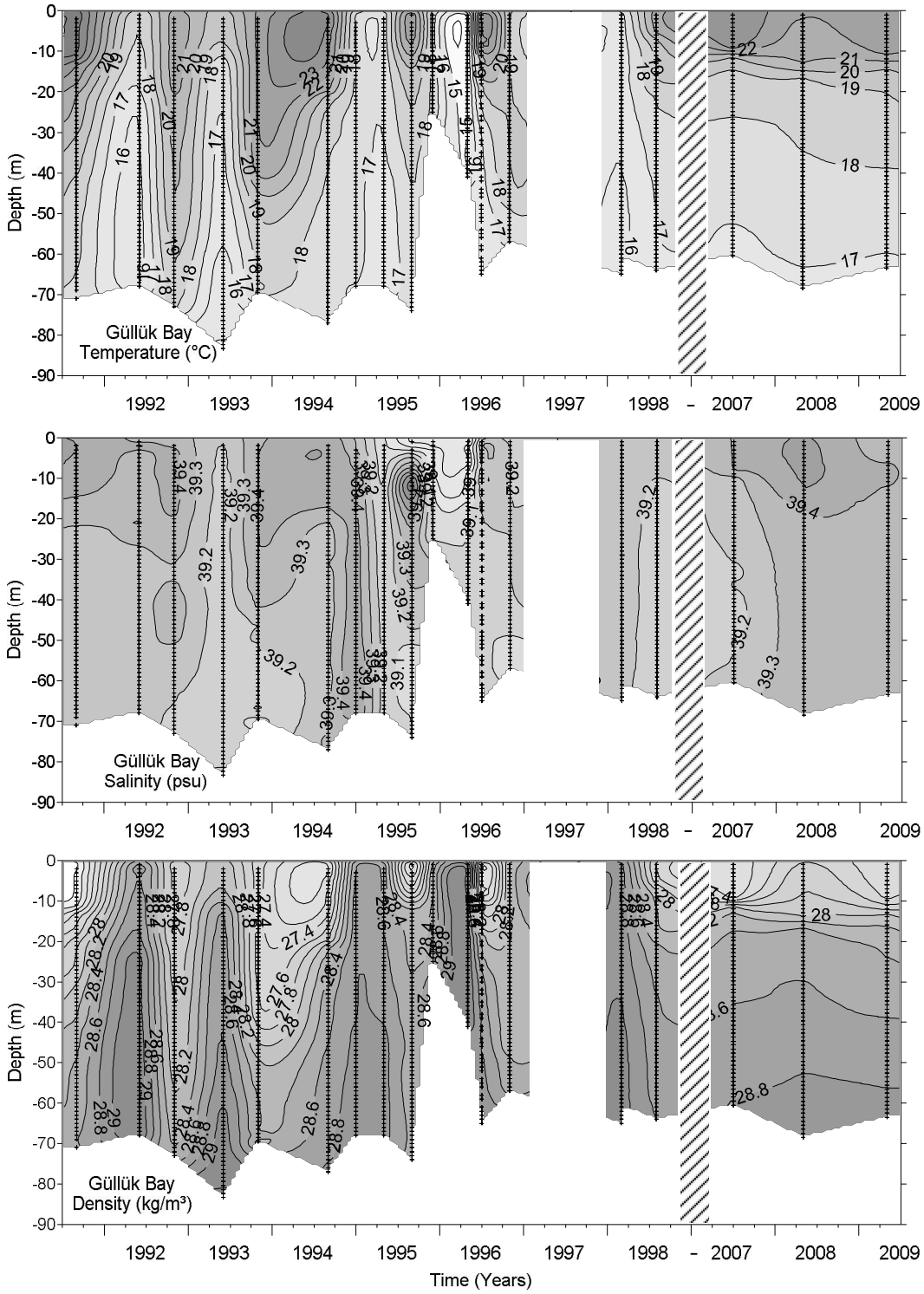

Figure 3.75 Temporal evaluations of temperature, salinity and density fields of Güllük region starting from 1991 up to 2009. The areas in white represent where data was not collected.

The Güllük and Kuşadası Bays show similar characteristics in the point of view of interannual variability of water masses. The isopycnal of 28.6 kg/m3 shoals near surface in spring 1992 and deepens to the depth of 5m, 15m and 35m in the spring 1992, 1993 and 2007 respectively. The water of Güllük Bay can be influenced by the water mass of Levantine origin even during spring 1995 and 1996. LIW (16 °C, 39.1 psu and 29.0 kg/m3) is seen in the depth greater than 25m and 60m before and after major peak time (winter 1993) respectively. LIW fills the surface of the Bay in spring 1996. The deepening of isopycnal of 28.6 kg/m3 continues and reaches up to 40m in spring 2009. Again the surface temperature increases reducing the surface density because of increasing air temperature at the same time the surface salinity increases due to the excess evaporation in Kuşadası region in the last years as observed in all bays.

3.7 Gökova Bay

3.7.1 Study Area

Gökova Bay, which is situated at the Southern Aegean Sea, as in a triangular form extending in the east-west direction (100 km long) between Bodrum on the northern and the Datça Peninsula on the southern part (Figure 3.76). It has two deep basin as eastern deep basin and western deep basin. The shelf depth reaches 104 m. The depth deepens to about 540 m. The oceanography of the Gökova Bay has not been studied until now.

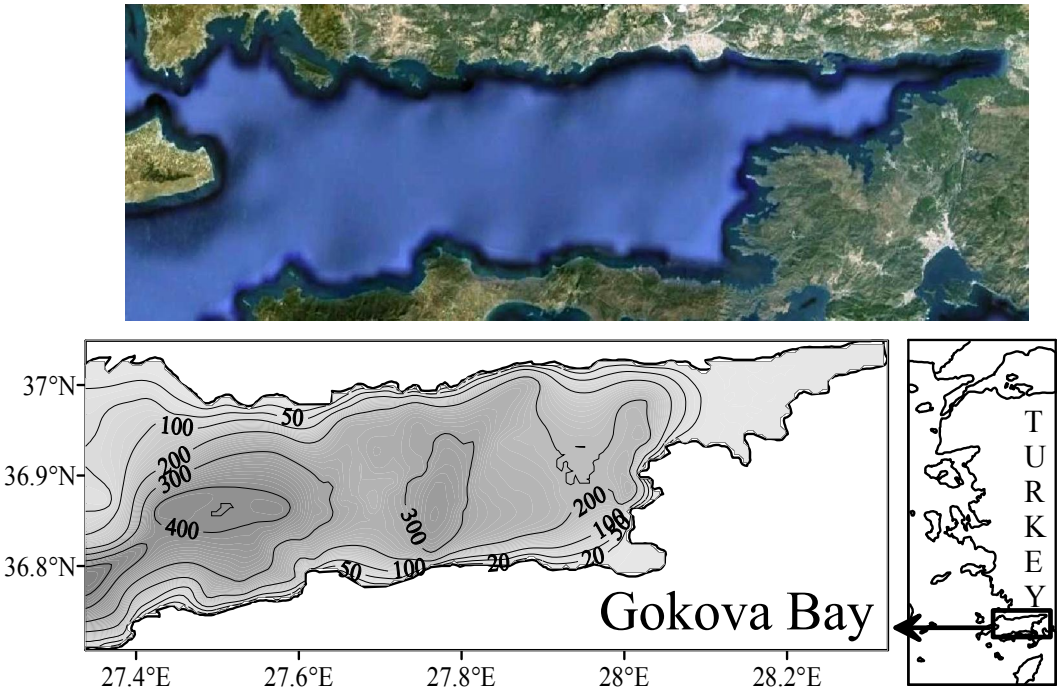

Figure 3.76 The view from Google Earth, bottom topography (from GEBCO, 2008 grided data) and location of the Gökova Bay.

3.7.2 Meteorological Conditions

The meteorological data from Marmaris Meteorological Centers for Gökova Bay area were recorded as hourly and include wind speed, wind direction, air temperature, precipitation, evaporation, relative humidity and air pressure. Figures 3.77-3.84 show the weather condition in the Gökova Bay, Turkey.

The temperature difference reaches approximately 20 °C between the summers and winters (Figure3.77). The maximum value ever measured in hourly data is 44.5 °C in July 1988 and minimum value is -3.4 °C in January 1964. The average over 47 year (between 1963 and 2010) is 18.92 °C.

The time series of yearly averaged data (Figure 3.77 bottom panel) shows negative air temperature anomalies before late 89 and positive anomalies after 1997. Air temperature anomaly gradually increases after 1990s as a result of global warming. with exception 1992, 1993 and between the years 1995-1997.

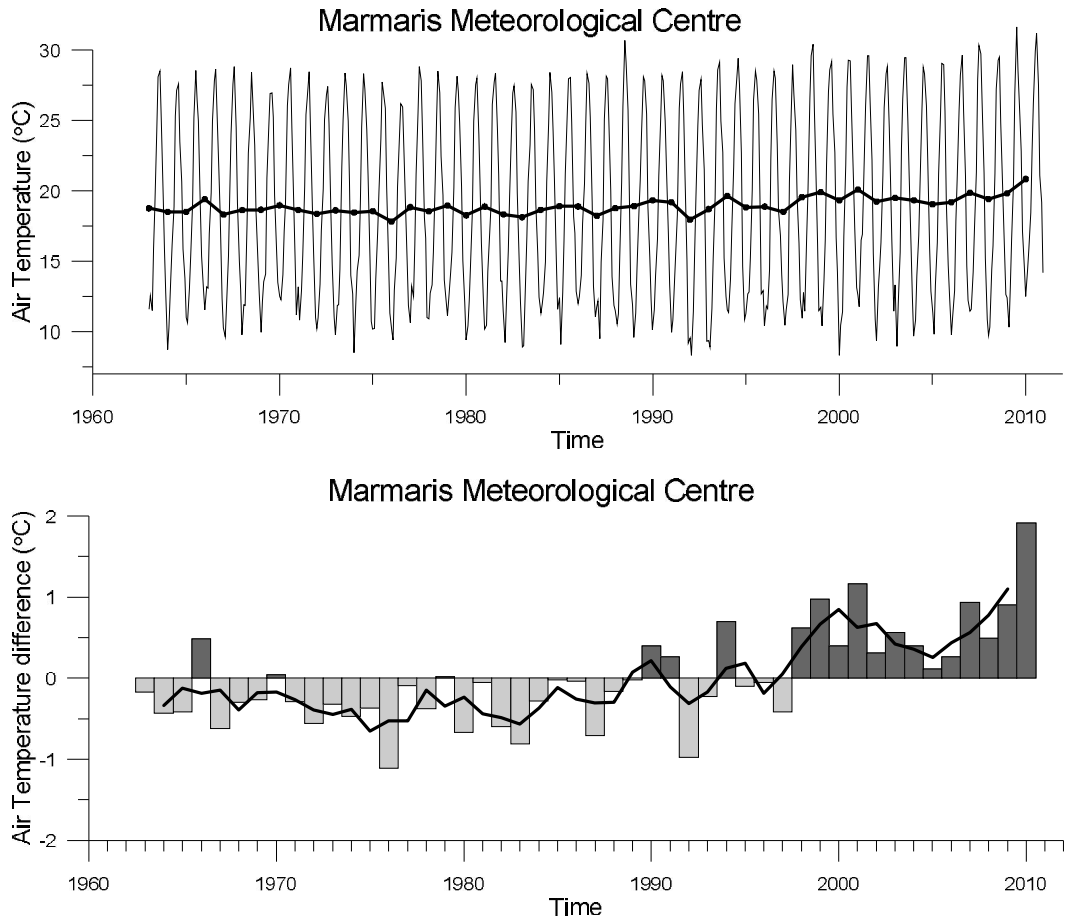

Figure 3.77 Time series of monthly average (thin line) and annual mean (thick line) air temperature (°C) (top), and yearly anomaly time series (bars) with moving averages (thick line) (bottom) for the Gökova Bay.

Hourly precipitation data is retrieved from Marmaris Meteorological Center. Monthly averaged precipitation data for the years 1959-2010 is shown in Figure 3.78. The maximum value ever measured in hourly data is 466.30 mm in December 1992. The average over 51 year is 14.28 mm. The rainfall is minimum in the months of summer according to monthly averaged values.

Precipitation anomaly time series data (Figure 3.78 bottom) does not show similar trend as the data belonging to the northerly bays does. It means that the negative precipitation anomaly observed in the northerly bays can be a sign for the forming dense water in the vicinity of the bays.

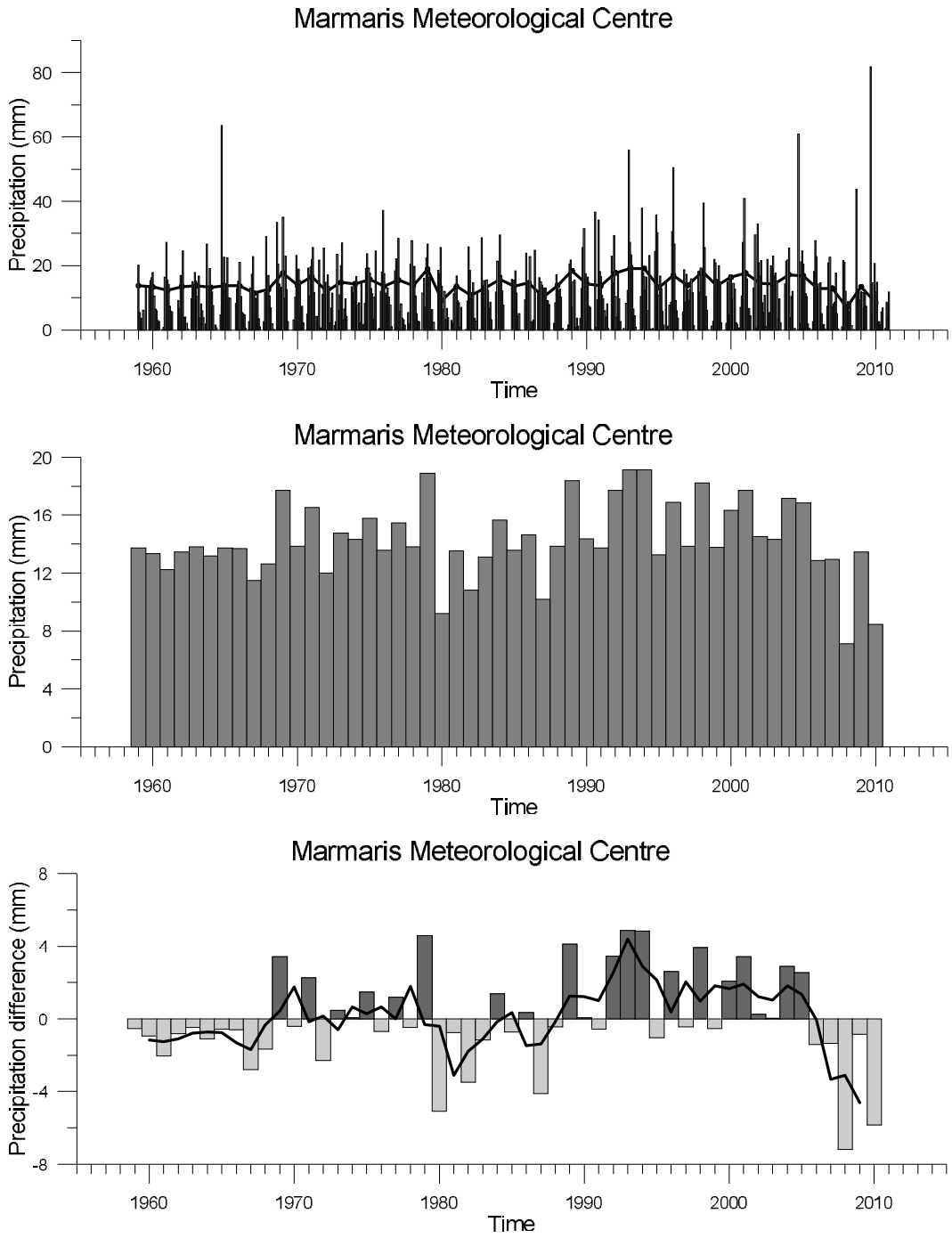

Figure 3.78 Time series of monthly averaged (top), annual mean precipitation (center) and yearly anomaly time series (bars) with moving averages (thick line) (bottom) for the Gökova Bay.

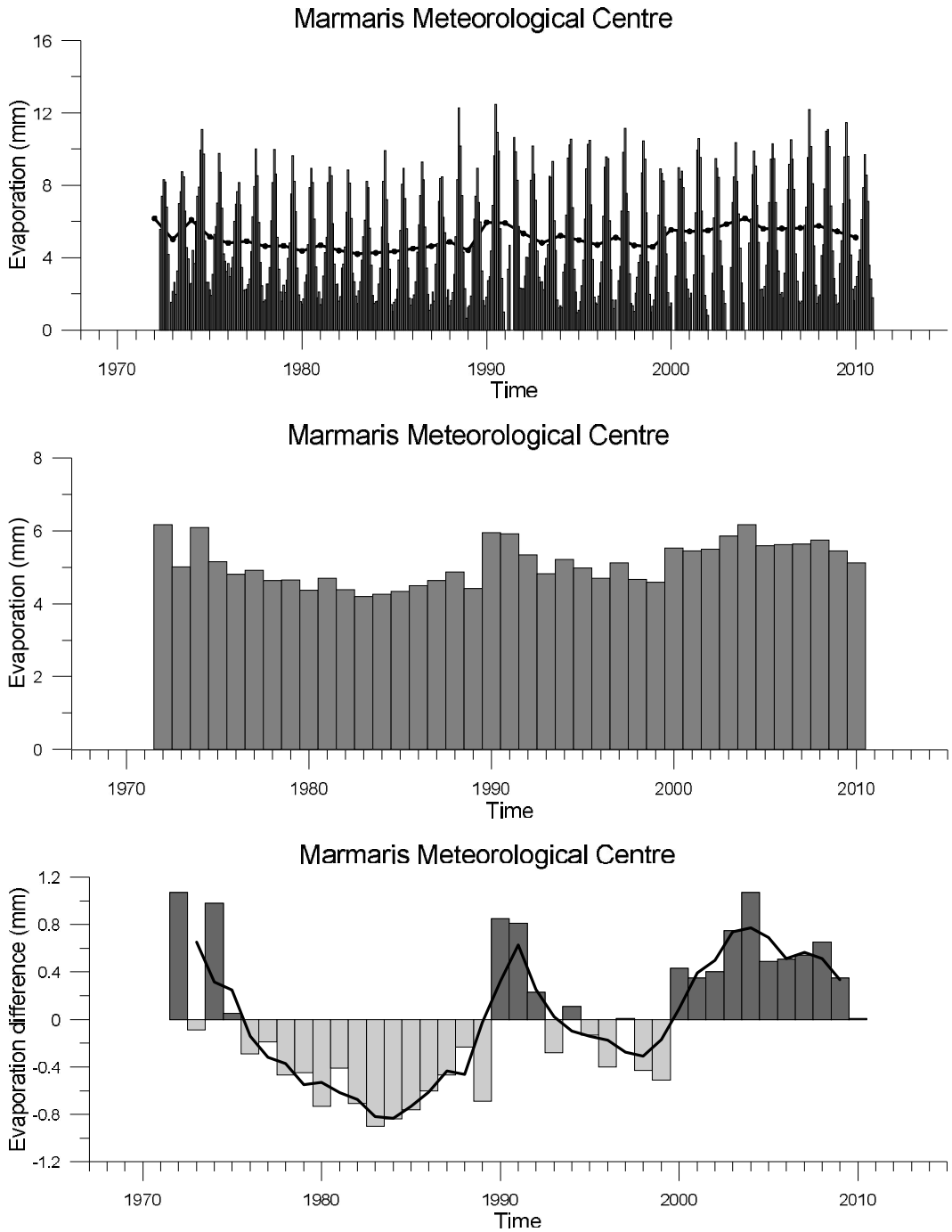

Figure 3.79 Time series of monthly averaged (top), annual mean evaporation (center) and yearly anomaly time series (bars) with moving averages (thick line) (bottom) for the Gökova Bay.

Hourly evaporation data is retrieved from Marmaris Meteorological Center for the years 1972-2010. Monthly averaged values are shown in figure 3.79. The maximum evaporation value ever measured in hourly data is 21.0 mm in July 1988. The

average over 38 year is 5.10 mm. The evaporation is minimum (0.66 mm) in winter and the maximum (12.48 mm) is in summer according to monthly averaged values.

Time series are used to see long-term trend in the evaporation data. Anomaly time series was usedthe time series of deviations of a quantity from mean of the all data (Figure 3.79 bottom). Evaporation anomaly shows negative anomalies extending from 1974 to 2000 with exception in the middle 1990s. As a result of the increasing air temperature the positive anomalies were observed in the last years after 1999.

Hourly humidity data is retrieved from Marmaris Meteorological Center for the years 1963-2010. Monthly averaged humidity time series is shown in figure 3.80. The average relative humidity over 47 year is % 65.45 mm. The humidity is minimum (% 44.22) in summer and the maximum (% 85.56) is in winter according to monthly averaged values.

Anomaly time series was used to see the deviations from the mean of the all data in time. The time series of yearly averaged data (Figure 3.80, bottom panel) shows negative humidity anomalies before 1980 and after positive anomalies up to 2001 making peak in the years 1986 and 1987. Big positive anomalies can be seen also between the years 1995-1999.. The negative anomaly values are observed after 2002 probably affected by warm air.

The highest pressure value in hourly data ever recorded in Gökova area is 1034.6 mbar in January 1973 and lowest value is 875.4 mbar in January 2004. The average over 45 year (between 1965 and 2010) is 1012.10 mbar. Anomaly time series of pressure data (Figure 3.81, bottom panel) shows that Gökova is a unique bay by the pressure anomalies that have no agreement with the anomalies in other bays ever detected.

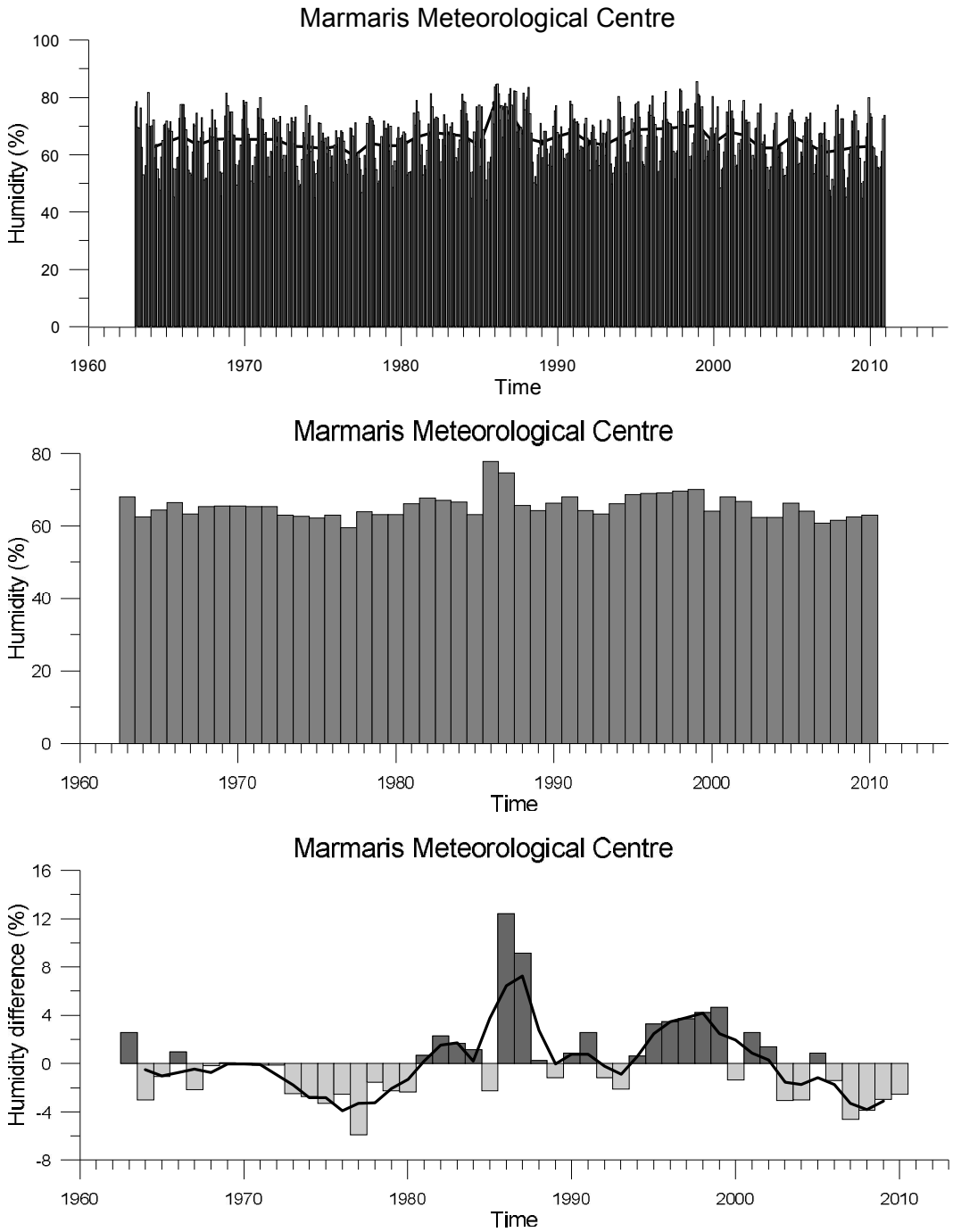

Figure 3.80 Time series of monthly averaged (top), annual mean humidity (center) and yearly anomaly time series (bars) with moving averages (thick line) (bottom) for the Gökova Bay.

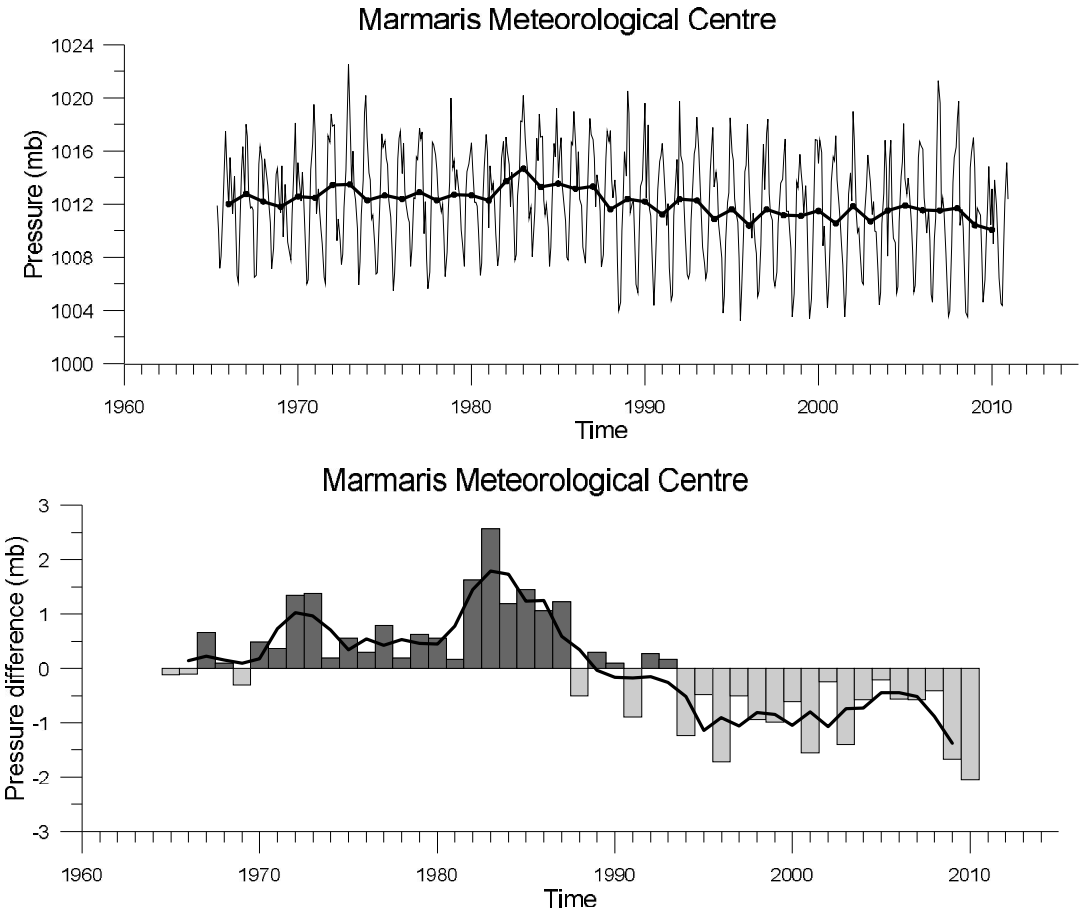

Figure 3.81 Time series of monthly average (thin line) and annual mean (thick line) pressure (mb) (top), and yearly anomaly time series (bars) with moving averages (thick line) (bottom) for the Gökova Bay.

3.7.3 Wind Analysis

In the region, wind from WNW direction dominates throughout the years with an average speed of 2.06 m/s is shown in Figure 3.82.

The prevailing wind over the Gökova area is WNW direction shown in the wind-rose map in Figure 3.82. Wind vectors of the monthly time series of wind speed and direction anomalies for 1966-2010, depending on the availability of the data, were constructed from hourly wind measurements in the Marmaris Meteorological Centre. The wind vectors of the monthly prevailing wind with average wind speed values for Gökova Bay data from Marmaris Meteorological Centre is shown in Figure 3.83.

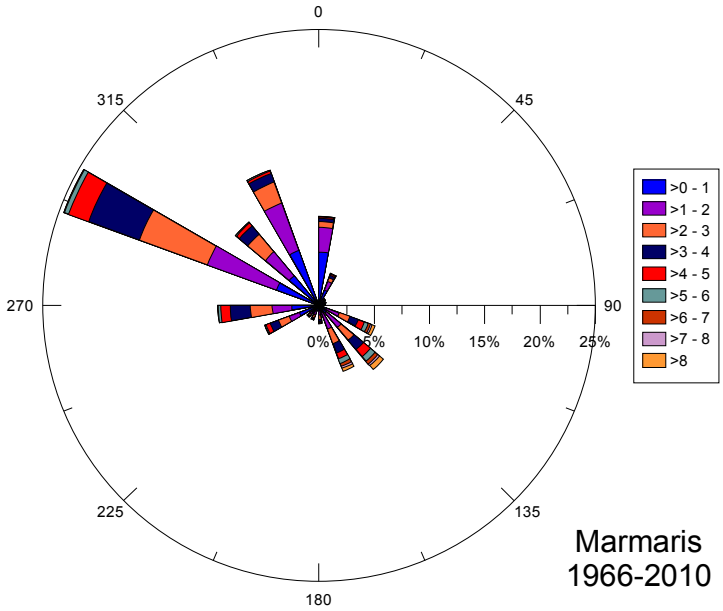

Figure 3.82 Wind chart of the prevailing wind for Gökova Bay data from Marmaris Meteorological Centre.

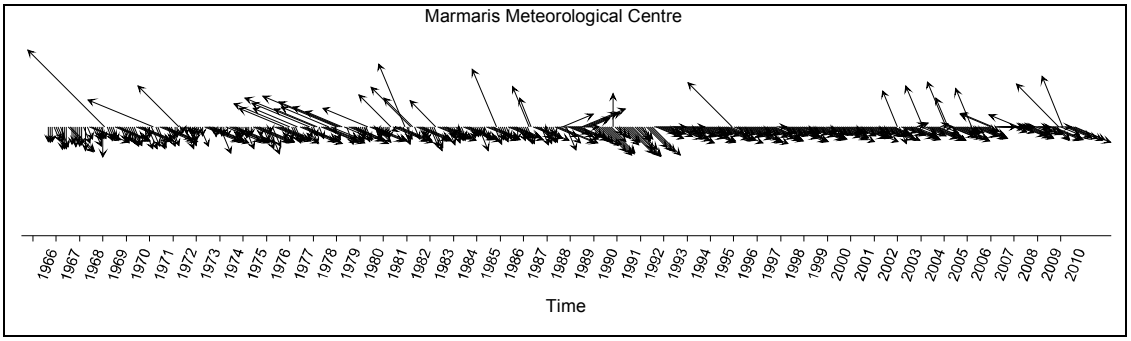

Figure 3.83 Wind vectors of the monthly prevailing wind with average wind speed values for Gökova Bay data from Marmaris Meteorological Centre. (V_{max}=17.09 m/s).

The changing wind in a reverse direction (ESE) is remarkable with increasing wind intensities. ESE is frequently seen direction by the winds blowing more than 12 hours in the Gökova region (Figure 3.84).

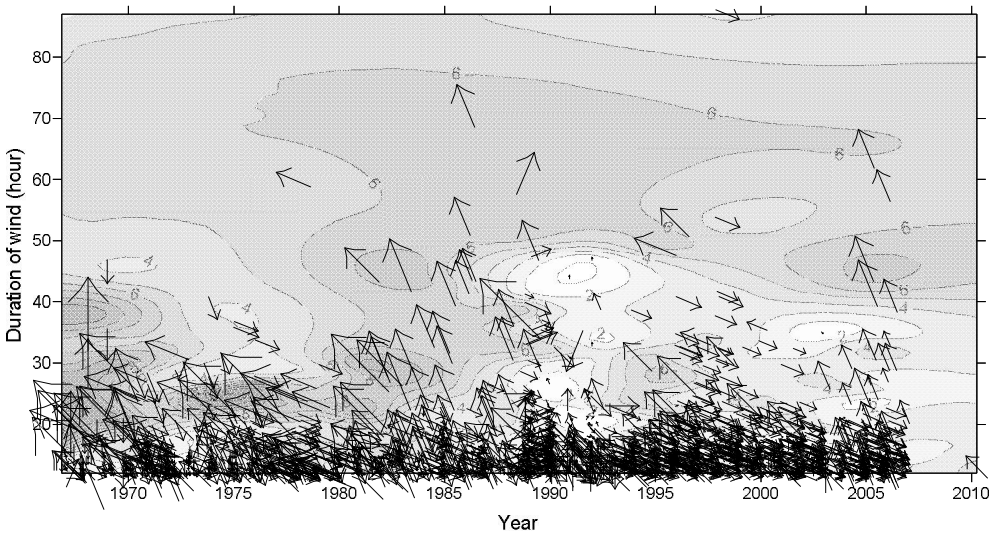

Figure 3.84 The wind vectors for the wind blowing more than 12 hours drawn on the average wind field.

3.7.4 Gökova Bay General Circulation Pattern

As a result of wind analysis it is found that the prevailing wind direction of the Gökova Bay (WNW) coincides circumstantially with the dominant wind direction in the winter cruise time. Therefore the model runs were conducted using the prevailing wind intensity and direction in order to obtain general water movements in the Bay. The circulation is based on the basin wide net current flowing along the water column.

The general circulation pattern that are frequently seen in the Gökova bay under the influence of prevailing wind (WNW) is shown schematically. After the kinetic energy reached a plateau the wind is let to blow over the model domain. One day after blowing WNW wind the Levantine waters enter the Bay from the southern and the northern shallow area of the entrance of the Bay. The expected flow characteristic near both coasts is that the currents more or less are to the wind direction in the case of a wind from WNW direction. Coastal jets are produced along both coasts and a slow return flow compensates the water budget in the central area of the basin. The cyclonic circulation settled down in the western basin in the earlier stage of model run. Two cyclonic gyres form in the two deep basins after three days. The Levantine waters exist in the western part of the Bay captured by the cyclonic

circulation. The developing westward costal current in the beginning changes its character and flows towards east because of existing persistent cyclonic movements in the western side of the Bay. The jet brings the water masses that are originated from the south Aegean Sea (MAW, LSW, LIW and TMW).

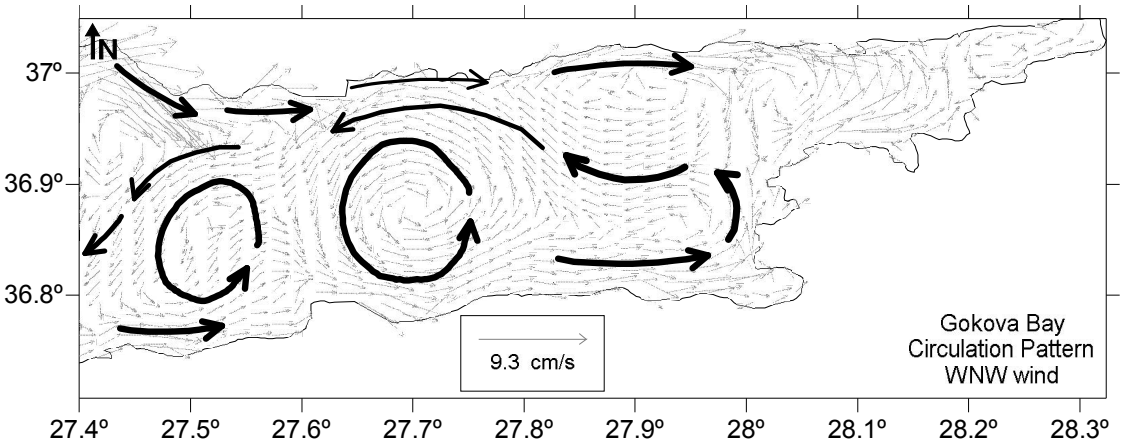

Figure 3.85 General circulation patterns of Gökova Bay.

The residence time which can be calculated dividing the water volume of the bays by the total water exchange through the vertical section in the entrance is 5 months for Gökova Bay. The fetch length is not long for the wind blowing from south and north directions in Gökova Bay. Therefore weak current velocity is expected by the wind-driven experiment done with the southerly and northerly wind lasted over the Gökova area. The existing anticyclones found near the entrance of the Gökova Bay could be responsible for the high residence time.

3.7.5 Time Series of the Gökova Bay

Gökova Bay is chosen as an area representing the southern Aegean water characteristics influenced by the waters originated from Levantine Basin. In summer 1991, we observed σ_θ = 29.0 kg/m^3 below 250m in the Gökova Bay while in spring 1992 σ_θ = 29.0 kg/m^3 isopycnal lifted up to 75m (Figure 3.86). This level continued until the end of 1993 possibly decreasing from surface layer in winter 1993. There was no data from 1994. In spring 1995 σ_θ = 29.0 kg/m^3 isopycnal was observed at the depth of about 230 m. It seems that the EMT relaxation episode has started already

and 29.0 kg/m^3 isopycnal level has reached 265m in spring 1996 and 280m in fall 1996. The decrease of density inside the basin continued in spring 2001 and winter 2002. The σ_θ = 29.0 kg/m^3 isopycnal level decreased to the depth of 320 m in spring 2001 and 350 m in winter 2002.

The winter convection is a seasonally occurring phenomenon that could have brought high salinity levels near the surface as observed in spring 1992 and 1993. The temperature values near surface were in accordance to the seasonal trend. But the subsurface temperature, for example 16°C was the typical LIW temperature observed in spring 1993 very near to the surface (80m). But the depth of 16°C isotherms reached the depth of 215m in spring 1995 and about 170m in spring 1996 showing more deep water formation in spring 1996. However, 29.0 isopycnal did not come to surface in spring 1996 as it was observed in spring 1993. The reason could be the existence of Modified Atlantic Water (MAW) (with temperature 16-18 °C and salinity less than 38.7) at the subsurface as a thin layer (25 m). The existence of such low density at the surface layer acts as an insulating lid that makes the air-sea interactions limited thus hindering the formation of dense water. Levantine Surface Water (LSW) filled the surface layer with the water mass containing high salinity and high temperature during fall 1996 as MAW disappeared. In the subsurface layer greater than 60m, the Levantine Intermediate Water (LIW) was identified by its salinity maximum. The Levantine Waters filled the Bay in spring 2001.

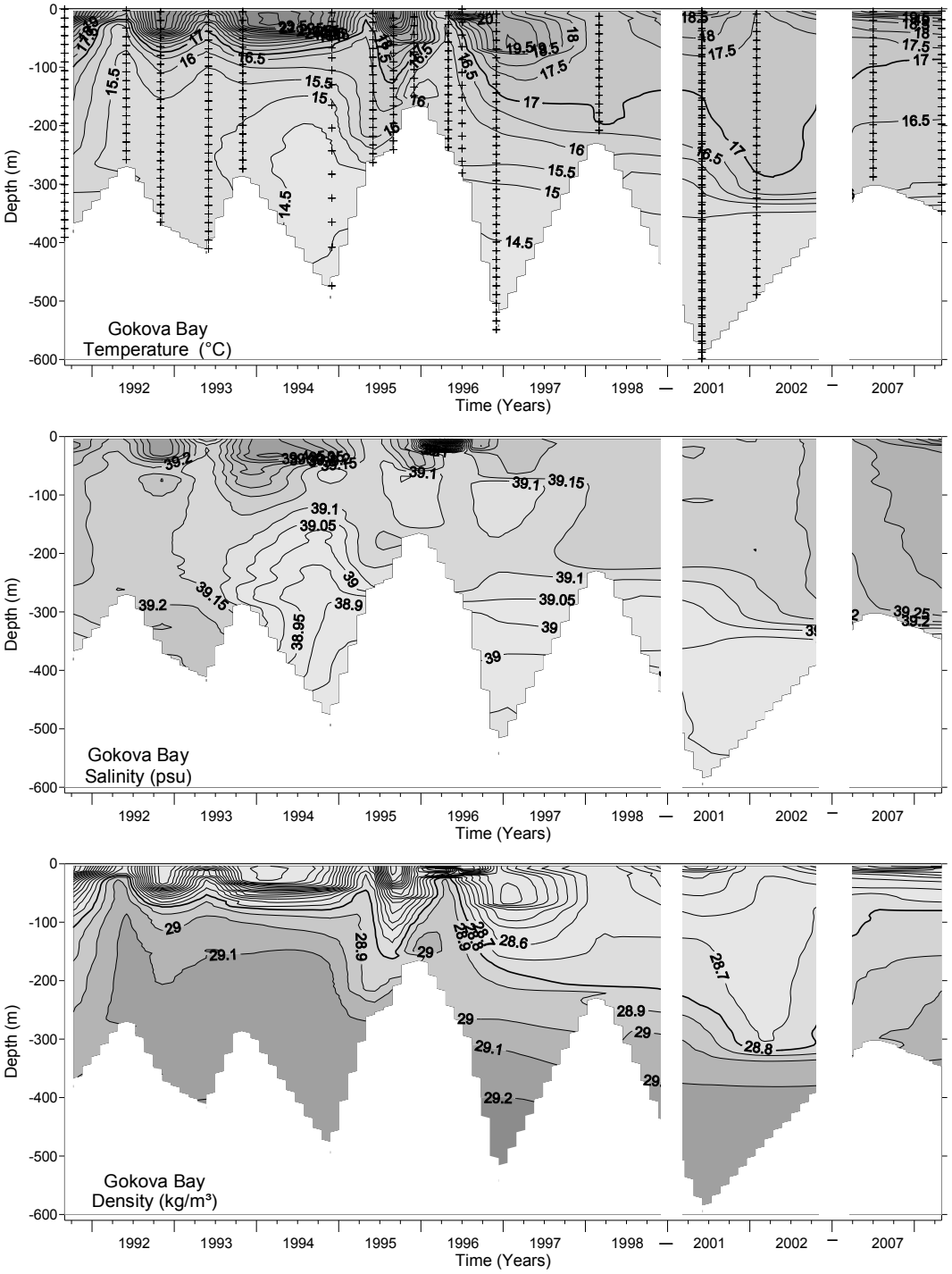

Figure 3.86 Temporal evaluations of temperature, salinity and density fields of Gökova region starting from summer 1991 up to summer 2008. The areas in white represent where data was not collected.

GIBW was at the surface with a temperature greater than 19^{o}C. LSW was under GSW between the depths of 10m and 40m with salinity about 39.2 psu. LSW was

separated from MAW by a halocline. MAW was slightly remarkable with its low salinity at the surface layer. The mixed layer was about 50m thick and the thickness of the LIW was about 150 meter. LIW existed between the depth of 100m and 250m. Its salinity was about 39.17 and its potential temperature 17 ^{o}C. The underlying water mass was Transient Mediterranean Water (TMW) that was detectable in the layer approximately 400m with the salinity slightly less than 39.0. TMW volume was not found in considerable amount. The water column was almost homogenized up to depth of 300 m because of influence of the wind and winter convective mixing in winter 2002. A strong seasonal termocline and halocline formed just under the depth of 300 m. The water masses LIW and TMW existed in the water column with slightly different characteristics than the same water masses in spring 2001. Again cold, salty dense water can be detectable in summer 2007 and 2008.

3.7.6 Hydrographic Characteristics of the Gökova Bay

3.7.6.1 Spring 2001

The water mass properties of the Gökova Bay are analyzed using the data obtained from the 19 stations during the spring 2001 cruise (19-23.05.2001) (Figure 3.87-3.89). The Asian Minor Current flowing between Turkish mainland and Rhodes Island brings the warm Levantine Surface Water (LSW) and the salty Levantine Intermediate Water (LIW) along the western Turkish coast into the Gökova Bay. Gökova Bay is open to the Aegean Sea from the west side. The opening part to the Aegean Sea, especially the southwest corner is appropriate for the LWs that enter the Bay. They penetrate up to the middle of the Bay as a result of general circulation evolving in the Bay. Kos Island is a barrier for the LWs flowing to the north. Therefore the station in the southwest corner of Gökova Bay has very similar water characteristics to the water of Levantine origin.

Gökova Inner Bay Water (GIBW) is a distinguished surface water mass of Gökova Inner Bay with high temperature and low density values (Table 3.5). LSW is below Gökova Inner Bay Water (GIBW) between 10m and 40m and with a higher salinity (Figure 3.89). LSW is the dominant surface water mass outside the Gökova

Inner Bay and separated from MAW by a strong halocline. MAW is slightly detectable with its low salinity (<38.8 psu) under the surface layer. MAW signal is lost towards the east and not detectable further in the shallow inner area. Thickness of the LIW is about 150 meter. LIW exists between the depths of 100m and 250m (Figure 3.89). Its temperature value (16.98 ^{o}C) is slightly higher than the LIW temperature value in the southern Aegean Sea (16.5 ^{o}C). The underlying water mass is the modified Transient Mediterranean Water (TMW) that is detectable in the layer approximately 400m with the salinity slightly less than 39.0. It is originating in the Levantine and Ionian basins (Balopoulos et al., 1999; Theocharis et al., 1999a). The temperature of TMW is slightly higher compared to the values obtained from different monitoring studies because of the relative shallowness of the Gökova area.

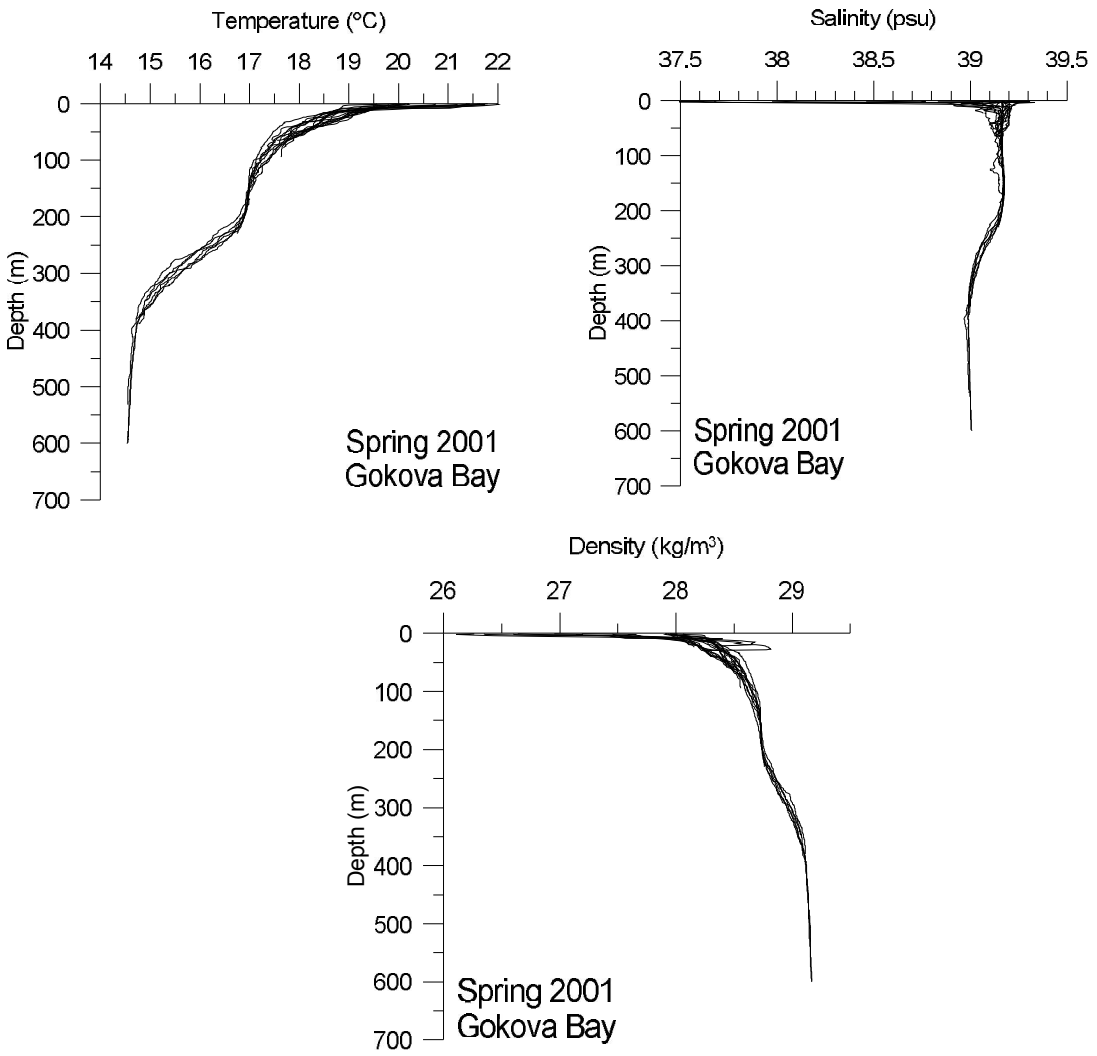

Figure 3.87 Temperature, salinity and density profiles of Gökova bay in Spring 2001.

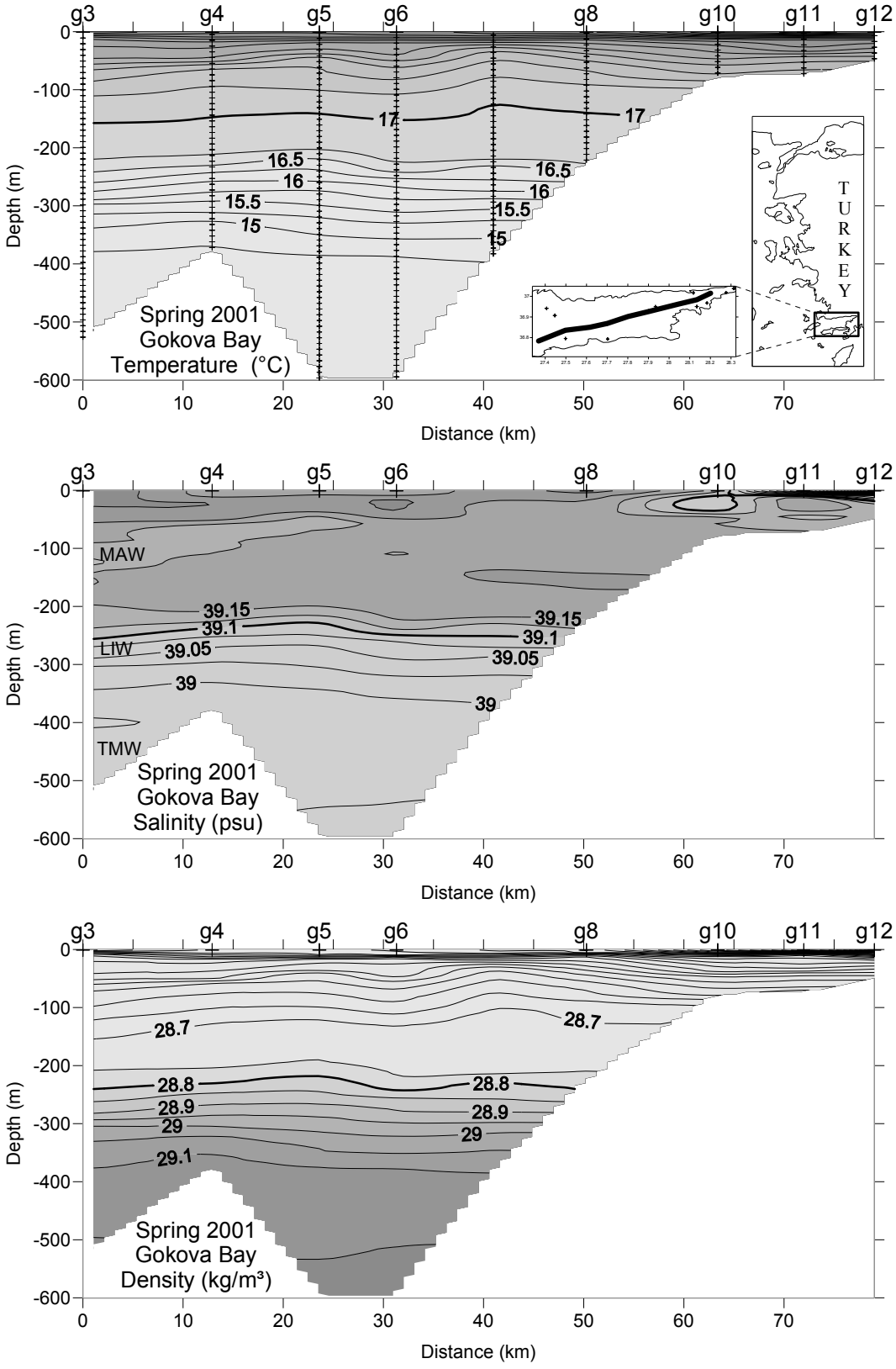

Figure 3.88 The salinity vertical section along the long axis of Gökova bay in spring 2001.

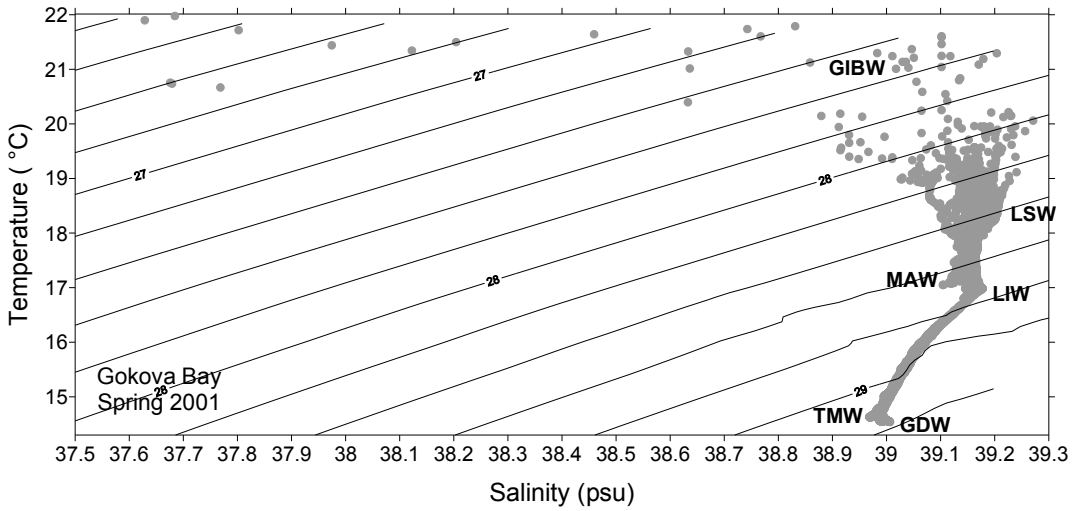

Figure 3.89 θ-S diagram of spring 2001 (Gökova Bay).

Table 3.5. The water masses existing in the Gökova bay and their range in spring 2001.

		Spring 2001		
	Water mass	Temperature (°C)	Salinity (psu)	Density (kg/m³)
GÖKOVA BAY	GIBW	> 20.0	37.7 - 39.2	< 27.8
	GDW	14.54	39.01	29.17
	MAW	17.17	39.1	28.63
	TMW	14.61	38.96	29.12
	LSW	18.31	39.2	28.41
	LIW	16.98	39.18	28.73

3.7.6.2 Winter 2002

The water masses of Gökova Bay are investigated through the data collected in 14 numbers of stations by the R/V K. Piri Reis in winter 2002 (27-29.01.2002) (Figure 3.90-3.92).

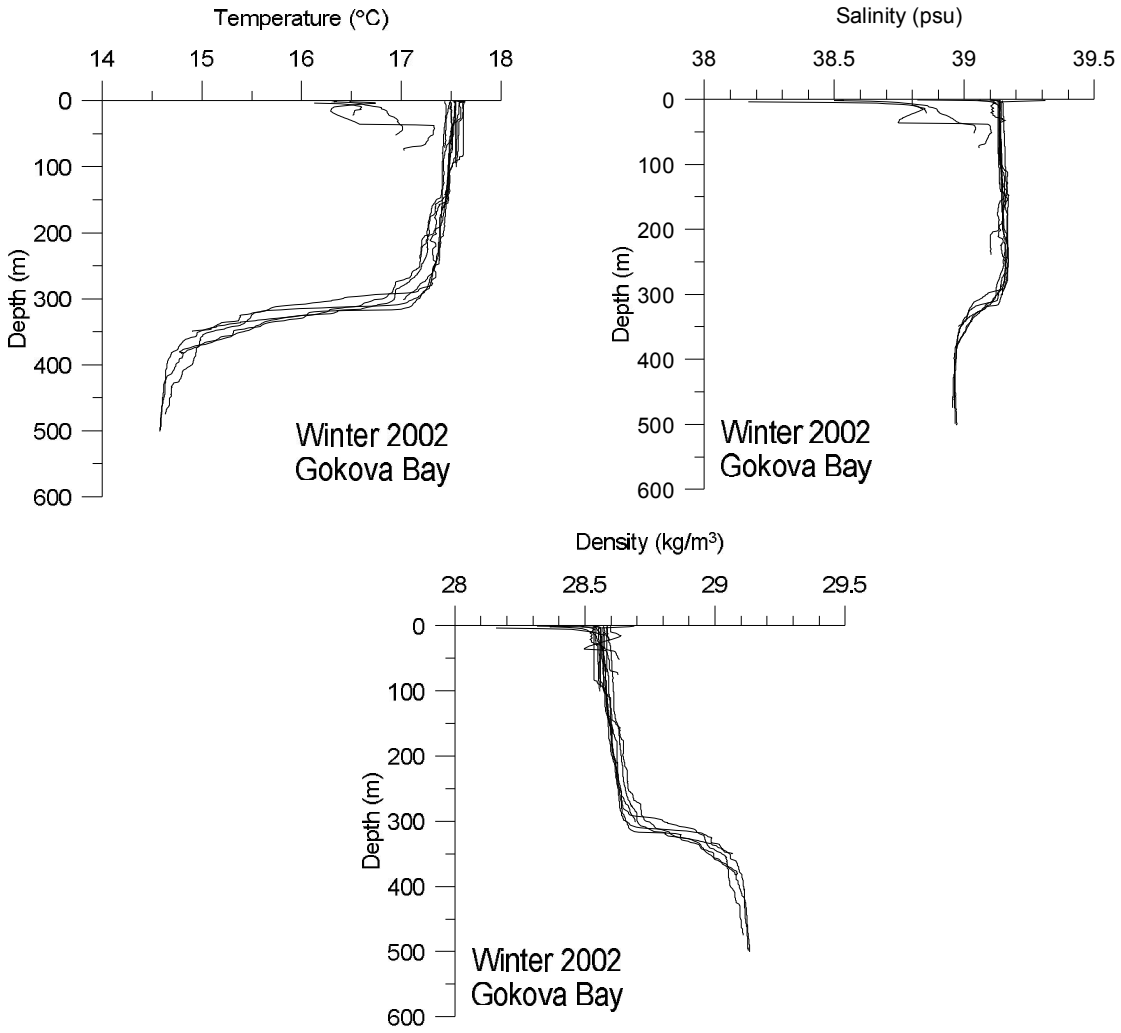

Figure 3.90 Temperature, salinity and density profiles of Gökova bay in winter 2002.

The water masses that are detected in the cruise spring 2001 could not be observed in winter 2002 cruise at the first glance. Water column is almost homogenized up to the depth of 300m because of the influence of wind and winter convective mixing. A permanent thermocline and halocline form just under 300m. The two layer system has also homogeneous water under thermocline (halocline) with a temperature of 14.6 ^{o}C and salinity of 38.95 psu. Bottom layer temperature does not change much; however but slight decreasing salinities make a sign of possible TMW formation in the fall season. The water masses that exist in the spring period can be seen after focusing the salinity range between 39.1 and 39.18. But the water masses are altered from original characters due to winter mixing processes. The signs of LSW and MAW are not detected in the winter period as strong as in the spring time (Figure 3.92).

Gökova Inner Bay Water (GIBW) has very distinguished water colder and less saline than the rest of water masses in the Bay (Figure 3.91, Table 3.6).

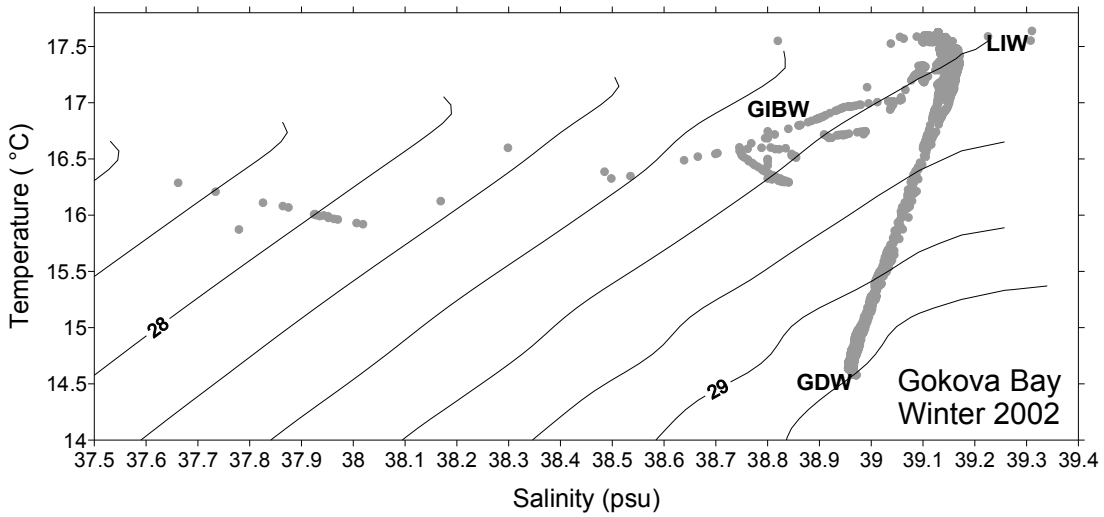

Figure 3.91 θ-S diagram of winter 2002 (Gökova Bay).

Table 3.6. The water masses existing in the Gökova bay and their range in winter 2002.

		Winter 2002		
	Water mass	Temperature (°C)	Salinity (psu)	Density (kg/m³)
GÖKOVA BAY	GIBW	< 17.0	< 39.04	28.37-28.65
	GDW	14.58	38.97	29.13
	MAW	----	----	----
	TMW	----	----	----
	LSW	----	----	----
	LIW	17.35	39.17	28.63

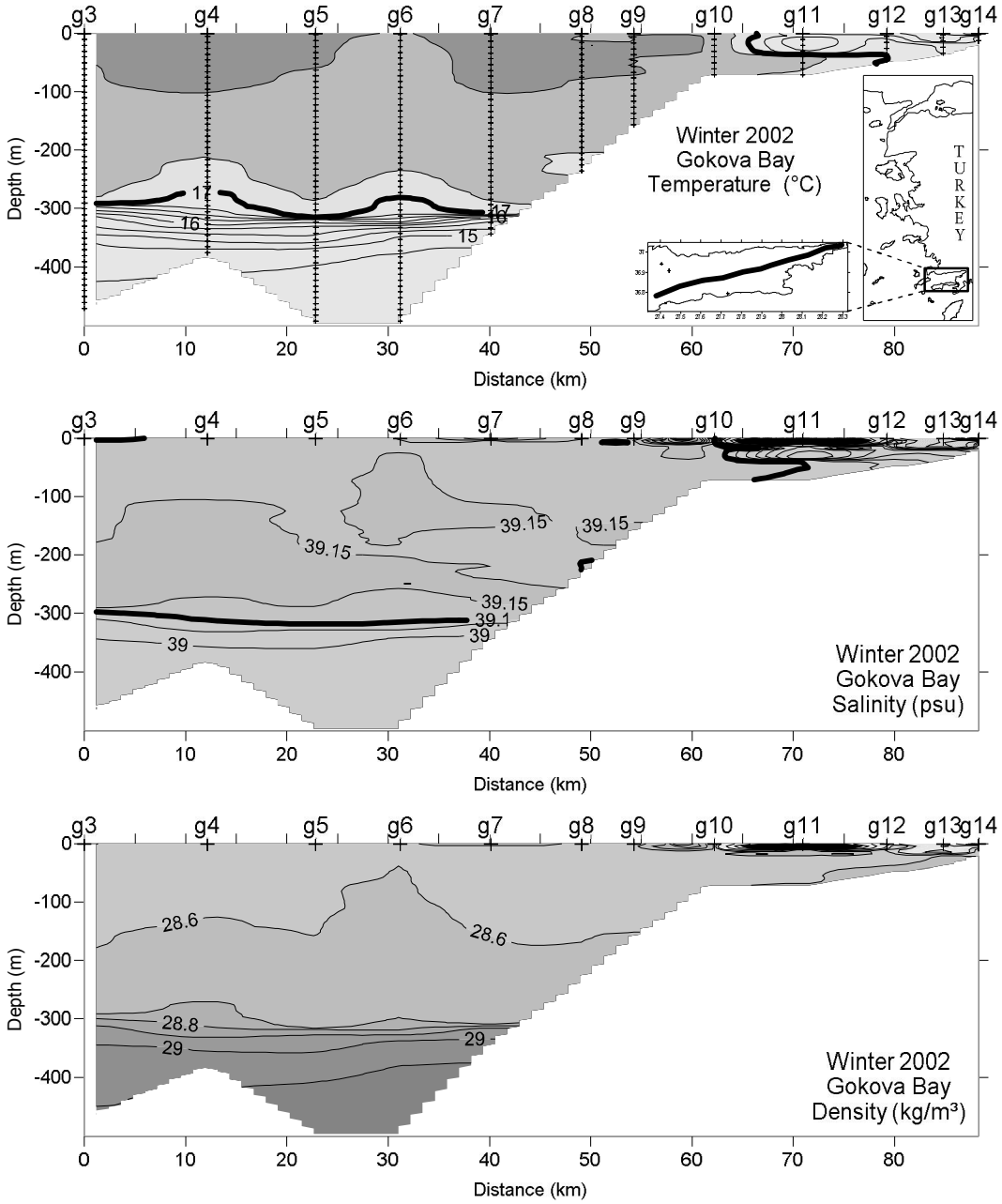

Figure 3.92 The salinity vertical section along the long axis of Gökova bay in winter 2002.

CHAPTER FOUR
DISCUSSION

Some studies asserted that the EMT (Eastern Mediterranean Transient) started in the years between 1987 and 1990 (Schlitzer et al. 1991; Theocharis et al. 1999a; Gertman et al. 2006). EMT event is relaxed by about 1995 (Theocharis et al. 2002). Zervakis et al. (2003) gave information about the EMT relaxation period of no ventilation of the deep waters of the North Aegean in the period from 1994 to 2000. The density levels in the northwestern Levantine Sea are decreased very moderately between 1995 and 2001 (Roether et al. 2007). The present work confirms the above studies and gives information about the evolution of density levels after EMT relaxation period in the Aegean Sea especially in the İzmir Bay and the Gökova Bay. It shows the different characteristics of the intermediate water masses of the Aegean's bays and tries to identify interannual variability consistent with the North-Central Aegean water characteristics. Figure 4.1 shows this consistency and also the evolution after 2000 (after relaxation period). The data of North-Central Aegean were obtained from the study of Veloaras and Lascaratos (2005). The stagnating intermediate water in the İzmir and Gökova Bays was denser after year of 2000 by gaining salt even though the temperature increases. The increasing of the density continued until 2007 in the Gökova and İzmir Bay even in the Saros Bay. Same trend cannot be observed in the North-Central Aegean Sea and Saros Bay by the intermediate temperature time series. They do not allow any solid conclusions to be drawn, apart from the salinity and density evolution with time. The high density values were observed near to surface level and the bays were again full with salty water and the isopycnal levels are comparable with the isopycnal levels of 1993.

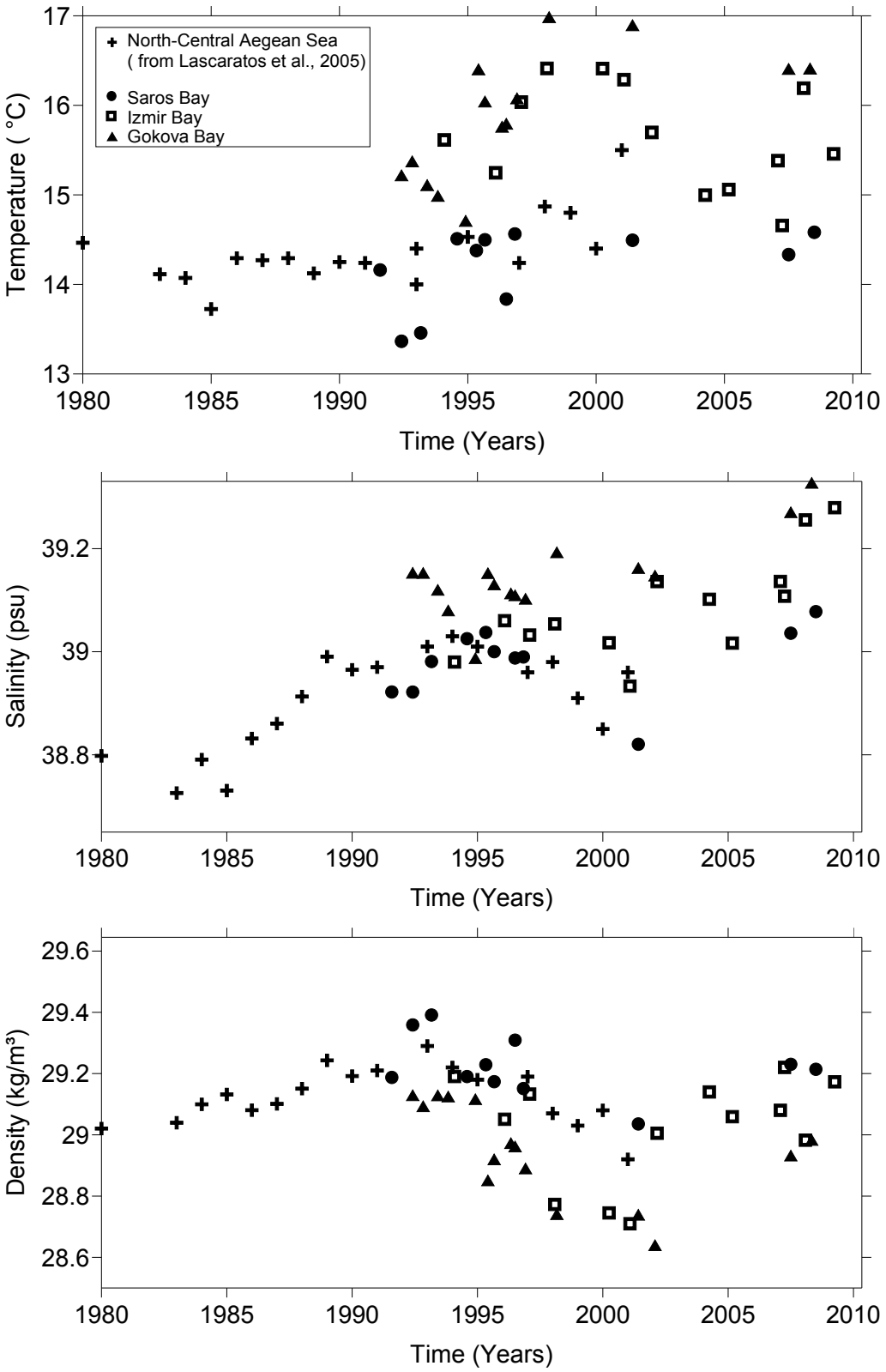

Figure 4.1 Time evolution of mean integrated values of temperature, salinity and density in the 100–300 dbar layer in the North-Central Aegean Sea (after Velaoras, D. and Lascaratos, A., 2005) in the Saros and in the Gökova Bay. İzmir Bay is very shallow area. The İzmir data is selected only for winter period from deep part of the Bay to rid of the influence of the seasonal variations.

This variability observed in the intermediate water of the bays showed that the bays have the potential to produce dense-water causing dense water cascade from coast to the Aegean Sea. However it depends on the meteorological conditions over the eastern Mediterranean and possibly, central/eastern Europe (Zervakis et al. 2004). The North Atlantic oscillation (NAO) appears to be responsible besides some regional variability. It is obvious from Figure 4.1 that intermediate water shows about 10 years oscillation independent of seasonal cycle.

In this part of the section the meteorological conditions of all bays are compared with each other. Similarities and differences especially during main EMT period (1990-1994) were revealed by overlaying the data retrieved from the meteorological center representative for the bays environment.

The air temperature of the all bays are overlaid (Figure 4.2). More or less all bays show similar variation in time. There is any certain oscillation period of data. Near 1990s 3 years time difference between two negative peak points (at 1993 and 1996). Especially the negative anomaly of 1993 is the lowest temperature anomaly of over 30 years. It means that the air temperature has big influence on the forming very dense water in the Aegean Sea in EMT time. Severe winter condition causes strong winter convection.

Air temperature influence on the formation of dense water is undisputed true. But it can not be alone to explain EMT event. Precipitation plays very crucial role on air-sea interactions (Figure 4.3). A big amount of precipitation hinders air-sea interaction. It isolates sea from air with maintaining a thin layer lid on the surface of sea. All precipitation data without any exception shows negative precipitation anomaly after 1989 until 1994.

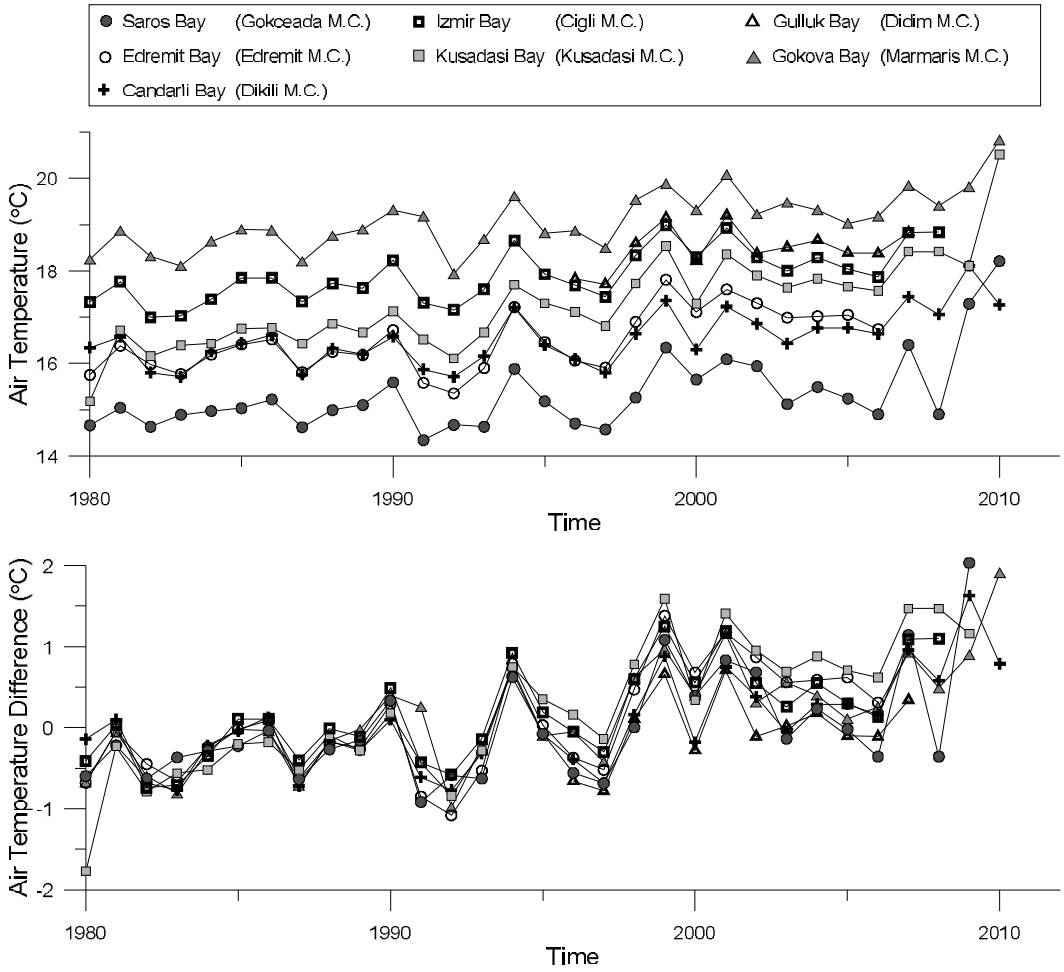

Figure 4.2 Overlaid time series of all bays, yearly averaged air temperature (upper panel) and their anomalies.

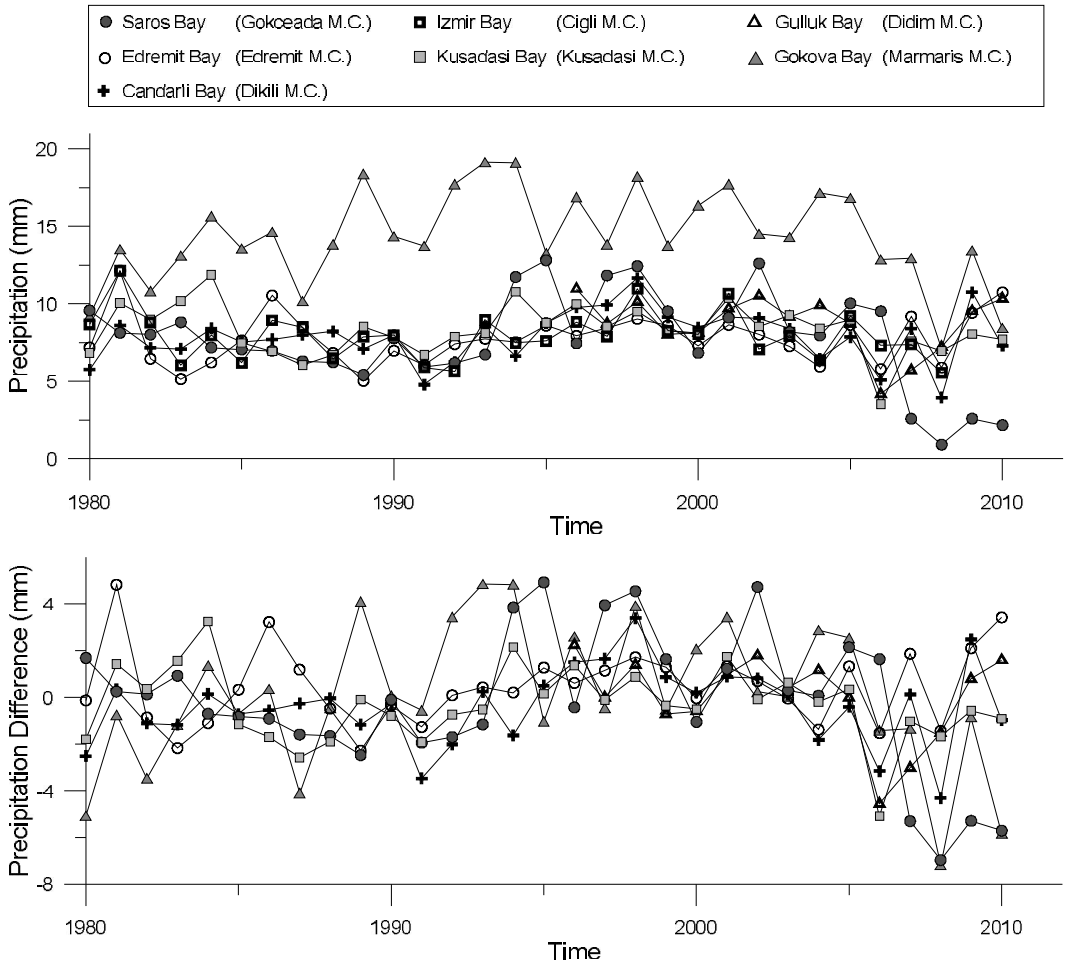

Figure 4.3 Overlaid time series of all bays, yearly averaged precipitation (upper panel) and their anomalies.

Except the southern regions of Kuşadası and Gökova, the data of other regions show negative evaporation anomaly during EMT period. The surface salinity is generally proportional to precipitation minus evaporation in middle latitude regions. Therefore we expect negative evaporation anomalies during EMT time together with the negative precipitation anomalies. Otherwise a salinity increase must be considered. It is the case for southern regions. Figure 3.86 (middle panel) shows excess salinities at the surface from 1992 until 1996. The negative evaporation anomalies are observed during EMT time for the northern and central Aegean bays shown in Figure 4.4.

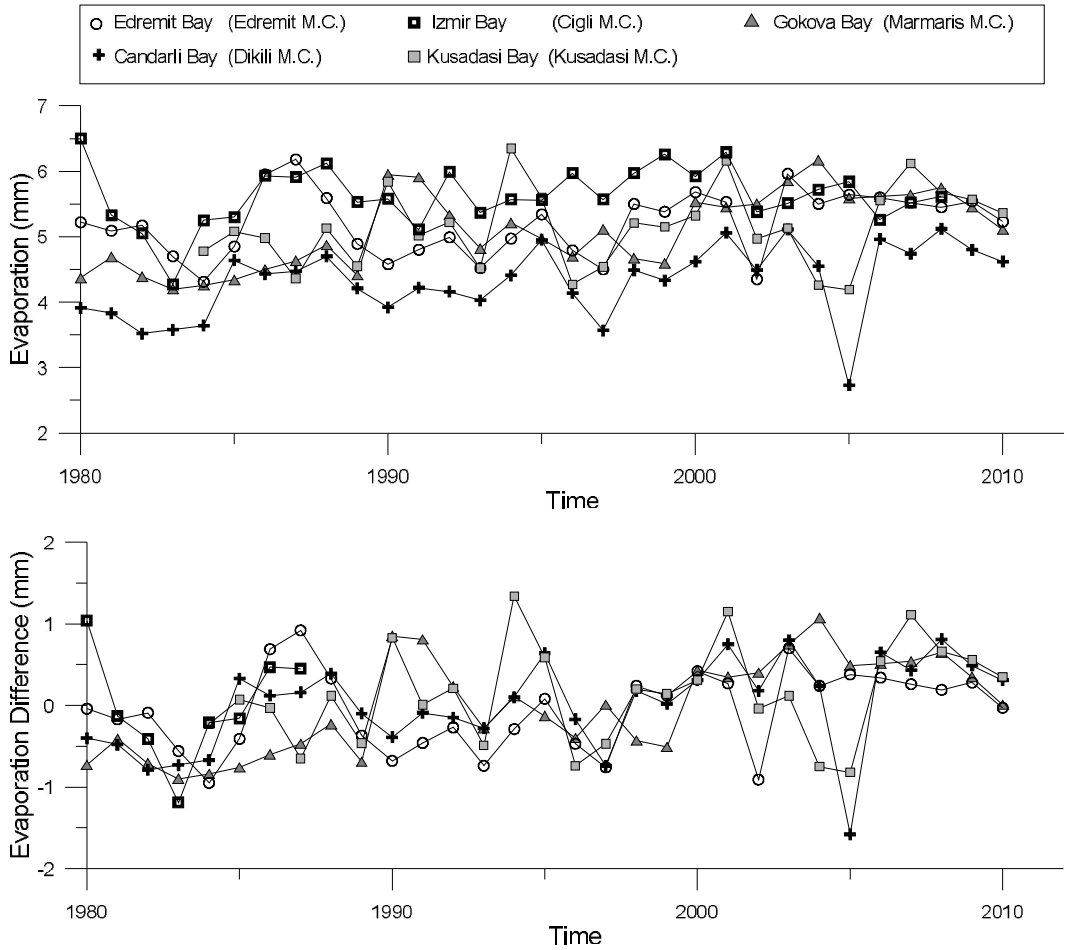

Figure 4.4 Overlaid time series of all bays, yearly averaged evaporation (upper panel) and their anomalies.

The all humidity curves belonging to the bays show similar trend with an exception of Kusadası (Figure 4.5). The humidity values increase from 1980 until 1986 and then begin to decrease after. There are no extraordinary changes during EMT period in the humidity data.

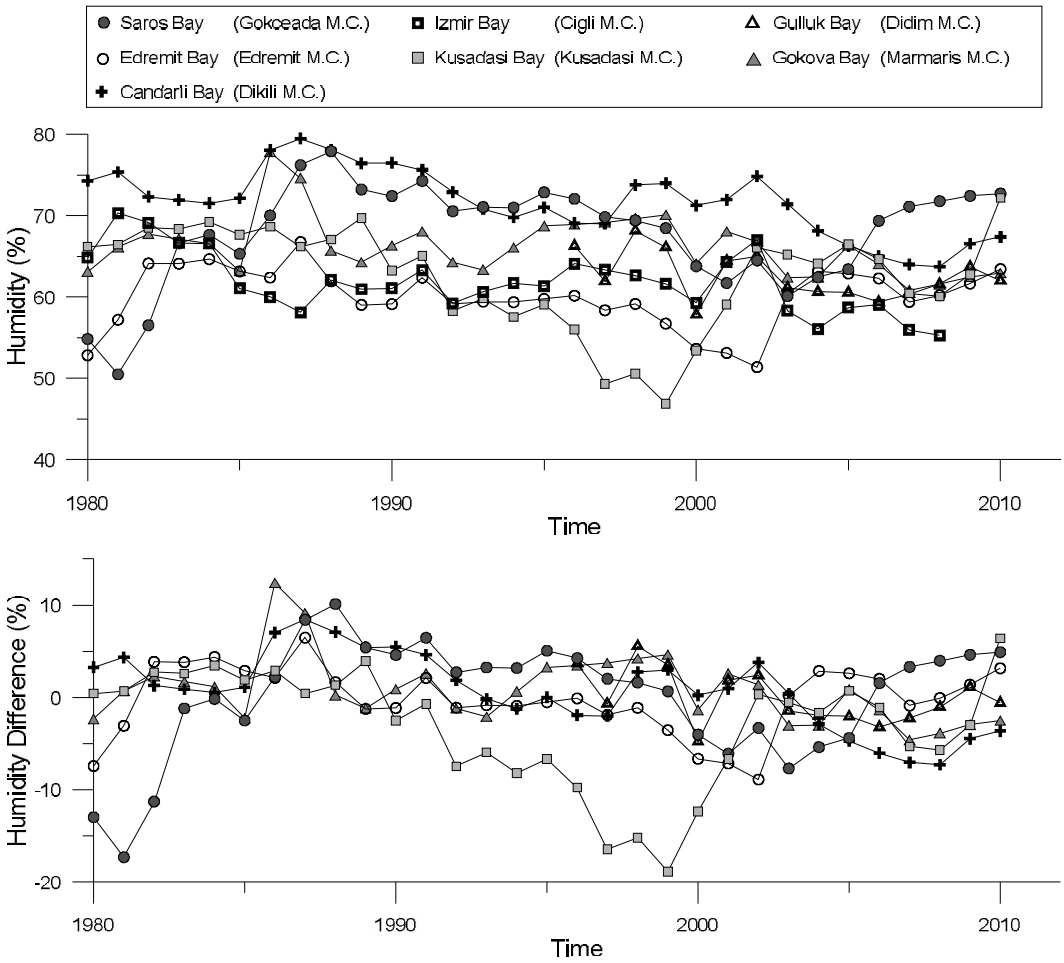

Figure 4.5 Overlaid time series of all bays, yearly averaged humidity (upper panel) and their anomalies.

It is an interesting evolution of high positive pressure anomalies that were observed similar in almost all bays during the years from 1989 until 1994 (Figure 4.6). Any significant positive pressure anomalies have been observed after this period. The big amount of Aegean Deep Water (ADW) flowed over the sills of the Cretan Arc into the Levantine Basin during this time. The pressure over a region can change the behavior of the wind. Wind changes the character of the circulation or establishing new cyclonic or anticyclonic movements in the bays. It is a question if these high pressure anomalies in the bays are related to the forming cyclonic gyres in the central Aegean. If it is the case together with very cold winter they play important role on the homogenization of the water column causing very deep winter convection remaining very dense water behind.

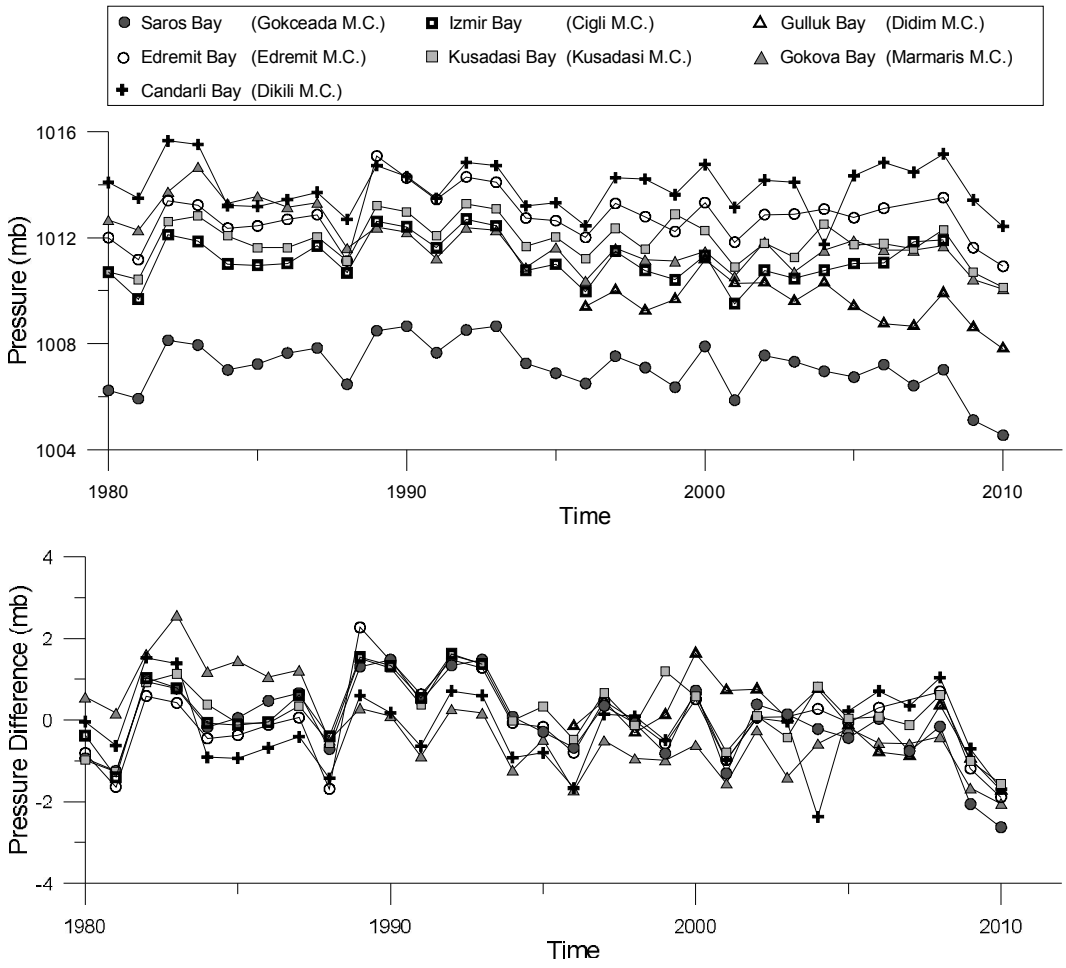

Figure 4.6 Overlaid time series of all bays, yearly averaged pressure (upper panel) and their anomalies.

The hydrography of three bays of Saros, İzmir and Gökova that are representative of the part of the Aegean Sea were analyzed separately in Chapter 3. The hydrographic parameters and water masses are treated together to indicate the differences and similarities of three parts of the Aegean Sea better.

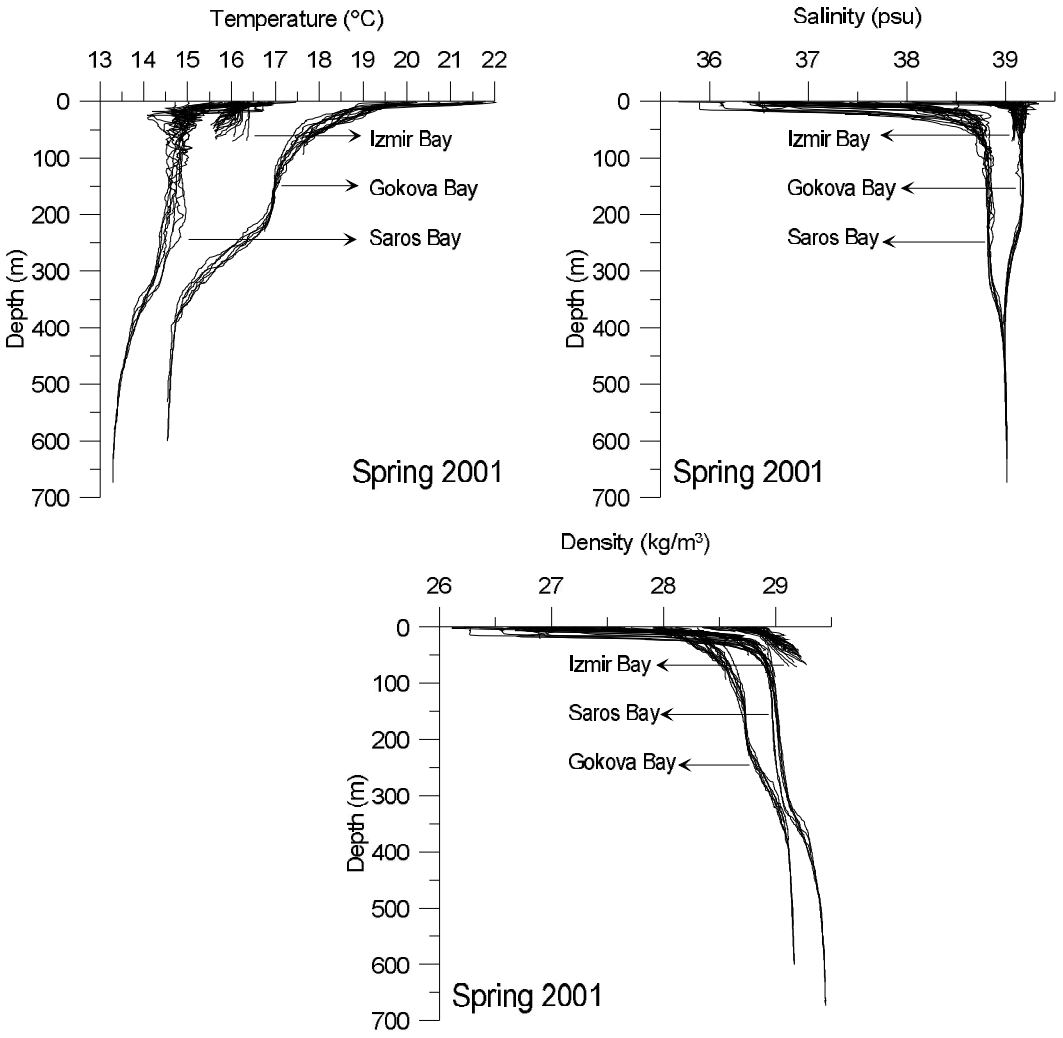

Figure 4.7 Temperature, salinity and density profiles of three bays in spring 2001.

Temperature value of the Central Aegean Sea (İzmir Bay) water is close to the temperature value observed in North Aegean Sea (Saros Bay) and approximately 1 ºC warmer than it and more than 3 ºC colder than the South Aegean Sea water (Gökova Bay) in spring 2001. On the other hand the salinity value of the Central

Aegean Sea (İzmir Bay) is very close the value of South Aegean Sea water (Gökova Bay) water. The North Aegean Sea (Saros Bay) is less saline compared the other two regions water in spring 2001 period (Figure 4.7). Therefore it can be understood why the Central Aegean has the densest water in the Aegean Sea.

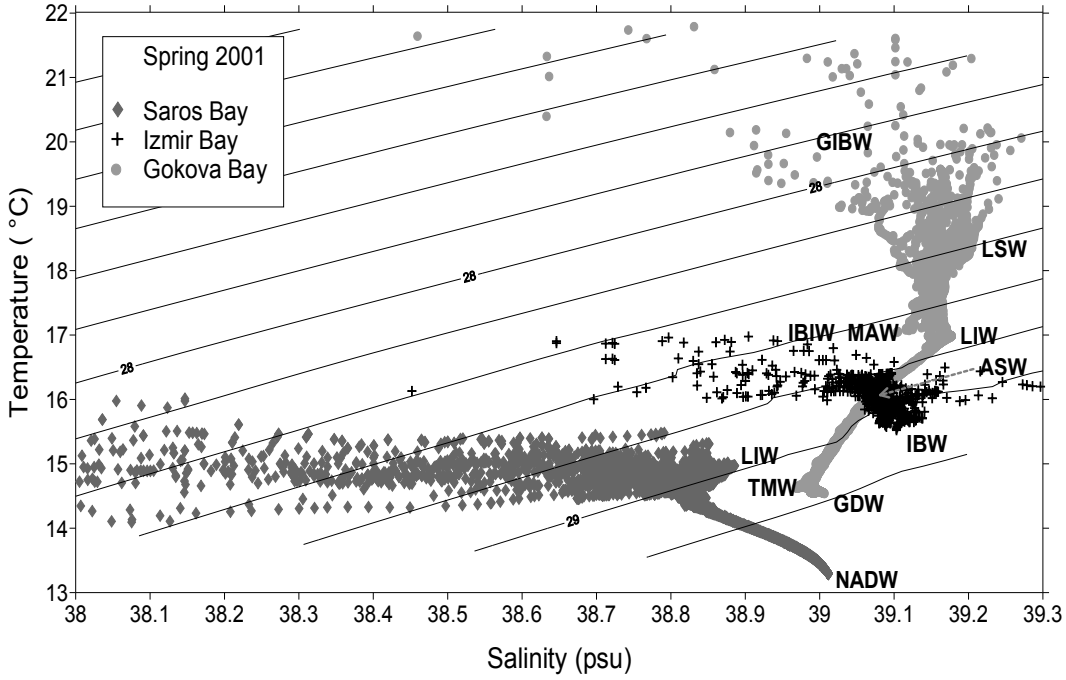

Figure 4.8 T-S diagram of spring 2001.

T-S diagram demonstrates the dense water of İzmir Bay at the surface and intermediate layer in another way Figure 4.8. LIW was found in both bays in the bays of Saros and Gökova. Its characteristics were modified on the way to the north. Its density decreased by gaining heat in the shallow Gökova Bay and by losing salt slightly in the Saros Bay.

The general characteristics of the water in the three bays do not change from spring 2001 to winter 2002. The water of the Gökova Bay is the warmest and saltiest in the three bays in winter 2002 as in spring the case is (Figure 4.9). Again the İzmir Bay water is the densest of three water masses (Figure 4.10). LIW was found clearly only in Gökova Bay. Its characteristics indicate that no big changes in salinity values different than original LIW. But its temperature increases on the way to Gökova Bay.

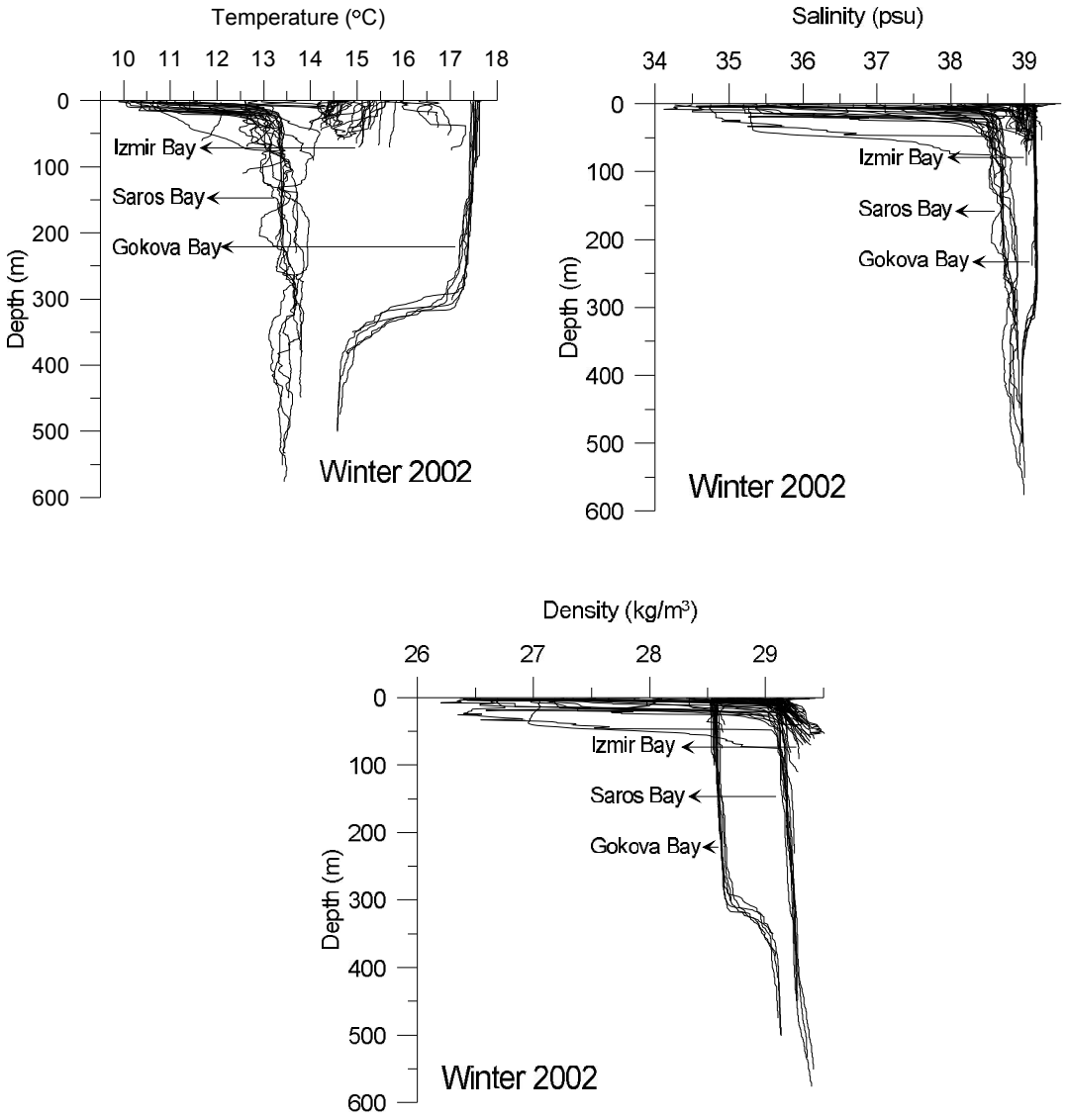

Figure 4.9 Temperature, salinity and density profiles of three bays in winter 2002.

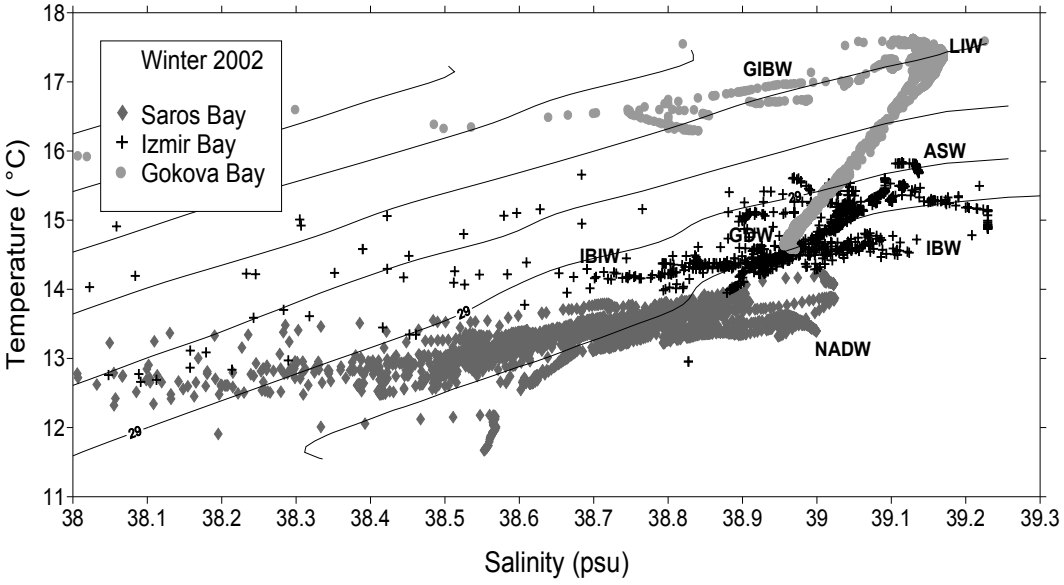

Figure 4.10 T-S diagram of winter 2002.

CHAPTER FIVE
CONCLUSION

The present study investigated the water masses in the bays (Saros, Edremit, Çandarlı, İzmir, Kuşadası, Güllük and Gökova Bays) along the eastern coast of Aegean Sea, in time and space. The important conclusion is the decrease of isopycnal levels in the bays after the peak EMT period with time starting from 1994 up to 2001. This confirms the study of Zervakis et al. (2003), Roether et al. (2007), Velaoras and Lascaratos (2010). The data of these bays shows that their salty, cold and dense waters change their characteristics during the EMT, EMT post-peak period and after. This is related to high salinity Levantine Waters reaching even to the North Aegean Sea. Due to their increased salinity they are the preconditioning for the outcropping of the isopycnals particularly after coinciding with severe cold winter episodes. The stagnating deep water in the bays gained slowly buoyancy by losing salt and gaining heat. After the EMT relaxation period the water started gradually to be denser until 2007. The bays were again full with salty water and the isopycnal levels are comparable with the isopycnal levels of 1993. It was the first time after 1993 there have been a new severe deep–water producing episodes in the Aegean. Unfortunately it is not known if these isopycnal levels were the sign of new time for new transient from the Aegean Sea to Levantine basin.

The general outcome is the waters in the three regions (Northern, Middle and Southern Aegean) show different characteristics. The water of the southern bays (Gökova, Güllük and Kuşadası) are warmer and saltier than the water of the bays in other regions in winter and spring. The water of the bays in the Middle Aegean (Ederemit, Çandarlı and İzmir) are denser compared to the bay waters in the other two regions. LIW was found clearly only in the southern bays and circumstantially in İzmir and Saros Bays. Its characteristics indicate that no big changes in salinity values different than original LIW. But its temperature increases on the way to the southern Aegean.

Air temperature influence on the formation of dense water is important. Especially the negative anomaly of 1993 is the lowest temperature anomaly of over 30 years. But it can not be alone to explain EMT event. All precipitation data without any exception shows negative anomalies after 1989 until 1994. Less rainfall plays also very crucial role on air-sea interactions. The very dense water formation period in the Aegean Sea is between 1990 and 1994. The evaporation data of the Aegean regions except southern regions (Kuşadası and Gökova Bays), show negative anomaly during EMT period. The evolution of high positive pressure anomalies were observed similar in almost all bays during the years from 1989 until 1994. Any significant positive pressure anomalies have been observed after this period.

The moderate or strong wind from north direction causes upwelling in southwest corner of entrance of the Saros Bay. Upwelling is a process that makes the surface water of this region denser. The transfer of this dense upwelling water to the Central Aegean Sea could be one of the several preconditions for the formation of dense water in the Central Aegean Sea. The southwest corner of Saros Bay was occupied with the BSW when the wind situation alters as in winter 2002. This time, instead of dense surface water, a buoyant BSW influences the area. LIW exists in the Saros Basin from time to time as in spring 2001. It penetrates the bay from the North Aegean Sea with the flow compensating the outflowing water.

In the middle of the İzmir Bay, a cyclonic gyre occurs frequently as a result of wind driven circulation. This cyclonic circulation brings the dense water to the surface especially in winter period. The forming water in the middle of the İzmir Bay is denser than the water of Aegean Sea entering from the northwest corner of the bay. This means temperature-controlled dense water cascading occurs from the İzmir Bay to the Aegean Sea along the east coast of the İzmir Bay during winter, and a salinity-controlled dense water cascading during summer.

The other important conclusion is the finding of most of the south Aegean Sea water masses in the Gökova Bay as LSW, LIW, MAW and TMW. GIBW is the only

distinguished water mass forming in the inner part of the bay independent from the south Aegean water masses. The jet from southwest and northwest entrance of the bay brings the water masses that are originated from the south Aegean Sea especially to the core of western cyclonic gyre. Coastal jets are produced along both coasts and a slow return flow compensates the water budget in the central area of the basin. The movements always over the eastern and western deep basins have cyclonic character in winter time.

REFERENCES

Balopoulos, E., Theocharis, A., Kontoyiannis, H., Varnavas, S., Voutsinou-Taliadouri, F., Iona, A., Souvermezoglou, A., Ignadiades, L., Gotsis-Scretas, O., & Pavlidou, A. (1999). Major advances in the oceanography of the southern Aegean Sea - Cretan Straits system (eastern Mediterranean). *Progress in Oceanography 44,* 109-130.

Gertman, I. F., Pinardi, N., Popov, Y., & Hecht, A. (2006). Aegean Sea water masses during the early stages of the Eastern Mediterranean Climatic Transient (1988–1990), *Journal of Physical Oceanography*, *36* (9), 1841–1859.

Killworth, P. D., Stainforth, D., Webb, D. J. & Paterson, S. M. (1989). A free surface Bryan-Cox-Semtner model. *Institute of Oceanographic Sciences, Deacon Laboratory Internal Rep*. 270.

Klein, B., Roether, W., Manca, B.B., Bregant, D., Beitzel, V., Kovac˘evic, V., & Lucchetta, A. (1999). The large deep water transient in the Eastern Mediterranean. *Deep-Sea Research I 46*, 371–414.

Lascaratos, A., Roether, W., Nittis, K., & Klein, B. (1999). Recent changes in deep water formation and spreading in the Mediterranean Sea: a review. *Progress in Oceanography 44,* 5–36.

Malanotte-Rizzoli, P., Manca, B. B., Ribera d'Alcala, M., Theocharis, A., Brenner, S., Budillon, G. & Ozsoy, E. (1999). The Eastern Mediterranean in the 80s and in the 90s: the big transition in the intermediate and deep circulations, *Dynamics of Atmospheres and Oceans 29* (2–4), 365–395.

Oguz, T., & Sur, H. I. (1989). A two-layer model of water exchange through the Dardanelles Strait. *Oceanologica Acta 12* (1), 23-31.

Pazi, I (2008). Water mass properties and chemical characteristics in the Saros Gulf, Northeast Aegean Sea (Eastern Mediterranean), *Journal of Marine Systems 74 (2008)* 698–710.

Roether, W., Manca, B. B., Klein, B., Bregant, D., Georgopoulos, D., Beitzel, V., Kovacevic, V., & Luchetta, A., (1996). Recent changes in the eastern Mediterranean deep waters. *Science, 271*, 333–335.

Roether, W., Klein, B., Manca, B.B., Theocharis, A., & Kioroglou, S. (2007). Transient Eastern Mediterranean deep waters in response to the massive dense-water output of the Aegean Sea in the 1990's, *Progress in Oceanography, 74*, 540-571.

Saner, E., Sayin, E. Ve Uslu, O., 1999, "Estimating the Water Quality of Izmir Bay by Using GCM", MEDCOAST 99 – EMECS 99 Joint Conference, Land Ocean Interactions: Managing Coastal Ecosystems, 9-13 Nov 1999, Antalya, Erdal Özhan (Ed.), pp. 1856-1871.

Sayin, E. (2003). Physical features of the İzmir Bay. *Continental Shelf Research 23*, 957-970.

Sayin, E., Pazi, İ. & Eronat, C. (2006). Investigation of Water Masses in İzmir Bay, Western Turkey, *Turkish J. Earth Sci., 15*, 343-372.

Sayin, E., Adalioglu, S. & Eronat, C. (2007). The light transmission and seiche depth of İzmir Bay, Western Turkey", *J. Earth Syst. Sci. 116*, 57–71.

Sayin, E., & Besiktepe, S. T. (2010): Temporal evolution of the water mass properties during the Eastern Mediterranean Transient (EMT) in the Aegean Sea, *J. Geophys. Res.,* doi:10.1029/2009JC005694.

Sayin, E., Eronat, C., Uckac, S. & Besiktepe, S. T. (2011). Hydrography of the Eastern Part of the Aegean Sea during the Eastern Mediterranean transient (EMT), *Journal of Marine Systems*, doi: 10.1016/j.jmarsys.2011.06.005

Schlitzer, R., Roether, W., Hausmann, M., Junghans, H. –G., Oster, H., Johannsen, H. & Michelato, A. (1991). Chlorofluoromethane and oxygen in the Eastern Mediterranean, *Deep-Sea Research I, 38*, 1531–1551.

Theocharis, A., Balopoulos, E., Kioroglou, S., Kontoyiannis, H., & Iona, A. (1999)a. A synthesis of the circulation and hydrography of the South Aegean Sea and the Straits of the Cretan Arc (March 1994–January 1995). *Progress in Oceanography, 44*, 469–509.

Theocharis, A., Klein, B., Nittis, K., & Roether, W. (2002). Evolution and status of the eastern Meditarranean Transient (1997-1999). *Journal of Marine Systems 33-34*, 91-116.

Tokat, E. (2006). Hydrological and biological water properties of Saros bay, M.Sc. Thesis, Dokuz Eylül University, İzmir, Turkey, 150 pp (Turkish).

Tokat, E. & Sayin, E. (2007). Water masses influencing the hydrographic properties of Saros bay, *Rapp. Comm. Int. Mer Medit.,Vol. 38* – p. 205.

Uckac, S. (2004). Determination of physical processes in the Aegean Sea, Phd. Thesis, Dokuz Eylül University, İzmir, Turkey, 98 pp.

Uluturhan E. (2010). Heavy metal concentrations in surface sediments from two regions (Saros and Gökova Gulfs) of the Eastern Aegean Sea. *Environ Monit Assess 165*, 675–684.

Unluata, U., Oguz, T., Latif, M.A., & Ozsoy, E. (1990). On the physical oceanography of the Turkish Straits. In: L. J. Pratt (Editor), *The Physical Oceanography of Sea Straits, Kluwer Academic Publishers,* 25-60.

Velaoras, D. & Lascaratos, A. (2005). Deep water mass characteristics and interannual variability in the North and Central Aegean Sea. *Journal of Marine Systems 53*, 59– 85

Velaoras, D. & Lascaratos, A. (2010). North – Central Aegean Sea surface and intermediate water masses and their role in triggering the Eastern Mediterranean Transient, *Journal of Marine Systems, 83*, 58-66.

Yaşar, D. (1994). Late glacial-holocene evolution of the Aegean Sea. Phd thesis Dokuz Eylül University, İzmir, Turkey.

Zervakis, V., Krasakopoulou, E., Georgopoulos, D., & Souvermezoglou, E. (2003). Vertical diffusion and oxygen consumption during relaxation periods in the deep North Aegean. *Deep Sea Research I, 50*, 53–71.

Zervakis, V., Georgopoulos, D., Karageorgisa, A A. P., & Theocharis, A. (2004). On the response of the Aegean Sea to climatic variability: A Review. *International Journal Of Climatology 24,* 1845–1858.